Stony Brook University

Assessing the nature of rip currents along the south shore of Long Island, NY: Dominant rip type and insights into possible forcing mechanisms

A Dissertation Presented

By

Michael Patrick Slattery

to

The Graduate School

In Partial Fulfillment of the

Requirements

for the Degree of

Doctor of Philosophy

in

Marine and Atmospheric Science

Stony Brook University

December 2010

Stony Brook University

The Graduate School

Michael Patrick Slattery

We, the dissertation committee for the above can for the

Doctor of Philosophy degree, hereby recommend

acceptance of this dissertation.

Henry Bokuniewicz-Dissertation Advisor
Associate Professor, School of Marine and Atmospheric Sciences

Malcolm Bowman-Chairperson of Defense
Associate Professor, School of Marine and Atmospheric Sciences

David Black
Associate Professor, School of Marine and Atmospheric Sciences

Henry Bokuniewicz
Associate Professor, School of Marine and Atmospheric Sciences

Frank Buonaiuto
Adjunct Faculty, School of Marine and Atmospheric Sciences

Paul Gayes
Burroughs & Chapin Center, Marine & Wetland Studies-Coastal Carolina University

This dissertation is accepted by the Graduate School

Lawrence Martin
Dean of the Graduate School

Abstract of the Dissertation

Assessing the nature of rip currents along the south shore of Long Island, NY: Dominant rip type and insights into possible forcing mechanisms

by

Michael Patrick Slattery

Doctor of Philosophy

in

Marine and Atmospheric Science

Stony Brook University

2010

The south shore of Long Island experiences periodic rip currents that pose a human threat as well as generate scientific intrigue. To address the type of rip currents present along Long Island's south shore, an integrated monitoring system that includes use of beach cameras, the SWAN wave model, and seismic recording stations was implemented. The original site was in East Hampton, NY in a private residence while a second camera was established in the Fire Island lighthouse and a second seismic station was placed in the Maidstone club (also in East Hampton, NY).

Statistics from camera observations indicate that rip currents are infrequent appearing less the 1% of the time along the two camera monitored beaches. They are also short in duration, with averages on the order of one minute, narrow, and short in offshore extent. In general, the offshore bar is too far beyond the surf zone to have the usually expected effect on rip current generation, though storm activity may drive rip current events. Instead, rip current traits and lack of dominant bar influence categorize these events as flash rip currents.

Seismic signals indicate that there is energy at longer periods affecting our coast. This energy is associated with infragravity waves capable of establishing standing edge waves, one mechanism attributed to rip current formation with the lack of strong bathymetric control. Both seismic stations recorded similar spectral peaks despite there distance of nearly three miles. The only coastal process that should be capable of generating these signals between 4 and 300 seconds are ocean wave fields. No direct measurement of a standing wave was possible, but spectral evidence supports their existence in the nearshore adjacent to our study.

The SWAN wave model was limited by accurate, high-resolution bathymetry. While the model accurately depicted incident wave field heights and direction, longer

period waves were not able to be modeled. In addition, the resolution was limited to scales approximately the same size as the average rip current making the model unlikely to accurately address flash rips, though it may be suited to fixed rip current studies.

Dedication

This body of work is dedicated to my family, my friends and my educators without whom my present and future would look much less interesting.

Table of Contents

List of Figures

Chapter 4:

List of Tables

Acknowledgements

I am grateful for the funding of my work by the New York Sea Grant, the East Hampton Beach Preservation Society and the Halpern Family Foundation. The study would not have been possible if not for the sacrifice of those locations in which I was allowed to deploy instruments which included: The Halpern Family Foundation, The Fire Island Lighthouse Preservation Society (Dave Griese) and the Maidstone Club (Ken Koch). I was fortunate to have the expert help of Mr. Porfirio Gonçalves in keeping me updated on the state of remotely located instrumentation. Preliminary seismic measurements which ultimately helped in determining the usefulness of seismics was completed by students from REU program students Jana Hirsch, Malik Kasmi (Lycee Louis-le-Grand, France) and Jeremiah Brower in 2005. Due to the extraordinary amount of time required to view this data set, the work of several other undergraduates were key in comparisons between the Fire Island Lighthouse and East Hampton imagery. The REU 2009 program students John Labold, Etienne Larangot, Allison Truhlar, and subsequently a Marine Science, undergraduate, Ashley Norton put in a lot of time to make it happen. My assorted office mates were helpful in talking through problems and sharing information and were always of help when needed. Eileen Doyle wasa pleasure to work with and made sure all of my paper work was always in order, on time, and on schedule. I'd also like to specially thank my advisor Henry Bokuniewicz as well as my dissertation committee Malcolm Bowman, David Black, Frank Bounaiuto and Paul Gayes.

Chapter 1: Occurrence of rip currents along the Long Island south shore

Introduction

Rip currents are features of nearshore circulation cells affecting sediment transport, exportation of nutrients, energy and biota from the shore, and the evolution shoreline morphology (Turner, et. al., 2007; Holman et al., 2006; MacMahan et.al., 2005; Yu and Slinn, 2003; Brander and Short, 2000; Aagaard et. al., 1997; Hammack et al., 1991). From a societal aspect, rip currents are the second most deadly natural hazard on bathing beaches in the United States (Figure 1; United States Lifesaving Association, 2010**).** These common features consume a large amount time and effort along monitored beaches for life guards; accounting for 80% of all rescues and 100 deaths annually (USLA). As a result, both the occurrence of rip currents along a stretch of beach and the ability to predict the rip current danger is of great scientific interest as well as practical importance.

Rip currents are strong, but narrow, shore-perpendicular jets of water that form along the beach (Turner, et. al., 2007; Johnson and Pattiaratchi, 2006). They have been observed at a wide variety of different spacings, durations, and widths (MacMahan et al. 2006). Brewster (1995) identified four different types of rips based on common traits including type of coastal setting and rip duration. The two main divisions are fixed rips, which remain in a single location for extended periods of time reacting directly to bathymetric forcing, and flash rips, which are short-lived, temporary rips widely thought unassociated with direct bathymetric forcing or undulation in the shoreline morphology.

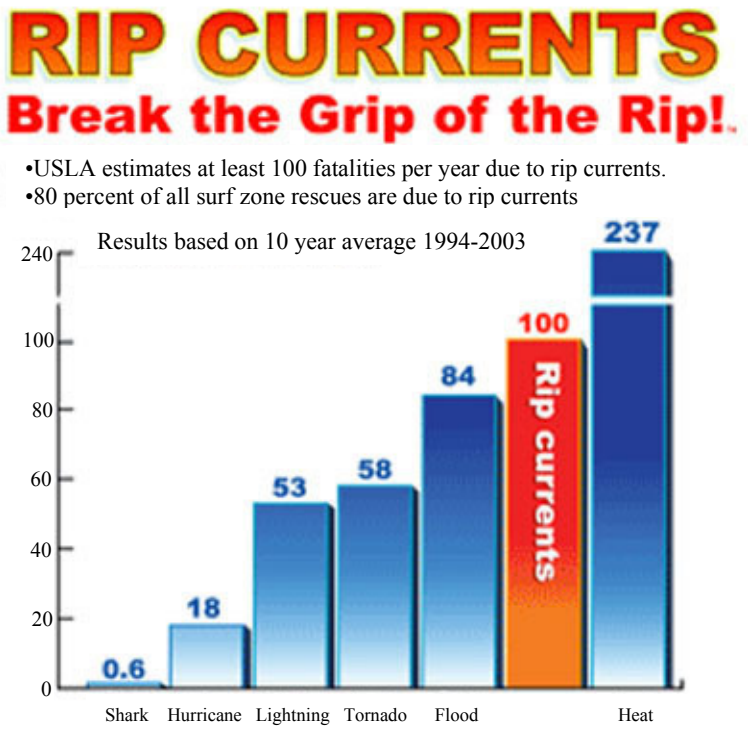

Figure 1. Commonly cited statistics from the United States Lifesaving Association regarding the biggest hazards for loss of life at beaches around the US for a 10 year period 1994-2003. (Online: http://www.ceoe.udel.edu/ripcurrents/safety/index.html).

Most studies on rip currents have focused on fixed rip currents which are controlled largely by local geomorphology, specifically, shoreline undulations or cuts through the bar known as rip channels, (Holman et al., 2006; Ranasinghe et al., 2004; van Enckevort and Ruessink, 2001; Brander and Short, 2000; LeBlond and Tang, 1974). Within the two larger divisions there are two other types of rips; permanent rips which are a fixed rip common along rocky coastlines with highly stable nearshore bathymetry allowing them to persist indefinitely, and traveling rips, a subset of flash rip currents, observed to migrate rapidly along the shore in the direction of longshore transport.

The rip current is, in fact, a portion of a larger circulation cell, where water transported shoreward by incident waves is directed alongshore to an area of low hydraulic head and is subsequently forced offshore as a focused jet of water. (Yu and Slinn, 2003; Aagaard et. al., 1997; Arthur, 1962). Many previous works on the persistence of rip currents do not directly measure the current, but rather, the evolution and migration of the rip channel as a proxy for the current itself by utilizing active observations made with video imaging. These studies have found fixed rip currents characterized by durations of days to weeks in a single location with some slow migration alongshore possible. Most often these are wide currents extending well offshore and appearing as a "hole" through the breakers. For example, MacMahan et al. (2008) used a sensor array to determine the presence of rip currents instead of video imaging and found weak rip flows to persist for long periods of time via wide, shallow rip channels. As such, the focus of rip current studies have been employed to gain better understanding of these long-lasting fixed rips and has left a gap in general knowledge when considering beaches which may not show persistent fixed rip-current presence or demonstrate

conditions that would suggest strong bathymetric controls. Instead, long straight coastlines with no (or ephemeral) offshore bars, or bars in deep water far from shore, still experience rip currents not widely addressed in terms of prevalence or duration in the literature.

The rip currents along straight coasts tend to be narrower and shorter in extent offshore and duration then fixed rip currents, often appearing as a line of foam perpendicular to the shoreline. Due to their highly mobile nature and short duration they have been termed "flash rips." The very nature of these rip currents makes long term studies difficult as commonly used, image-averaging techniques would miss these short duration events. The common practice of using dye to track water flow, too, would be cumbersome to arrange, because the exact location where a flash rip will form is currently not possible. Even sensor studies may miss these events; their narrow extent makes it difficult to be certain that deployed sensors will cover the area where a flash rip current forms. Even then, the sampling rate would have to be sufficiently rapid to record the short-lived phenomenon.

The first step in this study is to determine the nature of the rip currents found on the Long Island south shore and a get a feel for their general traits and morphological identity. Rip frequency, average duration, range of persistence, offshore extent and rip density all factor in to defining a rip current regime. With these data and better understanding of the rips on Long Island, I will address the possible causative forces. In chapter 2, I will present wave modeling results from the SWAN model and evaluate the model's accuracy in describing wave heights along the Long Island south shore. In chapter 3, I explore the use of land based seismic devices for use in surf zone wave

studies, specifically addressing dominant periods as an insight in nearshore physical processes. Chapter 4 will utilize these seismic techniques as evidence for infragravity waves which is a possible mechanism for rip current generation. Chapter 5 explores the predictive characteristics of my observations and direction for further study.

Study Setting

The Long Island south shore is a fairly uniform and largely swell dominated, though rapid short term changes in the morphology can result from storms such as Nor'easters and hurricanes (Kana, 1995; Howard, 1939). Discontinuous sets of groins and jetties can be found at several locations modifying the adjacent beaches, but in general it is a 190-km long, fairly straight, continuous coast broken by seven inlets. Tides are semi-diurnal and have a range between 0.8 m and 1.1 m (National Ocean Service, 2008). The wave climate for the nearshore is marked by average wave conditions of 1m, 7s, reaching maximum wave heights during storms of 3.5 m with 12-14 s periods (Buonaiuto, 2003; Kana, 1995). While past efforts had employed the use of nearshore sensors for short-term projects in Hampton Bays (Long Island Shores Project) and in Westhampton Beach (as run by the United States Army Corps of Engineers, sandbar project) no instruments providing nearshore wave conditions for any location have been in service since 2000. Instead, the nearest arrays from which real wave data is available stems from offshore buoys (44025 located offshore mid-island and 44017 located offshore of the eastern end of Long Island) operated by the National Oceanic and Atmospheric Administration's (NOAA) National Data Buoy Center (NDBC).

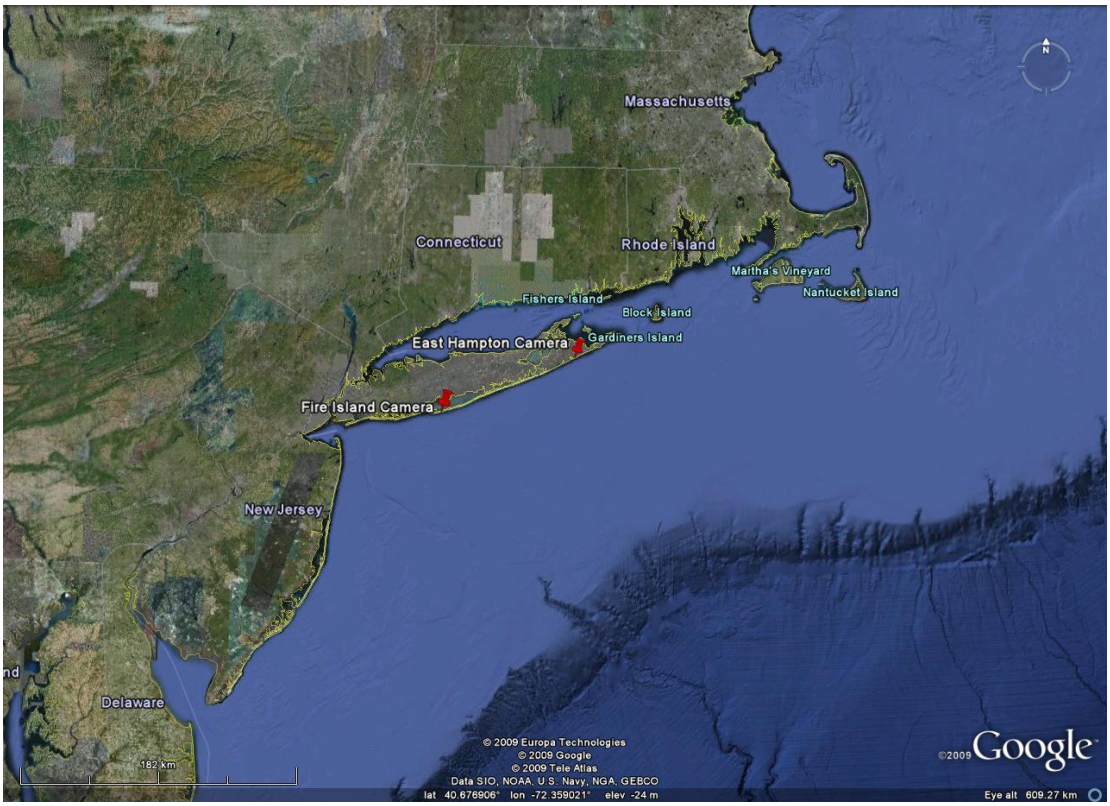

Figure 2. The location of the two camera systems along the Long Island south shore. Fire Island is located to the west while East Hampton is nearer the east end of the island

Figure 3. Set-up of the first coastal monitoring camera at the private residence in East Hampton, NY.

One of my study regions was located on the south shore of Long Island, NY in East Hampton (Figure 2). In March 2007, a camera was mounted 15 m elevation above mean sea level 120 m from low water (Figure 3) in order to monitor a stretch of beach between Main Beach (to the east) and Georgica Beach (to the west). Approximately 1000 meters to the west of the study location was the first of three groins which extend approximately 100 meters out from the dune and 23 meters into the ocean (Figure 4). The beach itself had a representative grain size of approximately 0.30 mm and a fairly steep slope of 1/7, with the surf zone slope decreasing to about 1/4 (Tsien, 1986). An ephemeral bar has been recorded approximately 220 meters offshore with the crest at 3 meters depth (Figure 5). To have a clearer idea of whether my study site was actually representative of a Long Island south shore beach, a second camera was established 92 Km west of the East Hampton location in April 2009. The second camera, on loan from Coastal Carolina University, was set in the Fire Island lighthouse lens room at 50.6 m above mean sea level and 350 m from the mean low water line (Figure 6). Similar to the situation in East Hampton an offshore bar that tended to be more permanent (though still ephemeral) was found around 220 m from the mean low water line (Figure 5). Prior personal observations and media accounts have noted rip currents at both locations.

Particular to the East Hampton study site, NOAA's buoy 44017 can be found 36 km offshore, southeast of the study site (Figure 7). Between 2002 and 2008, recorded offshore mean wave conditions at the buoy were 1.35 m, 7.46 s, and peak values of 6.77 m and 17.39 s (NOAA NDBC). Closer to the Fire Island location, NOAA buoy 44025 is located 42 km offshore in 36 m water depth (Figure 7). Between 2002 and 2008, recorded offshore mean wave conditions at the buoy were

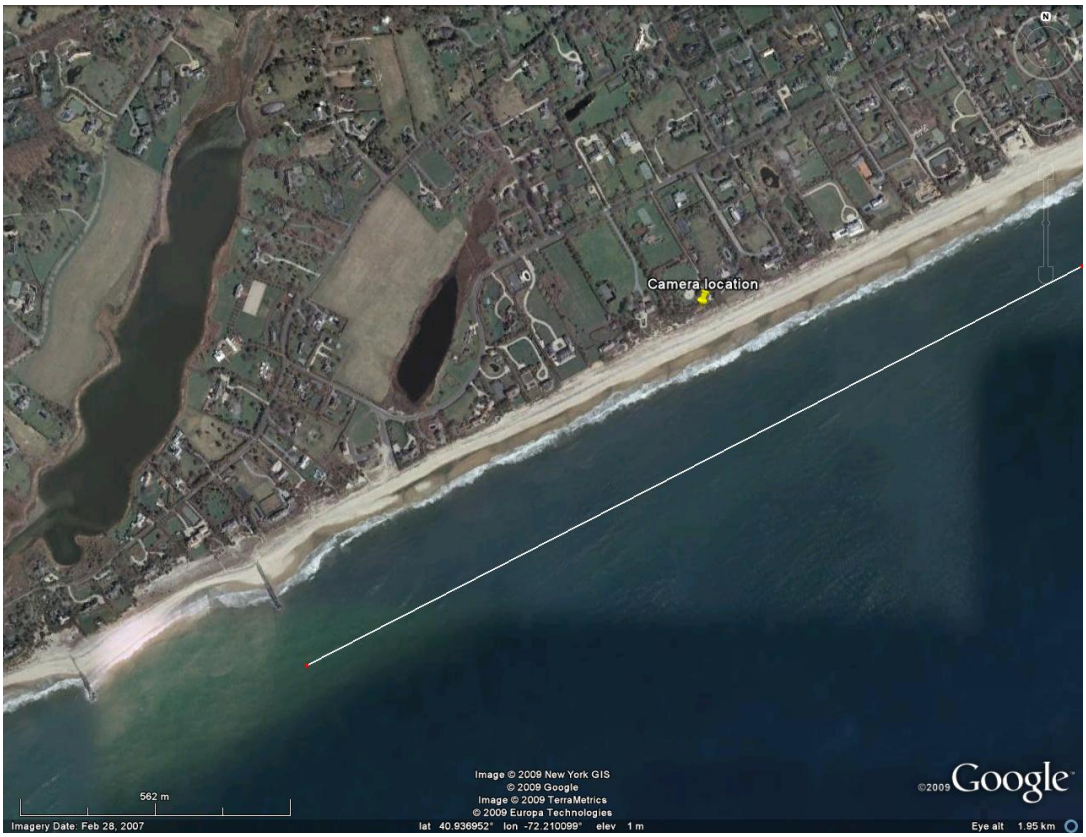

Figure 4. Physical setting of the study area in East Hampton, NY. Note the groins that start to the west and the approximate location of the bar denoted by the white line.

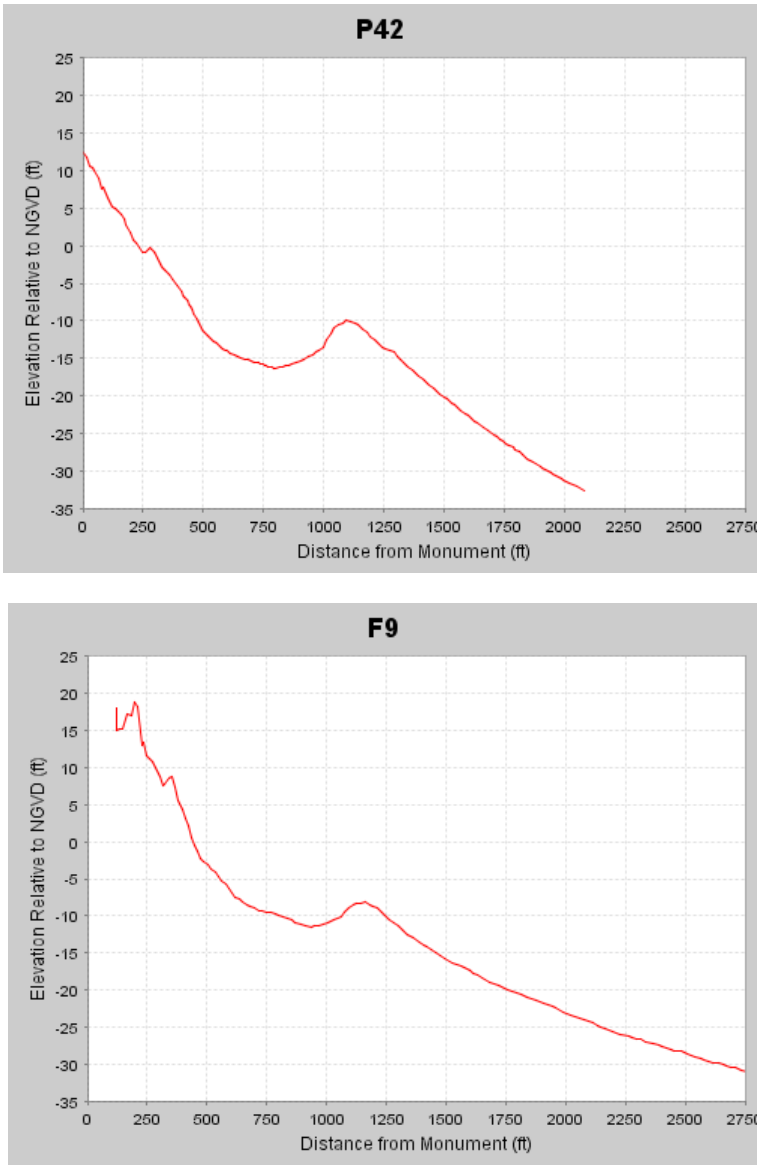

Figure 5. Location of ephemeral bar for P42 (East Hampton) and P9 (Fire Island) from the ACNYMP project (http://dune.seagrant.sunysb.edu/nycoast/). Note the depth of the bar crest at approximately 10 feet (>3 meters) and the distance offshore from mean low water at 750 feet (>227 meters).

Figure 6. Fire Island lighthouse camera. Camera is located in the lens room (inset) at the top of the lighthouse, visible here by the lamp.

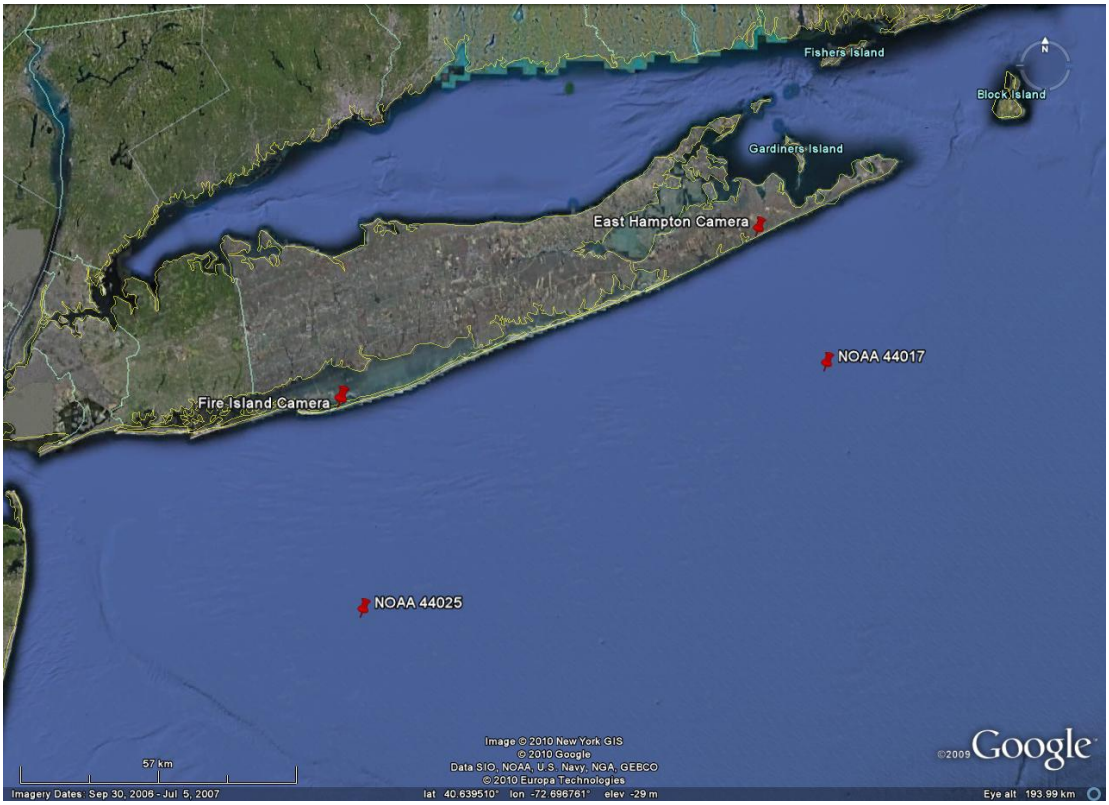

Figure 7. Position of offshore buoys in contrast to nearshore rip current monitoring stations at Fire Island and East Hampton.

1.32m, 7.28s, and peak values were 6.0 m and 17.39 s. Essentially, both buoys demonstrate the presence of similar wave conditions on the shelf approaching with little variability along the entire stretch of the Long Island south shore, therefore, it seems safe to assume variability in incident wave conditions alongshore would be controlled by nearshore transformations and local forcing.

These two study locations were primarily sites-of-opportunity. Researchers at SoMAS have been monitoring conditions at the East Hampton Village Beach since 1979. Previous observations at East Hampton have noted the presence of rip currents and I am grateful to the East Hampton Beach Preservation Society for providing a site upon which the camera could be mounted for a fairly clear surf zone view. The Fire Island Lighthouse has an incredible unobstructed view of a large portion of the Fire Island shoreline, coupled with its elevation and the lack of other structures at the open-ocean coast for the barrier island portion of the island on which to deploy video instruments the support of the Fire Island Lighthouse Preservation Society was sought. Communication with their organizational heads were quite encouraging and allowed for another positive research relationship that allowed for me to expand the study to a geographically different section of the Long Island south shore. As far as the coastal geomorphology, each of the two sites were located in the one of the two major coastal divisions of Long Island as first described in Taney, 1961 and elaborated further by Zarillo and Liu, 1989 and Batten 2003.

The East Hampton site was located in the headlands section on the east end of Long Island, characterized in general, by sandy beaches, six-meter continuous dunes, and some coastal ponds (Taney, 1961; Batten, 2003). This section of the shore was shown to

have well-organized bathymetry and steeper shorefaces (Zarillo and Liu, 1989). Fire Island is centered in the barrier beach portion of the south shore characterized by sandy, barrier beaches which formed originally as spits across inlets (Batten, 2003). Zarillo and Liu, 1989 characterized the bathymetry as poorly organized and having a gentler shoreface. My East Hampton site was representative of the headland beaches along the east end of the island while the site at the Fire Island Lighthouse represented the barrier island section of the coast.

Methods

Although a few studies using longshore and cross shore sensor arrays have also been completed, the method is difficult and expensive (Quartel, 2009; MacMahan et al. 2008; Turner et. al., 2007; MacMahan et al., 2005; MacMahan et al., 2004; van Enckevort and Ruessink, 2001). More frequently, researchers have used long-term video monitoring to create image averages and denote rip currents by cuts in the offshore bar.

An Erdman Systems ® camera recorded images every 15 seconds between 6:00 A.M (EST) and 9:00 P.M (EST) to observe surf activity in the region starting March 2007. From 6:00 A.M through 3:00 P.M. the camera was oriented 90 degrees to the ocean, but, due to sun glare, from 3:00 P.M. through 9:00 P.M. it was reoriented to look alongshore east. The images were retrieved from the remote camera location and inspected for the signs of rip currents which could be, for example, lines of foam and/or lack of breaking waves. Rip current duration and rip current frequency were compiled to

define rip current regime. This allowed for application of metrics to address what type of morphology was associated with rip currents along the Long Island south shore.

In April 2009, a second Erdman system was made available via Coastal Carolina University and it was mounted in the lens room atop the Fire Island Lighthouse for a second Long Island south shore study site. This location was 50.6 m above sea level and 350m from the shoreline. The camera had a sampling rate of 20 seconds and was oriented, generally, shore normal. The images for both locations were evaluated in the same way. Having two sites allowed some observational comparisons to essentially ground-truth results from the original study location.

The images were sampled by randomly picking days throughout a month and looking at each individual image with the intention that this would lead to a large representative sampling of the available images. While this method may not be accurate in determining the full duration of rip currents, it was able to accurately depict the occurrence, extent and general duration of rip currents that form in the study region statistically. Early efforts were spent on working cooperatively with the computer science department at Stony Brook University to try and utilize an automated computer recognition system based on pixel color. These attempts were not successful however, because the signature of rip currents depended too much on sun angle, cloudiness, the extent of white water, and rippling of the water surface due to wind.

Results

All told, 171,443 images covering 741 hours were examined from the East Hampton camera. Rip curents appeared to be present throughout the year with no seasonal preference. The rip currents at East Hampton almost always appeared as a line of foam through the surf zone (rather than as a large disturbed area of water like a "hole" through the breakers; Figure 8). A total of 49 rip currents were observed spanning 241 images with an average duration of nearly 76 seconds per rip currents and ranged from 30 to 150 seconds duration (Table 1). This means that rip currents existed in the study area 0.14% of the time and averaging about 2 rip currents per day per kilometer of beach (Table 1). Only one event was seen to contain multiple rip currents alongshore for the East Hampton site and this corresponded to the only rip current event that appeared as a gap in the line of breakers. There appeared to be no preference for location of rip currents alongshore and a few of these features were seen to migrate; almost exclusively westward. The rip currents were narrow, usually no wider then 15 meters. They rarely extended more than 50 meters offshore. Thirty of the 49 rip currents lasted between 45 and 75 seconds (Figure 9).

Rip currents at Fire Island were widespread through the months for which data were available and did not seem to show any seasonal trend. The rip currents appeared as both the line of foam and gap through the breaker zone for this location (Figure 10). In all, 155,677 images spanning 865 hours of footage were viewed. Rip currents were observed as 130 separate events, spanning 338 images. This gives an average duration of

Figure 8. Representative "line of foam" type rip current as noted by the arrow at East Hampton, NY on a day with small surf.

Table 1: Rip current regime for East Hampton, New York

Scenes observed	171443
Scenes with rip currents	241
% frequency	0.14%
Distinct rip events	49
Rips/Km/day	2.00

Time Observed (hr)	714
Average Rip Duration (s)	76
Minimum Duration (s)	30
Maximum Duration (s)	150
Rip Activity	1.44E-06

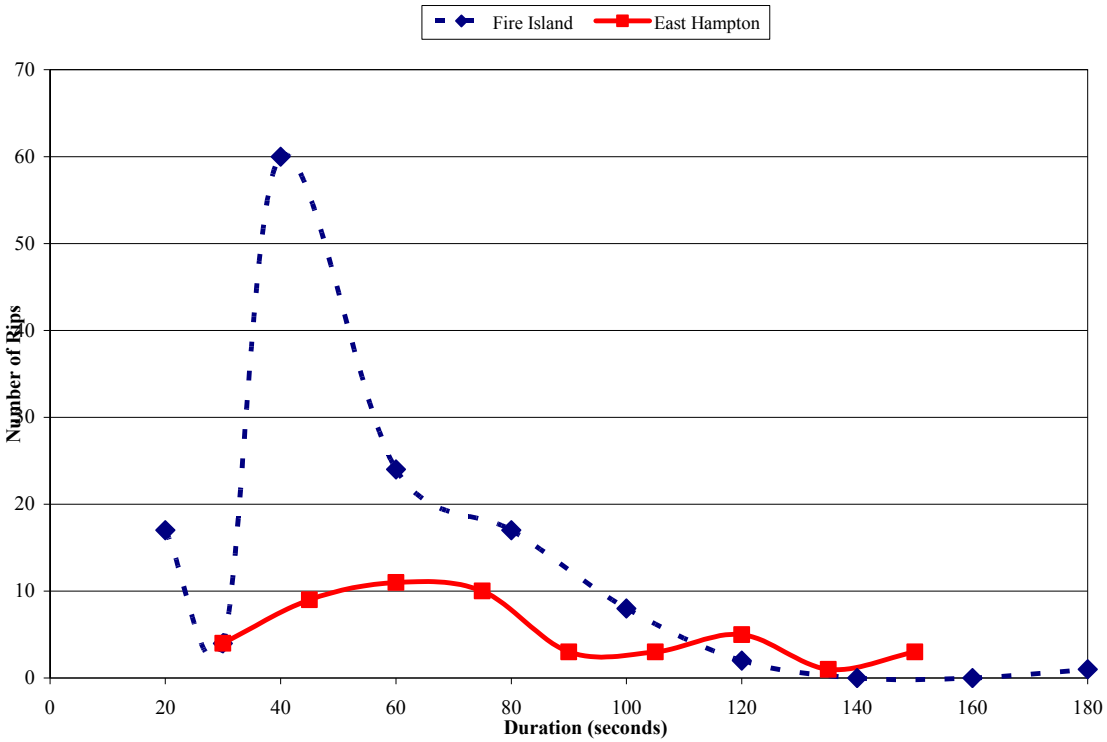

Figure 9. The number of rip currents plotted versus duration of rip currents seen at Fire Island (blue) and East Hampton (red).

Figure 10. Rip currents at Fire Island. Note the multiple rip currents as indicated by the two arrows and the expression as a “hole” through the breakers.

Table 2: Rip current regime for Fire Island, New York

Time Observed (hr)	865
Average Rip Duration (s)	47
Minimum Duration (s)	20
Maximum Duration (s)	180
Rip activity	4.65E-04

Scenes observed	155677
Scenes with rip currents	338
% frequency	0.22%
Distinct rip events	130
Rips/Km/day	13

52 seconds ranging from 20 to 180 seconds in total duration. A rip current frequency of 0.22% was calculated and a density of 13 rip current/km/day (Table 2). Multiple rip currents were seen on several occasions, though still not the dominant condition. There was a slight preference for rip currents to appear at the east end of the study area, although this did not seem to persist or affect subsequent rips that may have formed to produce a multiple rip scenario. These rips appeared to stretch for between 20 and 30 meters alongshore and extend up to 75 meters offshore. Of the observed rip currents, 101 (78%) lasted between 40-80 seconds (Figure 9).

Discussion

The first indicator of the type of rip-current setting present on the Long Island south shore comes from viewing the physical nature of the observed rip currents. Dominant in East Hampton, and common at Fire Island, rip-current events were evident as shore-perpendicular lines of foam that extended through the surf zone and rarely seemed to extend to the nearshore bar; extending no more then 50 m offshore and had an infrequent tendency to migrate alongshore through the frames. Rip current appearing as a quiescent region through the surf zone were almost non-existent in East Hampton and, while more prevalent; such features were infrequent at Fire Island. This quiescence was the base premise for identifying rip currents in most prior video-image averaging studies since the lack of wave breaking in the rip channel denotes the rip location. Even had researchers noted the short duration and modified sampling to address the shorter lived rips, they would still have missed observing the rips based on their presence as lines of

foam instead of the more generally accepted mode of "hole through the breakers". Of further interest was the lack of events that demonstrated multiple rip currents at East Hampton, though again, these were more common at Fire Island. Common spacing for rip currents has been reported to be between 90 and 500 m and the field of vision at East Hampton was only 100 m at the 90 degree orientation and nearly a kilometer at the alongshore orientation. This, in itself, may have precluded the appearance of multiple rips, though personal observation on the beach seems to suggest multiple rips are indeed infrequent and the single rips are the normal condition for the East Hampton beach. Each of these morphological observations, in of themselves, can help to better understand the rip current regime common to the study site.

The anecdotal evidence of short lived rip currents was supported by the statistical findings for both study locations. At East Hampton, the average rip duration ranged from between 30 and 150 seconds with an average of 76 seconds, denoting extremely short-lived rip currents when compared with those more common throughout the literature; sometimes boasting durations on the order of a month (Holman et al., 2006). Instead Long Island's rip currents seem to appear and disappear at random over very short time scales as infrequent as two rip currents per day per kilometer of beach. In fact, the duration of over 60% of the rip currents fell between 40 and 80 seconds and another 30% exceeded 80 seconds in duration. At its longest, 2.5 minute rip currents were seen on three occasions; this still fell well short of the time periods generally cited (MacMahan, 2006). It would be difficult to describe such rip-currents in the category of fixed or permanent and both the basic statistical outcome as well as the observations regarding

rapid rip-current migration would, instead, support flash rips as the dominant form. With only slight differences, the general trend remained much the same at Fire Island.

The distribution was similar for Fire Island in that the majority (76%) of the rip currents lasted between 40 and 80 seconds. The remaining 24% were mainly shorter-lived rips (16%) with 8% being longer. Additionally, multiple rips were seen slightly more frequent, accounting for 20% of the cases. In instances of multiple rips, it was generally observed that rip currents persistent for longer then 80 seconds were seen in conjunction with a more ephemeral rip which lasted for 40 seconds or less. There was a slight tendency for a recurring rip current at the west of the frame during the study, but this usually did not reoccur within a single day, but rather spaced throughout the sampling. This could be due to a slight influence from shoreline, but I have no evidence of any specific features that would have lead to this trend.

The Fire Island set-up had a maximum sampling rate of 1 image every 20 seconds while the East Hampton camera generally took images once every 15 seconds. The nature of the different camera systems lead to a bit of difference in the way they could be handled and probably accounts for the greater number of short-lived rip currents detected at Fire Island. Since many of the rip currents seemed to fall in the 40-second range for both locations, there is a greater possibility of missing the event at Fire Island which could have lead, also, to the decrease in average rip duration being shorter by 52 seconds at Fire Island than that at Hampton Bays. Despite the slight variations between the rip current regimes at both sites, they each still demonstrate traits that would preclude a fixed-rip type system and instead support the idea of flash rips as the dominant mode along the Long Island south shore. This does not mean, necessarily, that the entire south

shore is devoid of the occasional fixed rip, but perhaps the lack of larger, stronger, more persistent rip currents on a regular basis explains the relatively low number of rip current drownings (14/decade) when viewed from a national average (100/year).

Conclusions

Rip morphology and the rip regime observed from rip current statistics at East Hampton and Fire Island, denote similar traits. These traits presented in the discussion would seem to preclude strong bathymetric forcing for the majority of the time at the Long Island south shore. Instead, these short lived, small, rip currents are more indicative of flash rip currents which are typically harder to observe and describe due to their highly ephemeral nature. It would seem, then, reasonable to proceed with the rip current investigation with a focus of driving mechanisms possibly associated with flash rip currents.

References

Aagaard, T., B. Greenwood, J. Nielsen. 1997. Mean currents and sediment transport in a rip channel. Marine Geology, 140: 25-45.

Arthur, R.S. 1962. A note on the dynamics of rip currents. Journal of Geophysical Research, 67 (7): 2777-2779.

Batten, B.K. 2003. Morphologic typologies and sediment budget for the ocean shoreline of Long Island, New York. Ph.D. Dissertation, Stony Brook University, 92 pp. +appendices.

Brander, R.W., A.D. Short. 2000. Morphodynamics of a large-scale rip current system at Muriwai Beach, New Zealand. Marine Geology, 165: 27-39.

Brewster, B. C. 1995. *The United States lifesaving association manual of open water lifesaving*, BRADY/Prentice Hall, Upper Saddle River, New Jersey, 07458, 316 pp.

Buonaiuto, F.S. 2003. Morphological evolution of Shinnecock Inlet, NY. Ph.D. Dissertation, Stony Brook University, 84 pp. + appendices.

Hammack J., N. Scheffner, H. Segur. 1991. A note on the generation and narrowness of Periodic rip currents. Journal of Geophysical Research, 96(C3): 4909-4914.

Holman R.A., G. Symonds, E.B. Thornton, R. Ranasinghe. 2006. Rip spacing and persistence on an embayed beach. Journal of Geophysical Research, 111: 1-17.

Howard, A.D. 1939. Hurricane modifications of the offshore bar of Long Island, NY. Geographical Review, 29(3): 400-415.

Johnson, D., C. Pattiaratchi. 2006. Boussinesq modeling of transient rip currents. Coastal Engineering, 53: 419-439.

Kana, T.W. 1995. A mesoscale sediment budget for Long Island, New York. Marine Geology, 126: 87-110.

Leblond, P.H., C.L. Tang. 1974. On energy coupling between waves and rip currents. Journal of Geophysical Research, 79(6): 811-816.

Long Island Shores. Last accessed March 22, 2010. http://www.lishore.org/sites.htm.

Macmahan, J.H., E.B. Thornton, A.J.H.M. Reniers, T.P. Stanton, G. Symonds. 2008. Low-Energy Rip Currents Associated With Small Bathymetric Variations. Marine Geology, 255: 156-164.

MacMahan, J.H., E.B. Thornton, A.J.H.M Reniers. 2006. Rip Current Review. Coastal Engineering, 53: 191-208.

MacMahan, J.H., E.B. Thornton, T.P. Stanton, A.J.H.M. Reniers. 2005. RIPEX: observations of a rip current system. Marine Geology, 218: 113-134.

MacMahan, J.H., A.J.H.M. Reniers, E.B. Thornton, T.P. Stanton. 2004. Infragravity rip current pulsations. Journal of Geophysical Research, 109(C01033): 1-9.

National Oceanic and Atmospheric Administration, National Data Buoy Center. Last accessed, March 2, 2010. http://www.ndbc.noaa.gov/station_hisoty.php?station=44017

Quartel, S. 2009. Temporal and special behavior of rip channels in a multiple-barred coastal system. Earth Surface Processes and Landforms, 34: 163-176.

Ranasinghe, R., G. Symonds, K. Black, R. Holman. 2004. Morphodynamics of Intermediate beaches: a video imaging and numerical modeling study. Coastal Engineering, 51: 629-655.

Taney, N.E. 1961. Geomorphology of the south shore of Long Island, New York. U.S. Army Corps of Engineers, Beach Erosion Board, TM No. 128: 67pp.

Tsien, H-S. 1986. Differential transport of sand on the south shore of Long Island. M.S. Thesis, Stony Brook University.

Turner, I.L., D. Whyte, B.G. Ruessink, R. Ranasinghe. 2007. Observations of rip spacing, persistence and mobility at a long, straight coastline. Marine Geology, 236: 209-221.

United States Army Corps of Engineers (USACE). Last accessed, March 22, 2010. http://sandbar.wes.army.mil/public_html/pmab2web/htdocs/newyork/westhampton/ny001/ny001.html.

United States Life Saving Association (USLA). Last accessed, September 17, 2010. http://www.usla.org/ripcurrents/.

Van Enckevort, I.M.J., B.G. Ruessink. 2001. Effects of hydrodynamics and bathymetry on video estimates of nearshore sandbar position. Journal of Geophysical Research, 106(C8): 16969-16979.

Yu, J., D.N. Slinn. 2003. Effects of wave-current interaction on rip currents. Journal of Geophysical Research, 108(C3): 33(1)-33(19).

Zarillo, G.A., J.T. Liu. 1988. Resolving bathymetric components of the upper shoreface on a wave-dominated coast. Marine Geology, 82: 169-186.

Chapter 2: Verification of the SWAN wave model for implementation along the Long Island south shore

Introduction

Still a matter of contention among rip current scientists regarding the specific processes, there seems to be at least a general consensus that incident waves play a role in rip current formation. As nearshore sensors are not present anywhere along the Long Island, south shore study region, it seemed wise to try and establish nearshore physical conditions through the implementation of a nearshore wave model. To get a true verification, a time period for which nearshore sensors were available for ground truthing would be necessary and required looking back to 1999 for data to which to compare model results. It also seemed prudent to choose a time period over which no extreme storm events took place in order to try and find a simple baseline for exploring results. While most of the focus for large scale storm systems along the United States east coast is concentrated on hurricanes that regularly impact the southeast United States, it is in fact winter cyclones (nor'easter storms) that are more prevalent to the ortheast seaboard of the country, which can easily be as destructive, if not more so, then hurricanes (Davis and Dolan, 1993). In fact, of the ten worst storms of the century as voted on by meteorologist experts at the Weather Channel in 1999, three were nor'easters including: "Great Appalachian" storm 1950, "superstorm" 1993, and "Ash Wednesday" storm 1962 (http://www.weather.com/newscenter/specialreports/sotc/topten/results.html, 2006).

The wave transformations that occur as incident waves move across the shelf into shallow coastal waters is a key component in establishing an ability to forecast hazardous coastal conditions. Whether it is the threat of rip currents and loss of life, enhanced wave set-up inducing flooding, or large erosive waves, no accurate warning system or forecasting can be implemented without a solid grasp on the wave conditions. SWAN (Simulating Waves Nearshore), a third generation wave model, is intended to predict nearshore wave conditions from offshore incident wave heights. SWAN allows for the user to predict the transformations waves undergo as they move into shallower waters, specifically it was designed to "…estimate wave conditions in small-scale, coastal regions with shallow water, barrier islands, tidal flats, local wind, and ambient currents." (Ris et al., 1999). Because discrepancies between the SWAN model output and observed data have been detected in prior studies, (Rogers et al, 2003) it was necessary to first verify the effectiveness of SWAN in the specific study area for the prediction of wave heights. In this chapter SWAN will be applied to the ocean coast of Long Island and verified with limited wave gauge measurements in order to accurately depict nearshore wave transformations that occur as waves move into the shallows along the Long Island south shore. I will show that SWAN sufficiently modeled the wave transformations that occur as the wave energy propagates to the Long Island south shore and therefore is a reasonable tool in better describing nearshore wave conditions for the general study regions presented in the prior chapters. In this way, we can gain some insight into local wave conditions that may ultimately lead to a better understanding of conditions preceding rip current formation.

Due to the nature of SWAN as a steady-state model (as the vast majority of nearshore models are) the instabilities needed to generate rip currents cannot be realized, but the model still gives insight into the incident wave conditions common for the south shore.

Description of the SWAN model

SWAN accounts for variations in wind energy, refraction, energy dissipation due to whitecapping, bottom friction, depth-induced breaking, and nonlinear wave-wave interactions (Booij et al, 1999). SWAN is based on the action balance equation, which is capable of describing wave spectrum evolution (1):

$$\frac{\partial}{\partial t}N+\frac{\partial}{\partial x}c_x N+\frac{\partial}{\partial y}c_y N+\frac{\partial}{\partial \sigma}c_\sigma N+\frac{\partial}{\partial \theta}c_\theta N=\frac{S}{\sigma} \qquad (1)$$

Where $\frac{\partial}{\partial t}N$ is the local rate of change, $\frac{\partial}{\partial x}c_x N+\frac{\partial}{\partial y}c_y N$ is the propagation of action in the x and y space (respectively), $\frac{\partial}{\partial \sigma}c_\sigma N$ denotes variability in relative frequency due to changes in the water depth and current interactions in x space and $\frac{\partial}{\partial \theta}c_\theta N$ represents transformation due to refraction induced by both depth and currents in θ space. S is a source term representing generation, dissipation and nonlinear wave-wave interactions and σ is the relative frequency. Formulations for each of these processes are described further in Booij et al. (1999).

Booij et al. (1999) provided the first validation of SWAN. SWAN model output was plotted initially against flume experiments for waves moving from deep water to shallow water over a bar and for simulating depth induced breaking. The predictions from SWAN were found to resemble conditions generated in the flume trials adequately. They concluded from the comparisons that SWAN, in addition to closely matching observed experimental data, agreed with analytical solutions.

Other experiments have focused, instead, on comparing SWAN output to environmental observations to test for real-world model performance instead of depending on flume and laboratory experiments. This step always contributes significantly in model development to test its portability to an array of real-world cases. Successful tests of this model compared to field data were completed in a variety of settings including: Lake Okeechobee (Jin and Ji, 2001), a portion of the Rhine estuary (Ris et al, 1999), off the outer banks of North Carolina, and on the Pacific shelf off of Washington (Palmsten, 2001). The first series of tests were completed by Ris et al. (1999) in back barrier tidal gaps of the Rhine Estuary, Germany.

Ris et al. (1999) demonstrated that SWAN reproduced most changes in significant wave height (86%) and mean wave period (73%), though the magnitude of the change was often over-predicted. Their explanation for this was the complexity of the systems in the area of the Rhine estuary that included bars, sheltered estuarine mouths, sluices, and areas of small fetch over which waves could regenerate. In addition, the magnitudes of the waves varied by up to 3 orders of magnitude during the tests between deep and shallow water with SWAN slightly over-predicting the decay of the waves by 1%. Additional studies of SWAN accuracy were completed in a variety of settings to gather

the full scope of applicability. In Lake Okeechobee (Jin and Ji, 2001) SWAN did reasonably well with the relatively noncomplex bathymetric geometry and coastal invariability, with changes in significant wave heights closely matching at multiple sample sites.

Methods

Input values of significant wave height (H_{sig}), wave period (T) and wave direction were all collected for the month of February 1999 from NOAA buoy 44025 located on the mid shelf. During this time no major storm events impacted the study region allowing for the simplest case study available for the verification. These data were averaged over three-hour time periods for the entire month resulting initial wave conditions for 196 separate SWAN model runs (with incident wave properties being updated at every three-hour intervals throughout the month) and propagated through the region over a bathymetric grid of resolution 0.0025° latitude by 0.0025° longitude (Figure 1).

Interpolation of the bathymetry grid was completed using the meshgrid command in Matlab version 6.5, and raw data provided by a compilation of readings from the US Army Corps of Engineers SHOALS (Scanning Hydrographic Operation Airborne Lidar Survey) and NOAA's SWATH (Small Water-Plane-Area Twin Hull). Gaps in the measured data were filled using the "fix gaps" command in Matlab which linearly interpolates missing data. "Fix gaps" was only used for a twelve hour period on February 1st, as NOAA buoy 44025 did not record data over this period from which incident

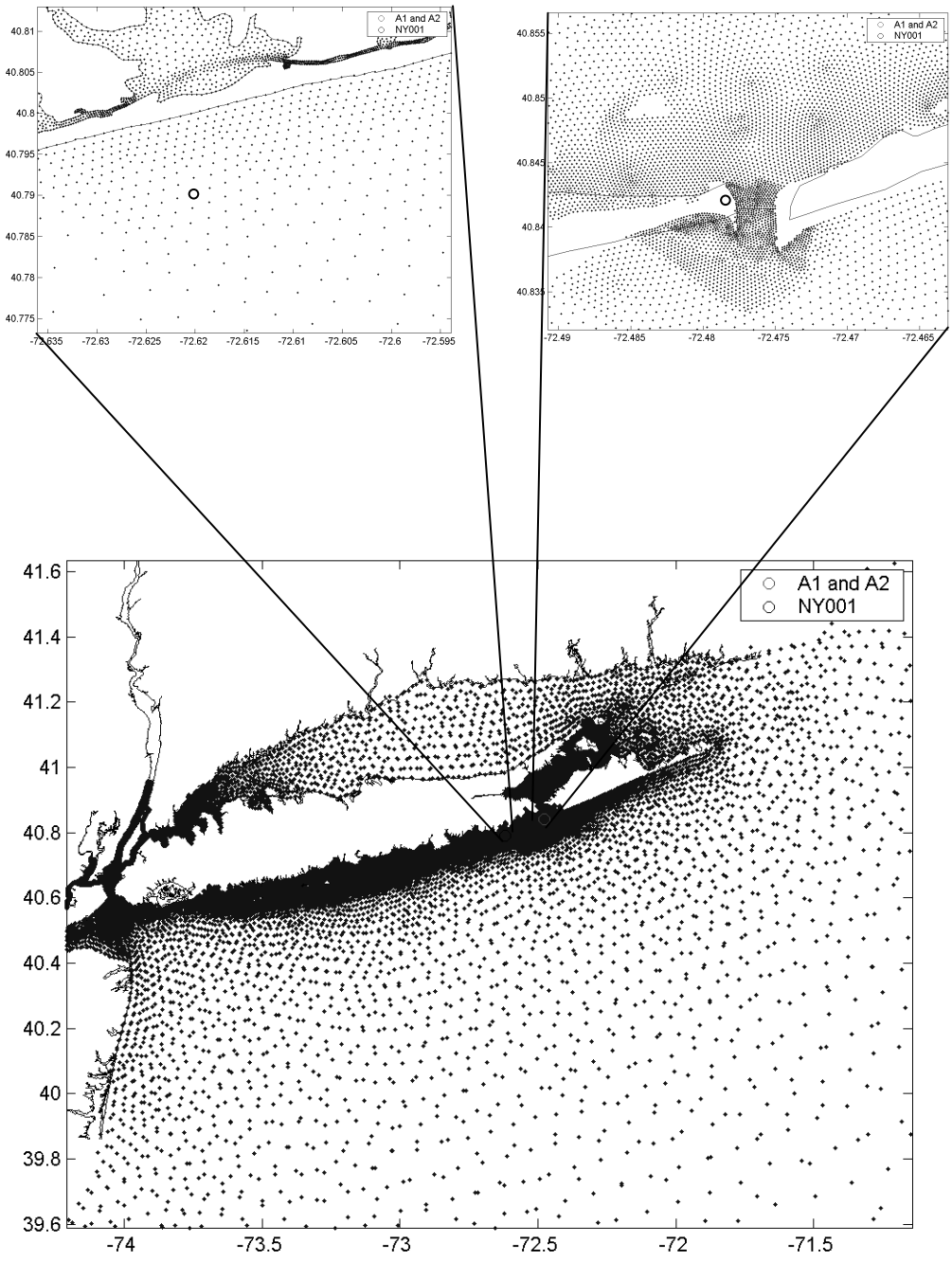

Figure 1. Grid resolution and locations of Westhampton (NY001, top left) and Shinnecock (A1 and A2, top right) measurement locations.

heights could be produced for the SWAN model runs. These conditions were utilized in SWAN version 40.41 with patches A and B running in generation one mode, which includes triad wave-wave interactions, depth-induced breaking, bottom friction, and obstacle transmission was used.

For model verification, data from three nearshore instruments measured significant wave heights. The records from station NY001 (Westhampton Beach) and stations A1 (Shinnecock Inlet offshore: Sontek Acoustic Doppler Velocimeter Ocean (ADVO)) and A2 (Shinnecock inlet onshore: ADVO) (Figure 1) were gathered from the LIShore project and plotted against the model results. Methods to assess model accuracy were taken directly from Ris' original work and included using root mean squared error (rmse) and Scatter Index (SI). The rmse is a measure of precision between a modeled outcome and observations. Scatter index is used to quantify model performance and is the rmse normalized to the average observed value.

No wind data was available. As a result, whitecapping was turned off for the model runs, though it is generally included in the generation one mode along with either exponential or linear wind growth. Limited wind conditions were gathered for the Shinnecock Inlet region from the LIShore project M1 station. Although this wind data was only a single point, and so, were not sufficient to generate a wind grid useable in SWAN, it did give some insight into how wind may have affected differences between the model and measured data. Onshore winds would be capable of generating larger than modeled H_{sig} and offshore winds may have acted to diminish H_{sig} from those produced by the model runs.

Results

Ocean conditions recorded at NOAA buoy 44025 showed a fairly quiet month in terms of wave activity. The average wave height was 1.03 m ranging 0.2-3.2 m. The average period of the approaching waves was 5.1 s ranging from 3.1-8.4 s. A period of larger wave heights occurred on February 25th and accompanied wave periods of just over 5 seconds. Generally the wave heights remained right around 1 m for the majority of the month.

Figure 2 shows the SWAN model output when plotted against the recorded data at NY001, Westhampton, NY location. Except for the time period from February 20-24 the SWAN model predictions followed conditions recorded at the buoy. The rmse was 0.398 and SI or 0.4313 for this run. To have an alternative comparison the rmse and SI were recalculated excluding the mentioned time from February 20-24. The results were an rms error of 0.307 and SI of 0.323.

Figure 3 demonstrates the comparison between the SWAN model results and wave heights recorded at Shinnecock Inlet. While general changes in wave heights seemed closely mimicked, SWAN produced smaller estimated wave heights than those measured at stations A1 and A2. For station A1 the rmse was 0.271 and SI was 0.414, while at station A2 the rmse was 0.340, and the SI was 0.452.

Wave direction as modeled was exclusively out of the southeast, matching well with the general direction of approach for Shinnecock, though at Westhampton there

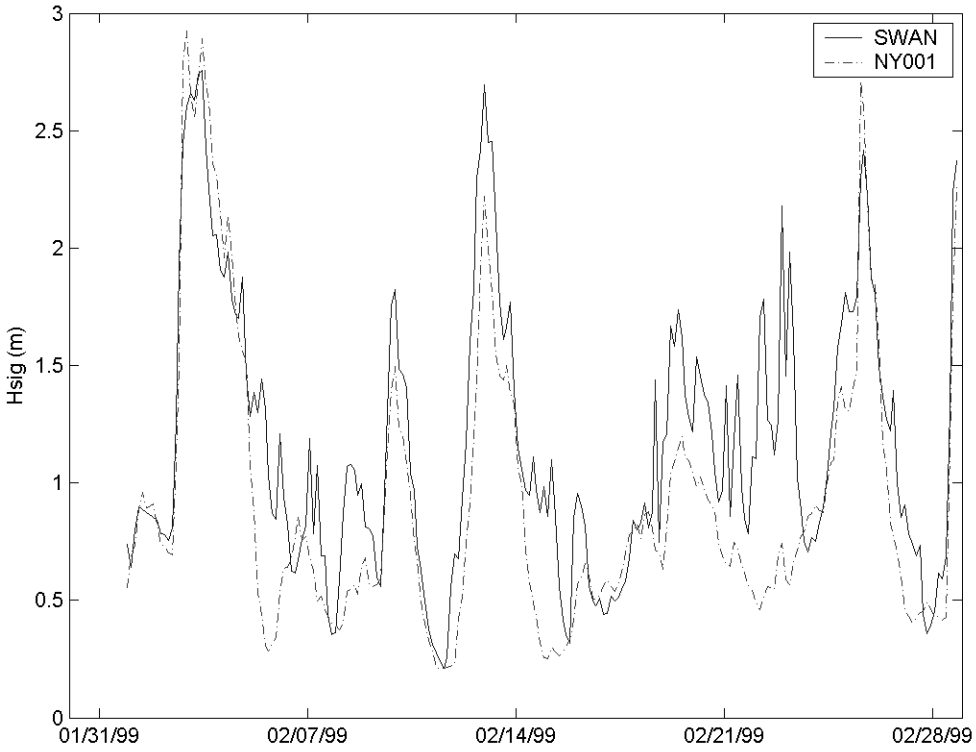

Figure 2. Results from SWAN model run at Westhampton Beach compared to measured significant wave heights at NY001.

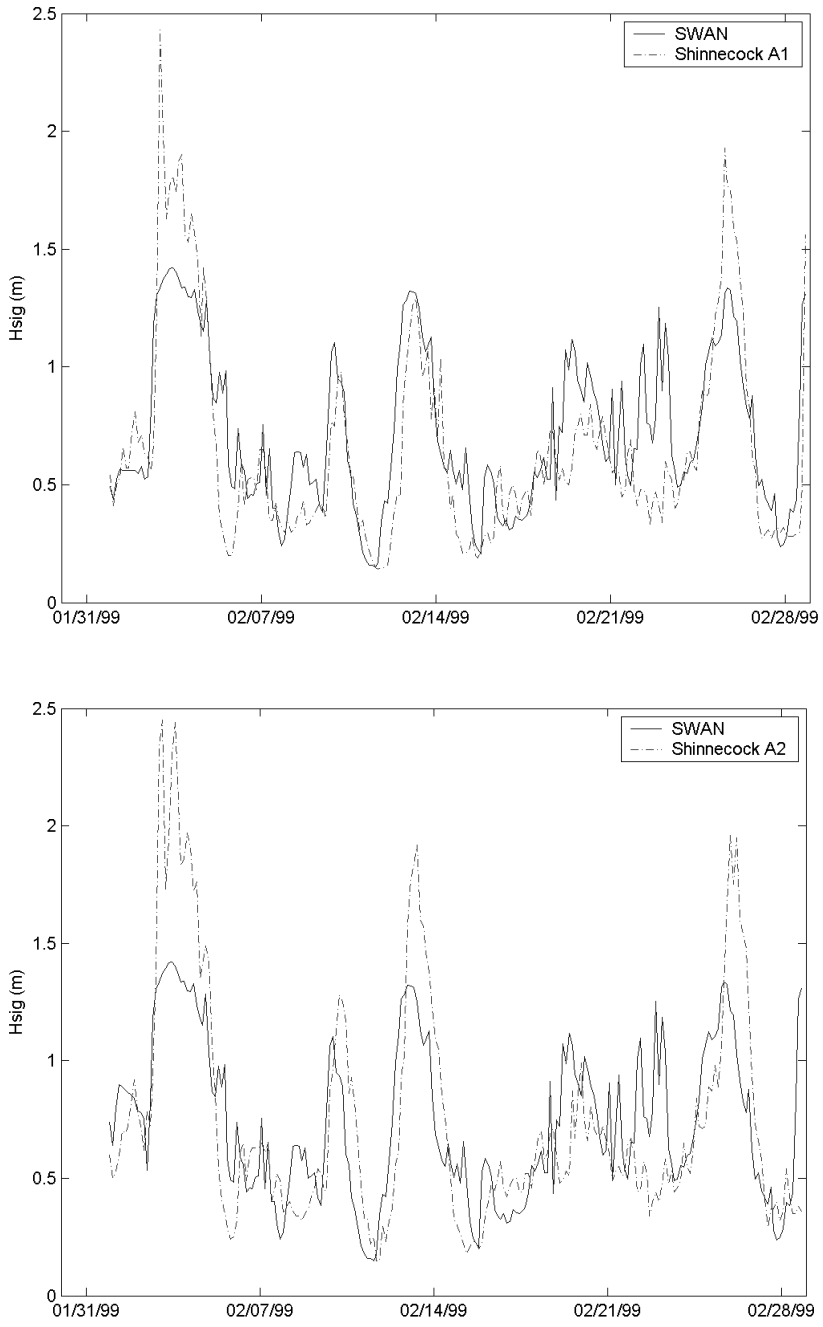

Figure 3. SWAN model results at Shinnecock inlet compared to measured significant wave heights at A1 (top) and A2 (bottom).

were approximately 30 hours (spread throughout the month) total that showed an average wave approach swinging more southwesterly.

Discussion

Similar to observations by Ris et al. (1999), SWAN had a tendency to under predict significant wave heights for our region. Generally the under prediction was not more than one meter and only occurred at times when wave heights were elevated to more than 1.5 meters. In our trials, lack of wind data which could further enhance wave heights during the study is the most likely source of this error. While no wind data was available for the region as a whole, some climatological data did lend itself to assess possible impacts wind may have had on measured data that would not have been accounted for in the model run. Overall the agreement between the model and measured data looked very good and showed promise for continued application of the SWAN model for the south shore of Long Island.

At Westhampton Beach, not only were most changes in height accurately depicted, but the timing of the changes in wave height was also accurate. Excluding the period from the 21st through the 24th wave heights from the SWAN model were fairly close to the measured data, but generally the peaks were over predicted in the model runs. This visual relationship is supported by the rmse (0.307) and SI (0.323). Over the time of greatest error between the model and observed wave conditions, point data from anemometers showed winds directed offshore from the north and northwest. This was the only time period where winds seemed to be blowing consistently from the north and

northwest for longer then few consecutive hours; possibly explaining the smaller measured wave heights compared to the modeled. The local wind blowing offshore could have acted to cause wave breaking or energy loss further offshore in the observed data, but, since not included in the model, would not have impacted the waves generated by the model. As wind data was unavailable it is difficult to draw any conclusions but local sea-state will certainly have an affect on incoming open-ocean swell.

A closer agreement was evident at both Shinnecock Inlet sites with a smaller rmse and for A1 a lower SI. The results would probably have been even stronger if not for what appeared to be an upper limit on maximum wave heights. Heights were under predicted throughout and held below 1.5 meters. Perhaps there was a seasonal shift in the local bathymetry not reflected in my bathymetric grid that could account for this type of discrepancy. As the Shinnecock sites were both in the Shinnecock inlet, local dynamics could be a strong influence on both real-world and modeled wave conditions. More specifically, local variability in the ebb shoal would be unaccounted for within the bathymetry and have an acute effect on altering nearshore waves. If my grid was from data collected at a time of a strong ebb shoal extending across the inlet mouth wave breaking and energy dissipation would have the effect of diminishing modeled wave heights, but, if no such shoal was present at the time the instruments were functioning this type of sheltering effect would not be impacting waves at the inlet. While the grid certainly seemed sufficient for the majority of the wave transformations, it is possible that this dynamic trait of the study region has an unexpected affect on the outcome of the model.

Conclusions

SWAN can be considered an accurate predictor of wave transformation due to influences in wind energy, refraction, and energy dissipation due to whitecapping, bottom friction, depth-induced breaking, and nonlinear wave-wave interactions (Booij et al, 1999) that has been verified for a variety of conditions. Though some discrepancies between observed and modeled conditions (usually only in magnitude) exist, the action balance equation terms can be modified to suit specific regions. It is reasonable then to assume that, with the results of this preliminary trial, SWAN could be successfully implemented as a predictor of wave transformations along the south shore of Long Island and utilized as a warning system for hazardous conditions, including enhanced beach erosion, rip current frequency, and wave induced flooding. This may take coordinating with a meteorological institute for accurate winds, though in prior communication with such bodies the grid resolution is generally poor (12 km). A grid no coarser then one km would be more fitting this study.

The overall reliability of SWAN seems (expectedly) sensitive to local forcing factors that vary on time scales beyond that which we can accurately update them based on funding and existing instrumentation or modeling efforts (i.e. bathymetry, currents, winds). As part of a related study, SWAN performed comparatively with another steady-state nearshore wave model, STwave (Steady state spectral wave); each model had time periods in which they were better suited (Figure 4, Buonaiuto et al., 2008 accepted with

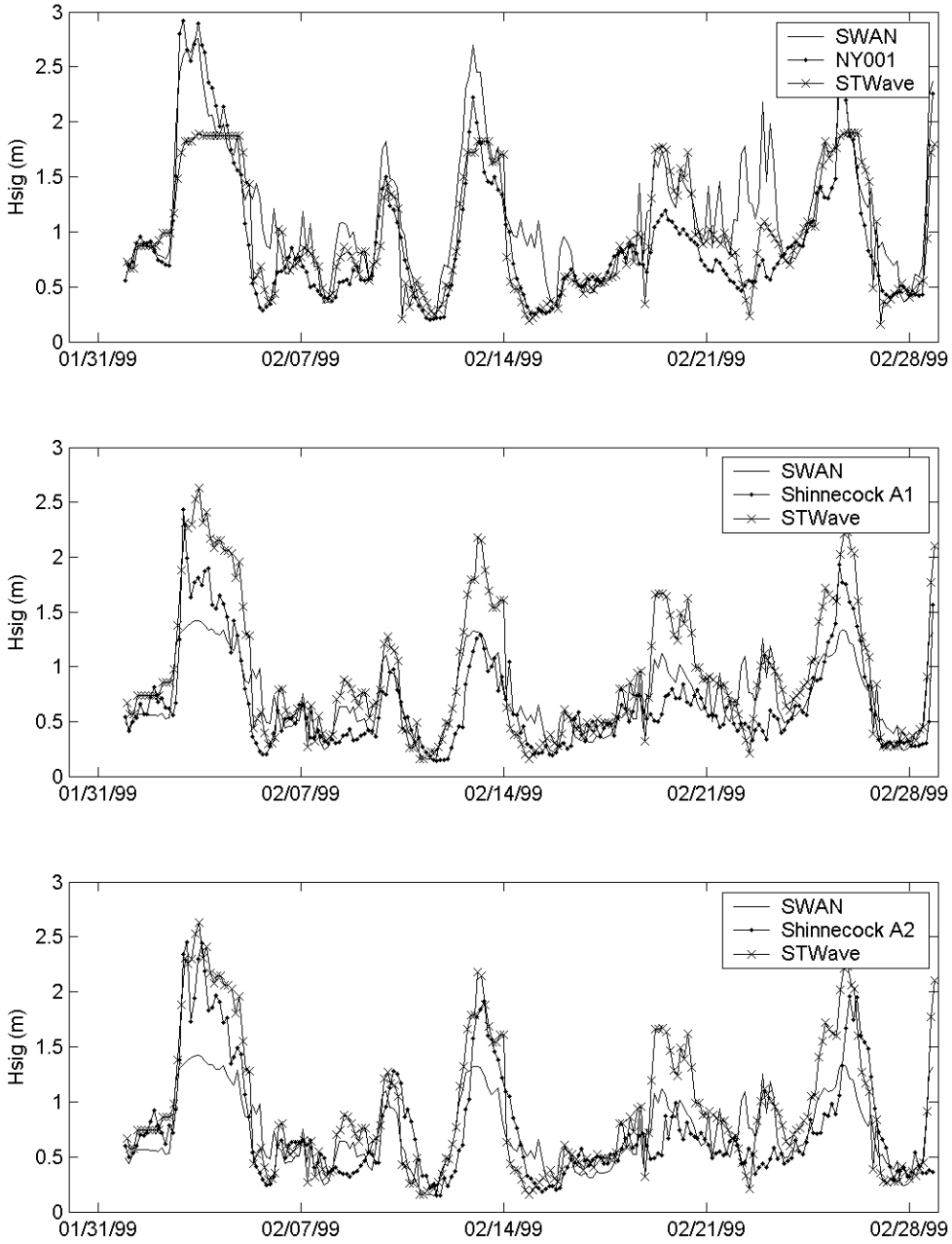

Figure 4. SWAN results compared to STWave, another typically used nearshore wave model. SWAN and STWave each had strong and week points depending on the location (From Buonaiuto et al., submitted)

revisions). In the case of Westhampton Beach, without the possible interference from local bathymetric changes related to ebb tidal shoals (as is the case at Shinnecock) SWAN better described peak wave conditions, while at the two Shinnecock sites SWAN seemed to hit a maximum threshold around 1.5 meters. This is most likely related to the nearshore bathymetric patterns that could have been in the model from the ebb tidal delta causing energy loss and early breaking over the shoals, whereas STwave seemed less affected by this possible early break. Rogers et al. (2002) first identified the consistent under prediction of low frequency wave energy off Duck, NC. A subsequent study by Rogers et al. (2003) sought to resolve these issues by: "1) by altering the weighting of the relative wave number term that exists in the whitecapping formulation and 2) by disallowing the breaking of swell." These modifications seemed to work when applied to the Sandy Duck, NC data as well in two other test cases.

In all, strong support remains from this research to the validity of the SWAN model for accurately depicting complex nearshore wave transformations. As can be expected the accuracy of the output seems dependent on the quality of the input parameters and with better data sets from which to draw model accuracy would be expected to be greatly enhanced. While frequent nearshore bathymetric surveys would certainly help elucidate fine scale nearshore wave transformations around structures and inlets; a reliable source of extensive wind conditions both offshore and nearshore would be, in my opinion, the best possible source of increased applicability.

References

Booij, N, R.C. Ris, L.H. Holthuijsen. 1999. A third-generation wave model for coastal regions 1. Model description and validation. Journal of Geophysical Research, 104(C4): 7649-7666.

Buonaiuto, F.S. M.P. Slattery, H.J. Bokuniewicz. Wave Modeling of Long Island Coastal Waters. Journal of Coastal Research, *Accepted with revisions, August 2008*.

Davis, R.E., R. Dolan. 1993. Nor'easters. American scientist, 81: 428-439.

Jin, Kang-Ren, Zhen-Gang Ji. 2001. Calibration and verification of the spectral wind-wave model for Lake Okeechobee. Ocean Engineering, 28: 571-584.

Palmsten, M.L. 2001. Application of the SWAN wave model to a high-energy continental shelf. MA thesis University of South Florida, 135 pp.

Ris, R.C., L.H. Holthuijsen, N. Booij. 1999. A third-generation wave model for coastal regions 2. Verification. Journal of Geophysical Research, 104(C4): 7667-7681.

Rogers, W.E., J.M. Kaihatu, H.A.H. Petit, N. Booij, L.H. Holthuijsen. 2002. Diffusion reduction in an arbitrary scale third generation wind wave model. Ocean Engineering, 29: 1357-1390.

Rogers, W.E., P.A. Hwang, D.W. Wang. 2003. Investigation of wave growth and decay in the SWAN model: three regional-scale applications. Journal of Physical Oceanography, 33: 366-389

Chapter 3: Seismic signature of surf

Introduction

Several studies have been used to determine wave traits via transmission of energy from the breaking of waves in coastal ocean, (Deane, 2000a; Deane, 2000b) but standing on the beach, vibrations from strong surf pounding can also often be felt through the sand itself. Indeed, even far from shore reports of feeling vibrations caused by waves are not uncommon in a number of coastal settings. In an extreme cases, people in Salerno, Italy, for example, report feeling buildings vibrate when there are storm waves affecting nearby coastal regions (E.P.E. Pugliese Carratelli 2007, University Consortium for Research on Great Hazards, personal communication), as do residents of the California coast. During some strong storm events residents of condominiums in Solana Beach, CA experience the shaking of their walls at regular intervals associated with surf action on the nearby cliffs (Benumof and Griggs, 1999). Phenomenologically, the vibrations should be associated with traits of the nearshore breaking waves.

Long term data, detailing characteristics of nearshore wave attack are required to accurately evaluate, interpret and forecast of coastal processes that respond to wave energy. Shorter study durations may not fully address underlying processes that act on time scales greater then incident wave periods or give poor temporal coverage; these underlying processes may display long-term trends that impact the ultimate outcome of nearshore dynamics. Wave monitoring projects, however, must not only bear the initial cost of instrumentation, but also that of maintaining sophisticated instruments in a high-

energy hostile environment that periodically can be directly impacted by severe climatological events. Routine, direct measurement of near shore waves poses an array of problems leading to their fairly infrequent implementation. Such studies are riddled with comments like "sensor failed" and "intermittent data only". Despite the obvious importance of these wave traits and their impacts on beach erosion, rip currents and coastal flooding associated with storm waves and surge the Long Island south shore currently has no active wave monitoring instruments (Tanski et al., 1990). Previous wave instrumentation from the LIShores study and the Army Corps of Engineers coastal hydraulics lab were removed shortly into the new millennium, leaving almost the entire south shore of Long Island unmonitored. As a result the nearest indicators of wave conditions are from NOAA buoys 44025, 42 km offshore and 44017, 36 km offshore.

An alternative to these surf-zone deployed sensor arrays may exist in the form of land-based seismic systems. These seismic devices should be able to be implemented in providing long-term, continuous data with a fine temporal resolution on wave conditions from a secure, easily accessible site. Seismic systems are relatively inexpensive when compared to in-situ devices, very reliable, and capable of real-time electronic transmission of data. Although such a system would provide information only on wave energy and, indirectly, wave height, the disadvantages are offset by the reliability and ease of maintenance of this method for routine monitoring. This type of instrumentation is especially feasible along coastal systems with a high density of beach homes, commercial buildings, or hotels/resorts as the monitoring system requires little room and can easily be tucked out of the way at ground level. Adding further data security, these

systems can use direct power (via converters) instead of batteries, better insuring uninterrupted data streams (Figure 1). The real difficulty is interpreting the data.

For those studying the earth's crust and more specifically earthquakes; their records have long been contaminated by noise, termed microseisms, most of which stems from energy carried in ocean waves (Webb, 1998). Below 0.03 Hz the signals seem to be related to surf zone eddies (SZE) with average periodicity of 13 minutes or more (MacMahan et al., 2004). Shubert and Bokuniewicz (1991) noticed energy near an inlet on Long Island's south shore that fell into the same frequency bands at a period of around 1000 seconds. The small band of energy between 0.003 and 0.05 Hz covers infragravity energy associated with surf beat and bound infragravity energy that has been released from breaking incident waves, subsequently the wave can reflect back to the open ocean as a free wave (Ruessink, 1998; Longuet-Higgins and Stewart, 1964; Oliver and Ewing, 1957). More broadly, the entire energy signal from 0.05 -1 Hz is traced back to ocean swell (Tindle and Murphy, 1999). There are two types of wave-generated microseisms—those that have the same frequency as the ocean waves that cause them, and those that have double the frequency of the ocean waves (Bromirski and Dunnebier, 2002). The microseism with the same frequency as the ocean waves are referred to as primary microseisms (Darbyshire and Okeke, 1969).

Breaking waves were recognized early on as a source of primary microseisms (Wiechert 1904 as cited in Howell, 1990). The strength of this source depends on the width of the surf zone (Darbyshire and Okeke, 1969). It has long been known that the longer wavelength, longer period waves, contribute substantially to the strength of the

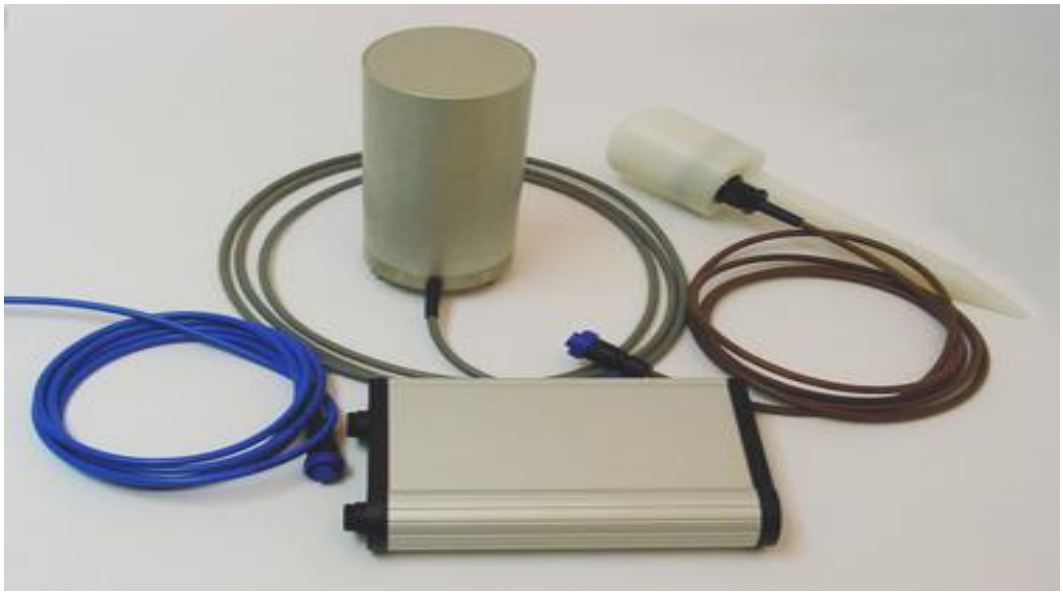

Figure 1. Typical seismometer set-up for study locations consisting of the seismometer cylinder, GPS receiver and controller box.

seismic signal (e.g. Oliver and Ewing, 1957). As water waves move into shallower water near shore, the energy is redistributed, in part, to longer period of the spectrum (Kinsman, 1965); these longer period waves should be expected to be more prominent in the microseism spectra (Hasselmann, 1963). Infragravity waves may be amplified by resonance in shallow water between the beach and the bar to produce edge waves implicated in the formation of rip currents. Ground motions are generated by local, breaking waves although the effect is usually undetected by seismic stations further than a kilometer from the shore (Tabulevich 1992; Webb, 1998; Hirsh, 2004). Sand is not a strong, natural conductor of acoustic signals; however, a seismic source can be detected after transmission through sand at close range. The seismic signal of the surf can be detected on seismometers within a few hundred meters of the shore on a sandy coast. Ship wakes and wind-waves, for example, produced measurable seismic signals at frequencies between 0.5 and 150 Hertz in dikes along the Elbe estuary (Schüttrumpt, 2006).

Another type of microseism, which is more far-reaching, is generated by standing, sea waves or other long period waves (Tabulevich, 1992). These microseisms occur at twice the frequency, half the period, of the generating water-waves and is created by reflected waves interacting with incoming wave fields (Darbyshire and Okeke, 1969). Standing waves can be produced in open water by the interaction of two, similar wave trains or by the reflection of waves off the shore, including edge waves. Large storms, remote from any particular seismic station, can produce detectable microseisms. Seismic signals were detected in New Mexico from the "Perfect Storm" off the Massachusetts coast in 1992 **(**Bromirski, 2001**)** and microseism caused by Hurricane Katrina in the

Gulf of Mexico in 2005 were detected at sites as far away as California (Gerstoft et al., 2006). Such a signal can be used to estimate wave climate (Beach and Sternberg, 1988).

Closer to the coast, direct reflection of infragravity waves, with frequencies between 0.003 and 0.05 Hz, at the shoreline can result in standing waves. These should appear as seismic energy at half the water wave period of the waves which generate them (Longuet-Higgins and Stewart, 1964). Shoaling water-wave energy dissipated along sea cliffs in California, possibly due to standing waves set up by the reflections of incident waves at the shoreline, have been detected on seismometers on the tableland (Adams et al., 2002). Similar experience is reported along the south coast of the United Kingdom (A. Brampton 2007, HR Wallingford Ltd. Personal communication). In addition, infragravity waves approaching the coast obliquely may produce standing edge waves along the coast, perhaps by reflection from shore-perpendicular structures in the surf zone. At alternating antinodes of the edge wave, rip currents may be formed (Bowman and Inman, 1969; Aagaard et. al., 1997).

The goal of this project portion is to effectively implement a coastal monitoring station. As part of the monitoring, a seismometer will be used to address the ability of seismic systems to measure vibrations from coastal energy. This energy should reflect an array of processes including incident wave energy and period, infragravity energy from surf beat, and infragravity energy from along or across shore directed waves.

Study Area

Initial coastal measurements were made at the same location as a camera system for rip current monitoring along the ocean shoreline in the Village of East Hampton, NY (Figure 2). The beach here faces south-southeast and our study is located approximately 1000 m east of the first in a series of four groins extending 100 meters out from the dune and 23 m into the surf zone. There is also one (barely exposed) groin 1700 meters to the east of the site. The beach width varies with season and tide but the range is generally between 30 and 60 meters, which could have an impact on the relative strength of the signal, but should not affect the accuracy of determining periodicities. A dune, approximately 25 meters wide and six meters high, separates the beach from the home in which the instrumentation is deployed on the slab floor of the basement.

Dominant wind direction for the south shore of Long Island is generally westerly, becoming predominately southwesterly in summer and northwesterly in winter (Kana, 1995). Easterly winds occur approximately 15% of the time (Baker Engineering, 1998). Average incident significant wave heights are approximately one meter with seven second periods, usually from the southeast; maximum wave heights of between 3 and 3.5 m, nearshore, 12 to 14 second periods have been observed during storm conditions (Buonaiuto, 2003). Like most south shore beaches the area undergoes annual winter erosion, though it generally recovers sand during the spring and summer. Beach erosion is generally related to storm conditions, specifically winter nor'easters, and long-period swell from Atlantic hurricanes and not in response to gradual sea-level rise.

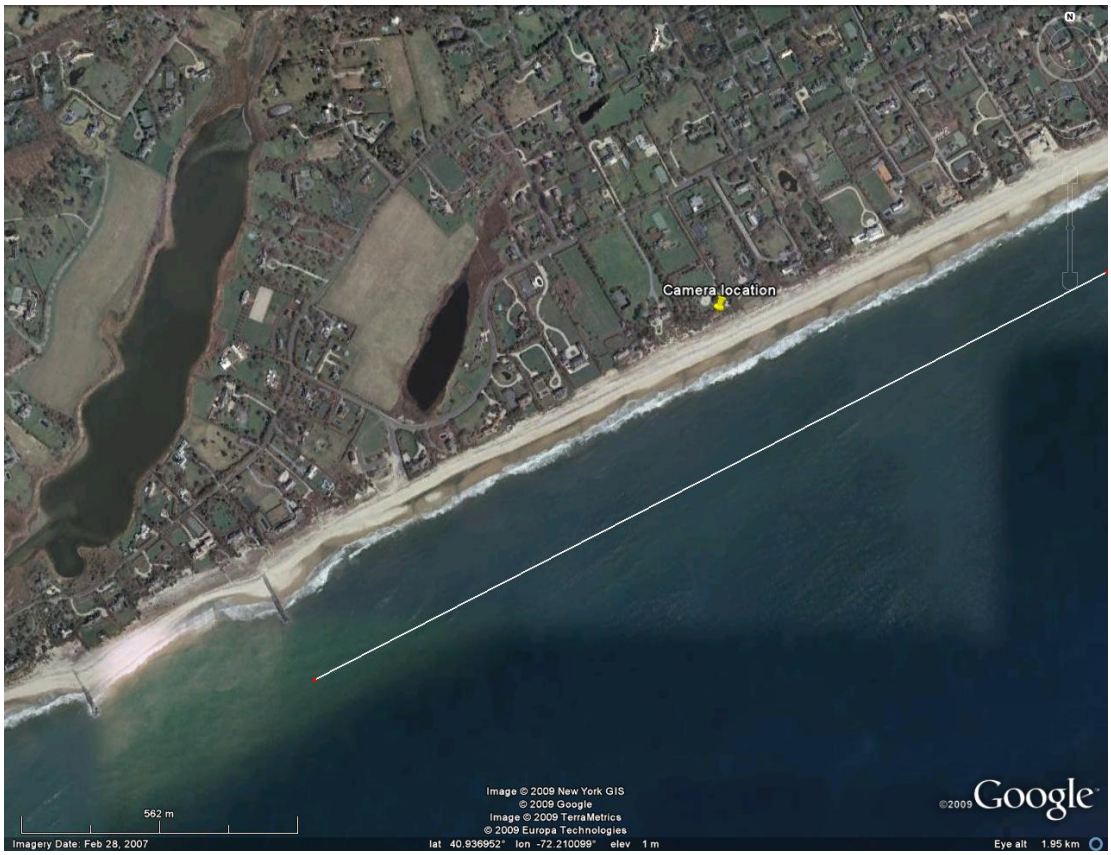

Figure 2. The study location located in East Hampton, NY. The seismometer is deployed in the basement of the private residence described in Chapter 1.

Methods

Measurements were made with Guralp systems CMG-EDU-V Digital Output Broadband Seismometer (equip with a CMG-EDU-V Processor box, and a time-code GPS receiver unit) and initial observations were made using filtering available with Guralp systems SCREAM! 4.3 software. The seismometer had previously been tested in four transects (along Further Lane, Beach Lane, Indian Wells Road and Atlantic Avenue in East Hampton, NY), at distances up to 0.38 km from the shore to record signals (J. Hirsch 2005, Stony Brook University, personal communication).

Tests were done in a transect using the seismometer at increasing distances from the shore to examine points at which a usable signal could be recorded, and to try and establish if the signal strength changed with distance from its, presumed, source in the surf zone. The preliminary observations at increasing distance from the shore showed that the signal amplitude was reduced by one-half at a distance of about 0.4 km though the instrument had to be located on the surface of any hard surfaces available like porches, sidewalks and driveways instead of being located subsurface. While the medium through which these waves travel can have an impact on their speed, no sources alluded to possible impacts dry versus wet sediment may have on the signal integrity (Hirsch, 2005; Bromirski and Dunnubier, 2002; Webb, 1998). Bromirski et al., 1999 did specify that attenuation can be dependent upon geologic make up and distance from the seismic source, but the sediment through which the signal propagates is assumed stable over time. No large scale alterations is sediment composition could be expected. The distance from

the source might vary slightly with tides (small tidal range and steep beaches should make this a non-issue) and wave height; each contributing to very subtle changes in distance between the breaking waves and the seismometer.

An initial trial of placing the device on the dune atop a post driven to the top of a revetment met with little success. Instead a permanent station was established in the basement of the residence within 60 m of the shoreline. A seismometer from Stony Brook University was used to determine if any differences or similarities existed between the periodicities measured at each location. Stony Brook is on the north shore and should not produce spectral peaks coincident with incident wave period on the south shore of Long Island.

The East Hampton seismometer records data twenty times every second resulting in 72000 points for the hourly output files. Spectral plots were created from ten-hour groups of records from each location for cross-spectral analysis. The Stony Brook seismometer records 100 samples/second and had to be averaged down to the same sampling rate of the East Hampton location (20 samples/second). Via this method, a comparison between the two sites, in terms of spectra peaks, was completed. For a short time (April 2009-February 2010) a second seismometer was placed further west in East Hampton, NY at the Maidstone club (Figure 3) to get a better idea of the accuracy of energy measured along this small region of the coast. Spectral plots of each location, too, were compared for similarities. This, second, East Hampton seismometer had a default sampling rate of 40 samples/sec and was sub sampled to the rate of the initial seismometer station.

Time periods to be analyzed were chosen initially based on offshore wave conditions gathered from the U.S. Department of Commerce National Oceanic and Atmospheric Administration (NOAA), National Weather Service, National Data Buoy Center, Station 44017, Long Island 23 NM Southwest of Montauk, NY (Figure 4). Buoy 44017 is a three-meter discus buoy with an ARES payload at 40.7 N; 72.1 W. Wave heights during the entire period of record ranged from less than 0.5 meters to greater than 3.0 meters. Later, time periods to be examined were chosen based on the occurrence of rip currents to determine the existence of power in the infragravity periods coincident with the presence of rips and on the availability of a second station for better ground-truthing. As I am looking at spectral signals for dominant periodicities and not looking directly at energy transmission over long time periods, any minor changes in attenuation due to slight distance variability with tides and wave height should not affect the outcome of this study.

Results

Two examples of the seismic record are shown in Figure 5. During the time period when the wave heights were near maximum values for this area (3.16 meters) there was a strong spectral signal below 0.25 Hz (associated with energy carried >4 second periodicities). However, during the time period when the wave heights were quite small (0.49 meters) the signal was comparably weak. Initial comparison between the

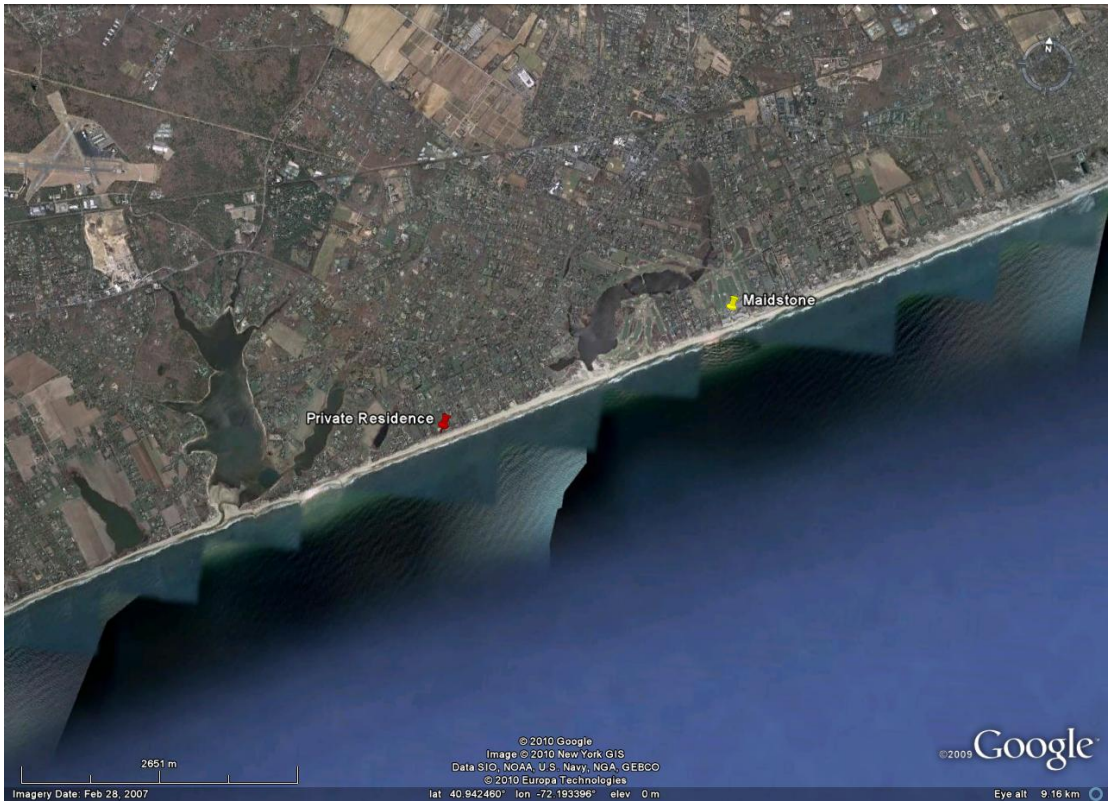

Figure 3. Location and proximity of two seismic stations at the private residence and the Maidstone Club in East Hampton, NY

Figure 4. Location of seismic stations with reference to NOAA's offshore buoy 44017.

root-mean-square (RMS) of the raw seismic signal and wave height squared showed a positive correlation with a linear correlation coefficient, r, of 0.92, that is, $r^2 = 0.85$ (Figure 6). Although this regression is site specific and instrument specific, such a correlation might still prove useful in monitoring wave attack at this location.

Earthquakes, such as the magnitude 6.7 Guatemalan earthquake on June 13, 2007, were detected by the seismometer at East Hampton as well as by the seismometer at Stony Brook University showing commonality for large energy events at distance (Figure 7). However, distinct differences of recorded energy became apparent for time periods without a dominant forcing source, in this case, when waves were over 3 meters, the seismic spectrums obtained at East Hampton showed a focus of energy in a broad band, especially at the incident water wave period of 4 seconds (Figure 8). This surf-related, seismic signature was sensitive to the incident wave height, decreasing by orders of magnitude in the band of incident, water-wave periods as the wave height decreased from 3.3 m to 0.5 m. This resulted in a non-linear relationship between the spectral power and the square of the water=wave height (shown as an exponential in Figure 9).

Further evaluation of the East Hampton seismic station came in the form of direct comparisons to the station established at the Maidstone club. Seismic records from both demonstrated the presence of spectral peaks at a range of frequencies, but in almost every case the two spectra were visually similar (Figure 10). Most peaks fell between 0.33 Hz (3s)-0.067 Hz(15s) and less then 0.05 Hz (>20s). Seventeen peaks were seen in the spectrum at the original site while twelve were evident from the Maidstone (Table 1). Nine of the peaks were common (within 10% of the value) to both locations for the same record. July showed no common peaks, while August 20th and 22nd had three each,

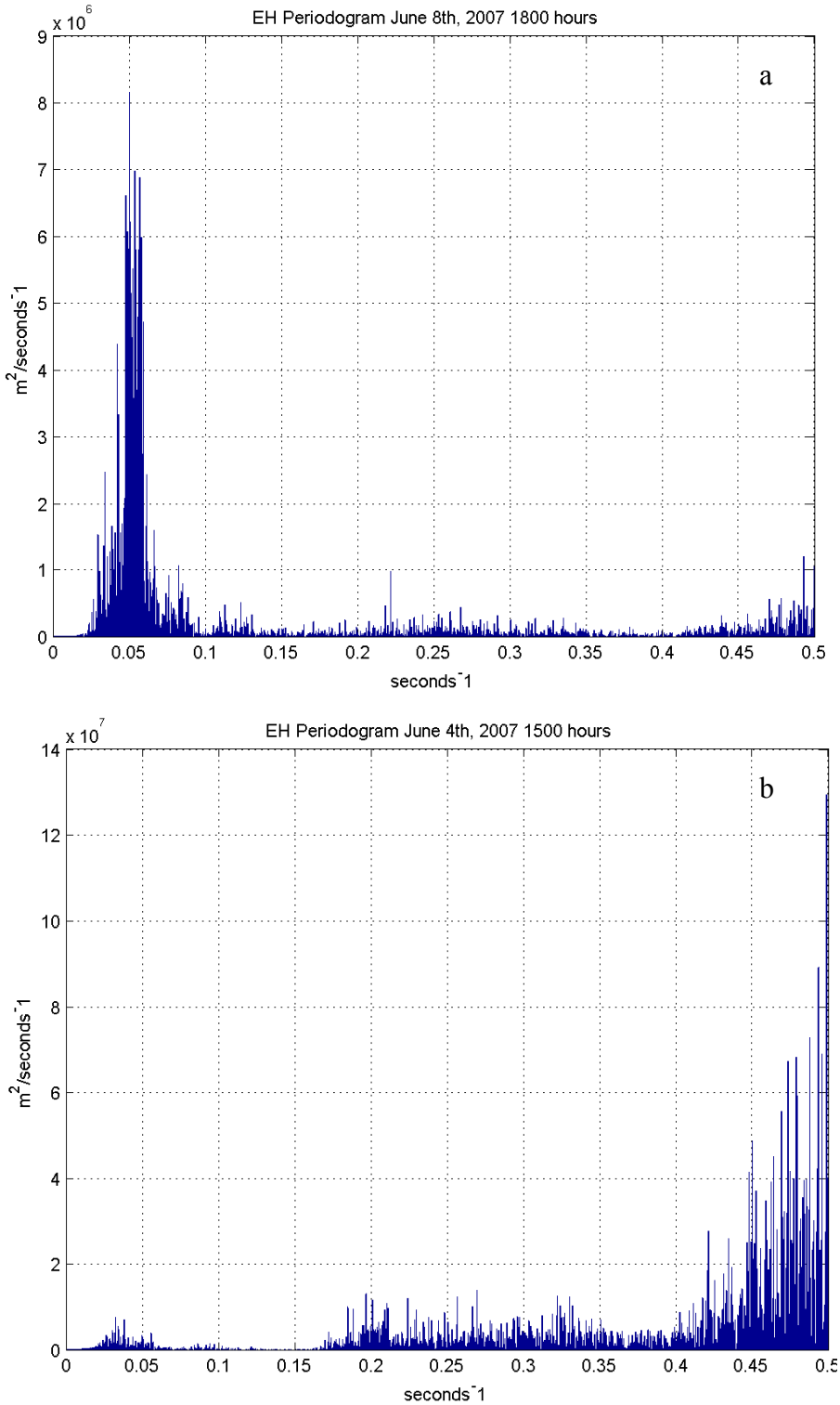

Figure 5. Periodogram of the seismic signal on a small wave day (a) and a large wave day (b). Note the scale, showing much greater energy during a large wave day.

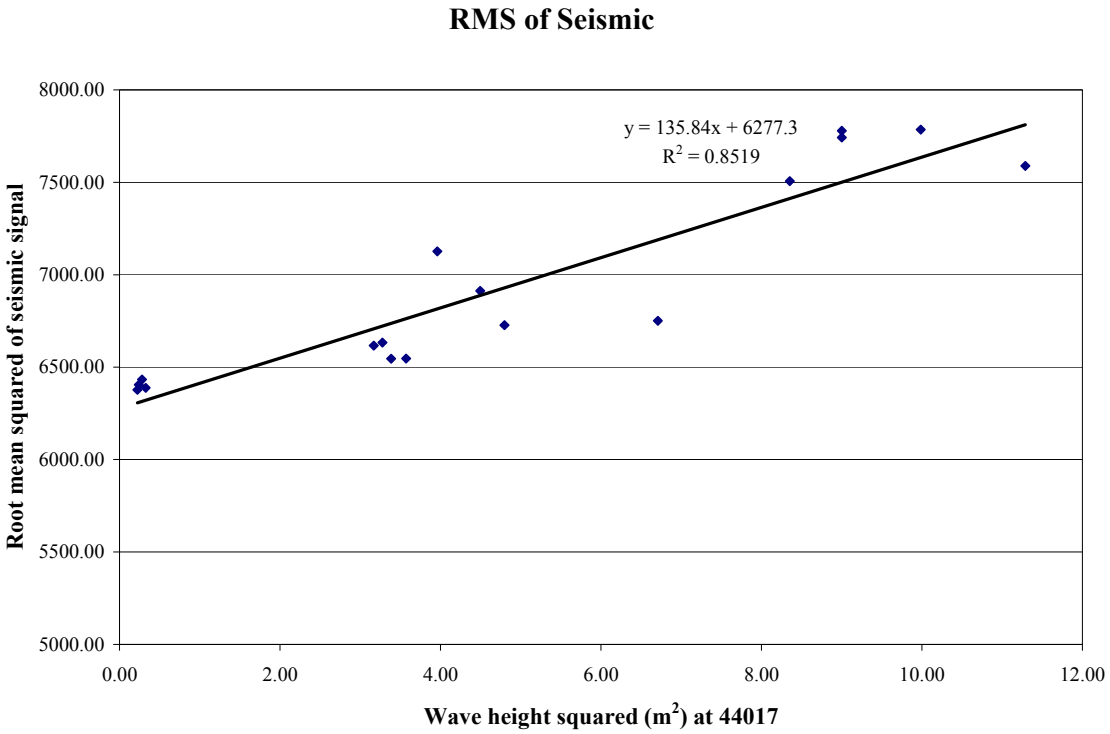

Figure 6. RMS of the raw seismic signal plotted against the incident wave height squared. R^2 value of 0.85 shows correlation between the two.

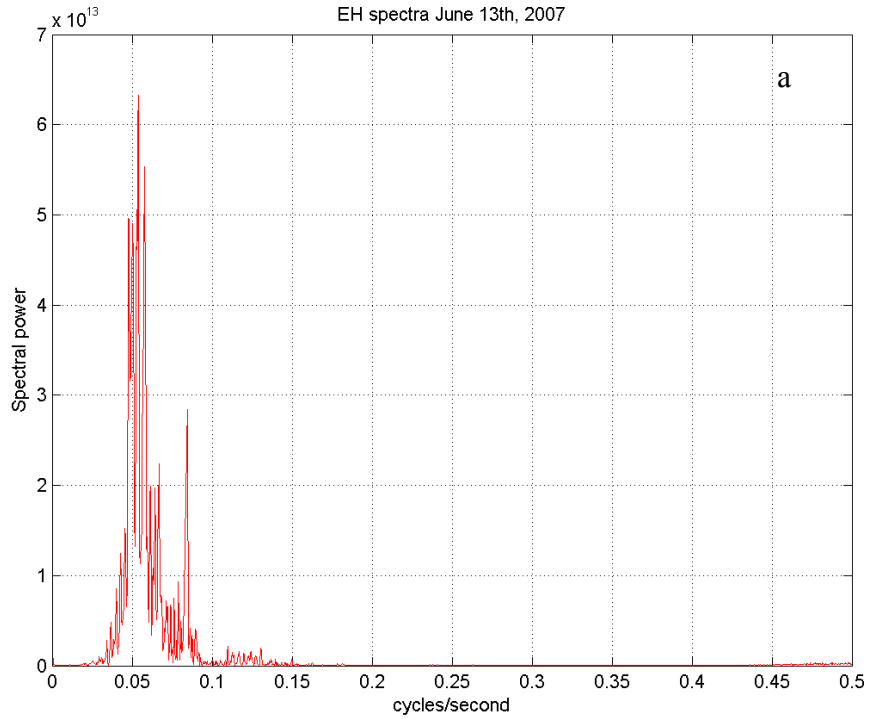
EH spectra June 13th, 2007
x 10^13
Spectral power
cycles/second
a

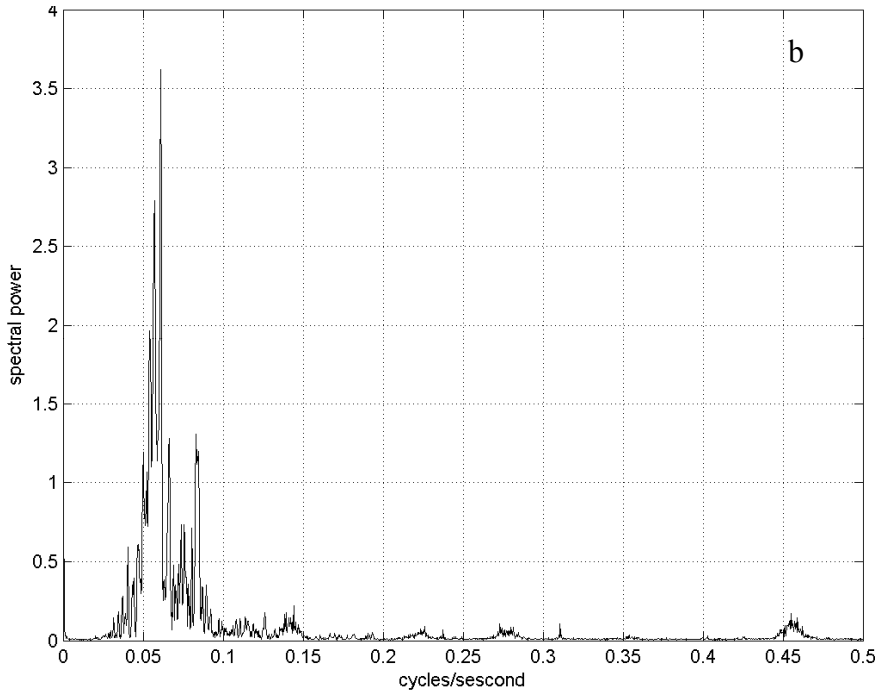
spectral power
cycles/sescond
b

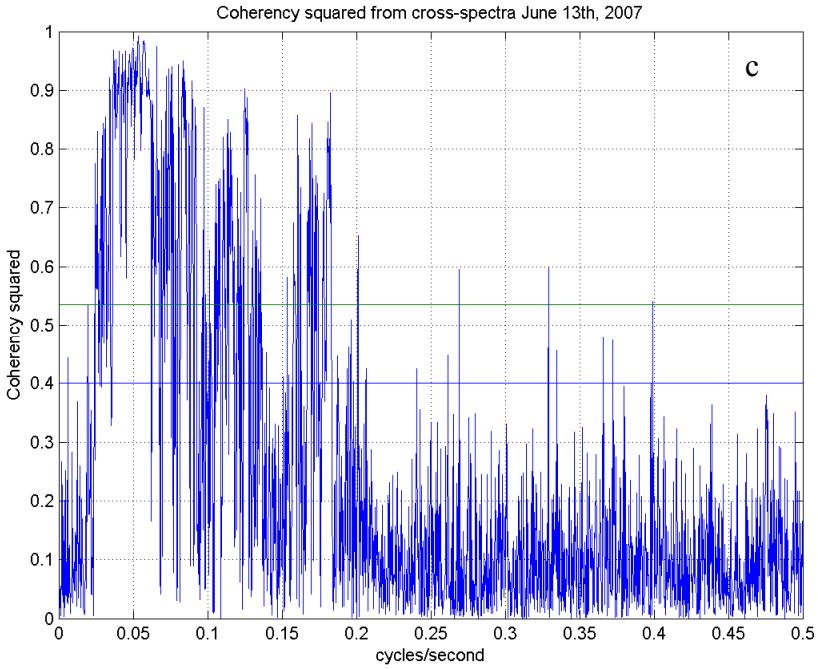

Figure 7. Spectral similarity between East Hampton (a) and Stony Brook (b) when dominated by a single event (earthquake). Evidenced in cross-spectral plot (c).

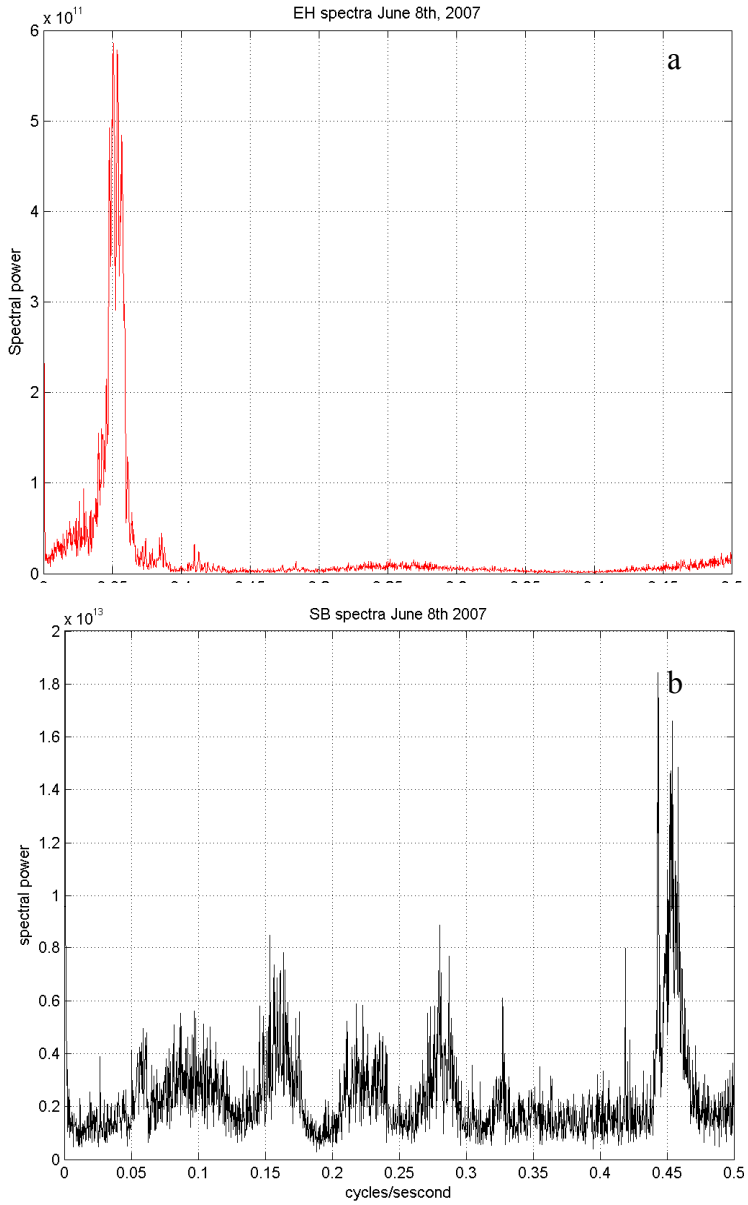

Figure 8. For this period of time the average wave period at East Hampton (a) was around 4 seconds which, despite a long period dominant signal, corresponds to the increase in power around 0.25. No such peak is seen in the Stony Brook (b) site.

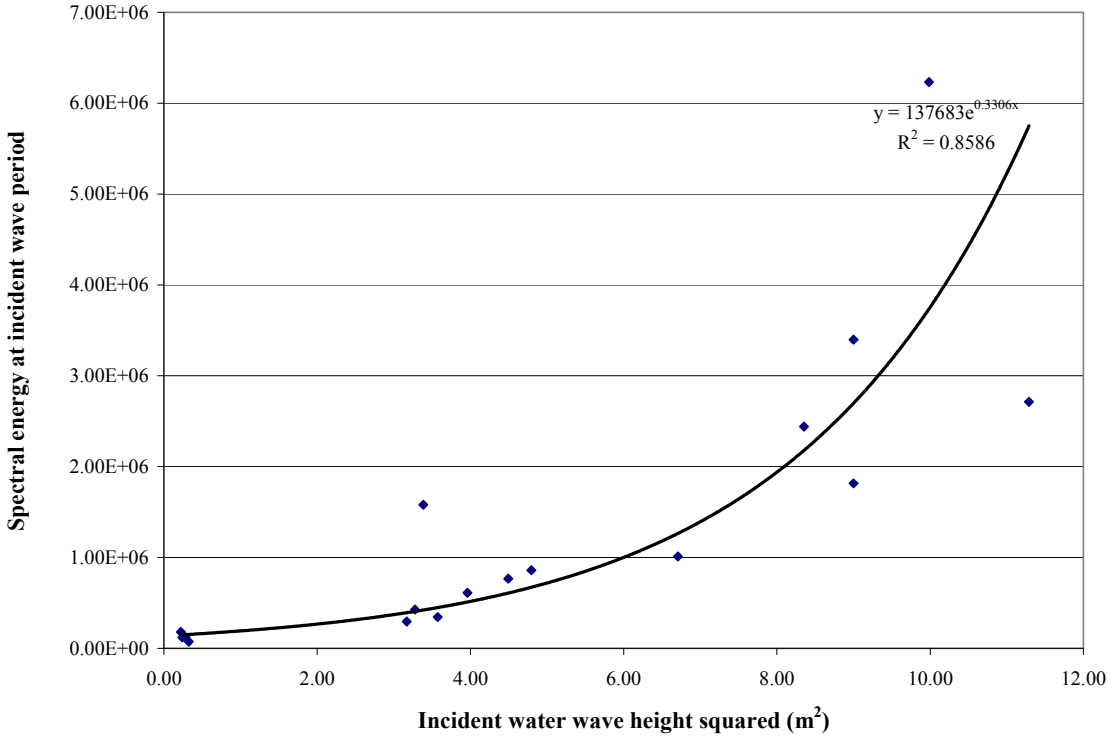

Figure 9. Spectral power at the incident water waves period against the wave height squared with an exponential fit.

October 2nd had two and October 6th had one. When viewed with respect to the measured wave periods at NOAA buoy 44017; a corresponding period was observed in the spectra all days for the private residence, while all but one day from the Maidstone seemed to be concurrent (Table 1). On two occasions the periods varied by more then 10% of the measured offshore periods for both study locations while spectra peaks were all but nonexistent for one day (October 6th) at the Maidstone.

The lack of common spectral peaks was almost exclusively confined to longer wave periods, while peaks at periods connected to reasonable incident wave periodicities showed good agreement. Other spectral peaks at longer periodicities (i.e. the range from 13-24 seconds on August 20th) could be a result of regional infragravity waves, perhaps an edge wave (at 26-50 seconds period). While shorter period peaks may result from differential wave breaking in choppy water conditions.

Discussion

The results give evidence to the effectiveness of a land based seismic station as a tool for monitoring nearshore wave activity. The continued implementation of this type of monitoring can be both inexpensive and easy to manage as deployment and retrieval become a trivial part of the study instead of, as is some times the case with subaqueous sensor arrays, a main focus.

The first test was of our instrumentation itself, but by showing a similar signal to Stony Brook University during a common forcing event (the Guatemalan earthquake) it would seem that the sensor was working properly. The next step was to show poor

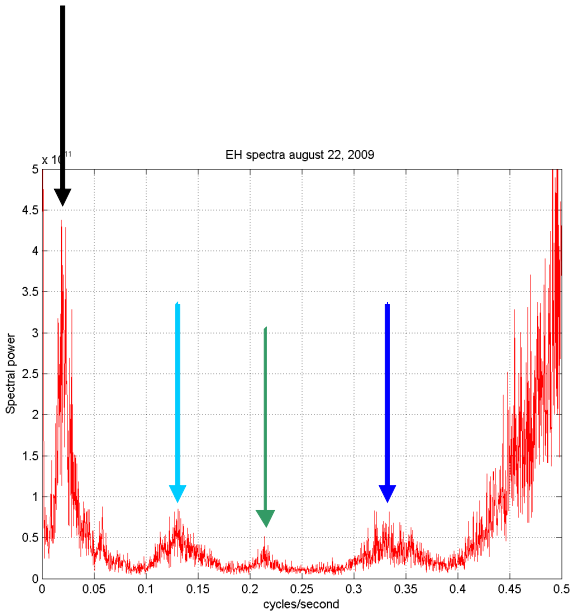
EH spectra august 22, 2009
Spectral power
cycles/second

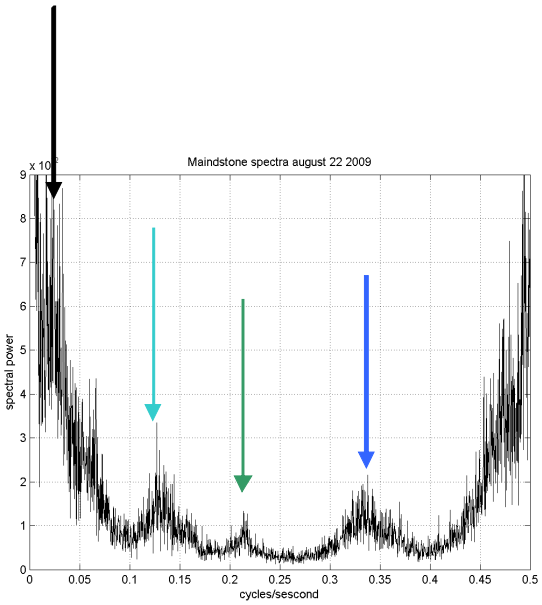
Maindstone spectra august 22 2009
spectral power
cycles/sescond

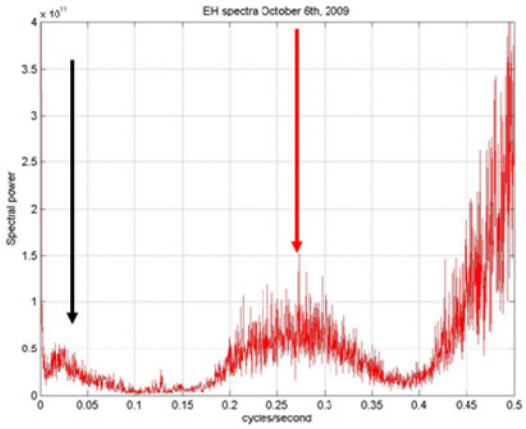
EH spectra October 6th, 2009
Spectral power
cycles/second

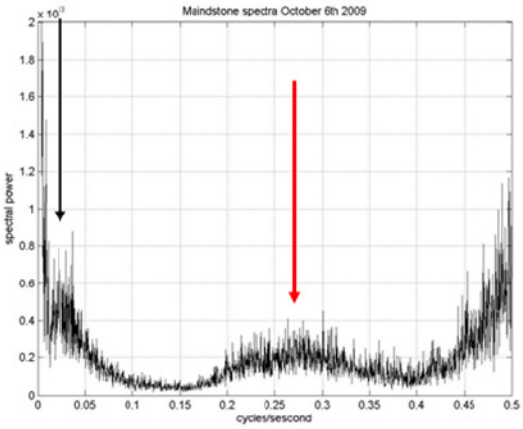
Maindstone spectra October 6th 2009
spectral power
cycles/sescond

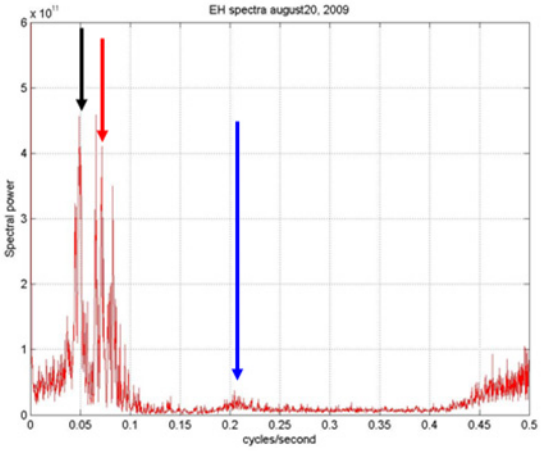
EH spectra august20, 2009
Spectral power
cycles/second

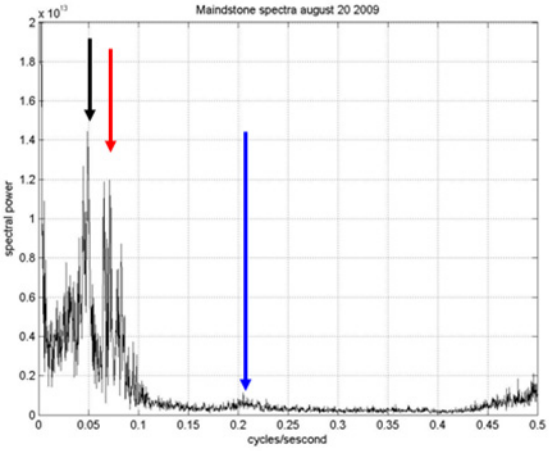
Maindstone spectra august 20 2009
spectral power
cycles/sescond

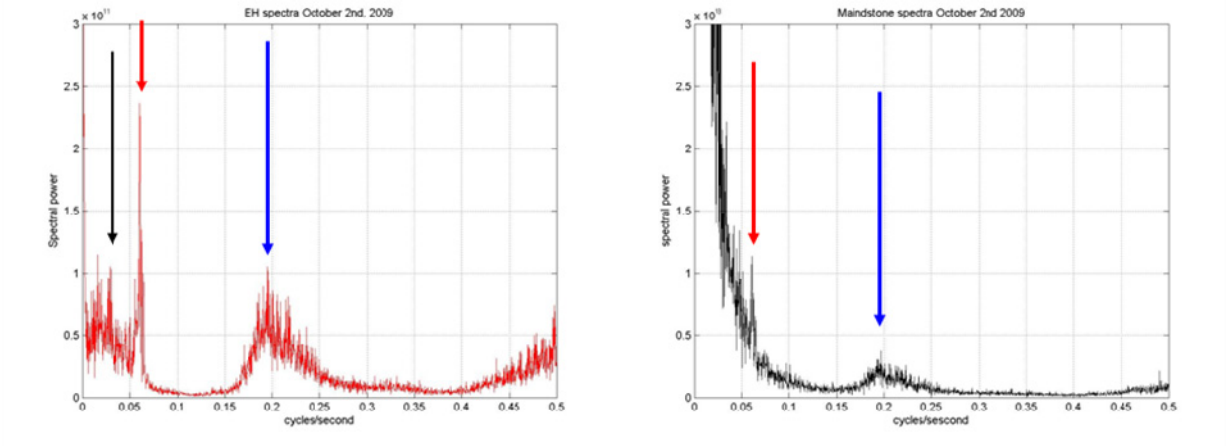

Figure 10. Spectra from East Hampton (left in red) and the Maidstone club (right in black). Note that each looks similar, visually, except for the final comparison. Common spectral peaks are noted in coordinating colored arrows between spectral pairings.

Table 1. Summary of spectral peaks from private residence and Maidstone club, and wave periodicity measured at buoy 44017.

Date	Period Private Residence	Period Maidstone	Average period 44017
July 17th	17.04	34.48	
	4.65		4.529
	8.33		
	3.03		
August 20th	4.878	4.878	4.806
	20.32	24.45	
	15.15	15.15	
	12.06		
	13.96	13.96	
Augusts 22nd	50		
	7.69	7.69	6.54
	4.65	4.65	
	3.01	2.99	
October 2nd	5.13	4.69	4.02
	16.53	16.67	
		8	
October 6th	40		
	3.68	3.57	3.852

agreement between the spectra at Stony Brook and East Hampton supportive of a difference in localized environmental forcing. Stony Brook University should be far enough away from the south shore that wave energy from breaking waves would go undetected though its proximity to the sound may not completely preclude the appearance of an ocean signal, and simply by chance may occasionally demonstrate swell periodicities from locally generated waves. The poor agreement between the two spectra during periods of increasing wave activity would support these conclusions. Of course this project had the added strength of deploying a second seismometer at a proximal alongshore site also on a slab floor to try and better access the signals at the south shore.

Cultural noise falls, generally, at a much higher frequency of 5 Hz owing mainly to the vibrations caused by machines (Webb, 1998). While we've seen that remote, large scale phenomenon can appear at distal sites (the Guatemalan earthquake); no environmental noise should dominate at frequencies commonly associated with incident wave periodicities 4-13 seconds. The seemingly poor relationship between energy at longer periodicities between the two site locations represents a discrepancy between infragravity (possible edge wave) modes between the private residence and the Maidstone Club. This would be expected as no groins are located adjacent to the Maidstone and any edge waves trapped would, by default, be progressive edge waves. Progressive edge waves may not be as readily describable with our instrumentation as it's a point reading. The presence of the groins would also isolate the East Hampton residence from the Maidstone for a continuous alongshore wave. This is especially true if the bound wave happened to resonate such that a node was coincident with the groin location (Komar, 1998). An offshore bar has been documented at a distance of 220 m

from shore (Figure 2). At the site near Georgica Beach a groin and associated headland is found about 1000 m east from the seismograph (Bokuniewicz, 2004). If the groin is taken as a structure reflecting longshore components of infragravity waves down a potentially resonant channel formed by the bar, then a resonant period of trapped edge waves can be calculated.

At East Hampton, at least, infragravity waves in the surf zone conceivably could generate standing edge waves. The groins at Georgica Pond may act as a reflective barrier to alongshore propagation, as described by Baquerizo et al. (2002), setting up a standing edge wave along the coast. Across shore component of infragravity waves reflected off the beach might be bound by the offshore bar (Bowman and Guza, 1978). If these conditions are, in fact, realized, standing, resonant edge waves might form.

In principle, the wave length of the edge wave might be:

$$L_e = \frac{gT_e^2}{2\pi}\sin\left[(2n+1)\beta\right] \quad (1)$$

Where T_e is the edge-wave period, g is the acceleration due to gravity, n is the modal number and β is the slope of the beach (Ursell, 1952 as cited by Komar, 1998). At the dominant mode the edge-wave period is expected to be twice the period of the incident wave (T_i) and the mode n=0 so equation (1) gives insight into beach cusp spacing as well and becomes:

$$L_e = \frac{g2T_i^2}{\pi}\sin(\beta) \quad (2)$$

Near the East Hampton study site, the beach slope is between 2.93 and 1.41 (Station P 42, ACNYMP); if the incident wave period is six seconds, the edge-wave wavelength would be 225 m.

The wavelength of an edge wave is twice the distance between the reflecting headlands (groins) divided by its mode number. The groins at Georgica Pond are 2.74 km from those at Hook Pond to the east, giving a hypothetical edge wave wavelength of 5.48 km for the first mode and 1.37 km for the fourth mode.

The offshore morphology, in this area (profile P42, ACNYMP) has the bar at a distance (L) of 221 m and the average water depth (h) between the bar and the shore at about 3.7m. The resonant period of $\frac{2L}{\sqrt{gh}}$ would be 73 seconds.

A calculation would predict an edge wave period between 70 and 100 seconds for the private residence location. Since the power in the spectra appears at half the frequency (twice the period) of the forcing edge wave, two of our measured, long period peaks (40 and 50 seconds) could stem from bound wave falling into that range.

At this stage we have no independent evidence of edge waves, but instead what we see unfolding is an ability to accurately depict nearshore energy both from incident waves and from infragravity waves. Despite the limitation of an isolated single-point resolution, the strong power signal focused, often, at one major band within the infragravity end of the spectra meets the requirements stated in van Enckevort et al., (2004) of "having a large amount of energy, but focused at a signal frequency", especially when considering the 10 hour time period used to generate the spectra. With this data and the known presence of rip currents, it would seem reasonable to address these infragravity waves in the surf zone as being intermittently trapped to the coast and possible of generating rip currents via the pre-prescribed criteria started by Bowen and Inman (1969). This is explored further in chapter 5.

References

Aagaard, T., B. Greenwood, J. Nielsen. 1997. Mean currents and sediment transport in a rip channel. Marine Geology, 140: 25-45

Adams, P.N., R.S. Anderson, J. Revenaugh. 2002. Microseismic measurement of wave energy delivery to a rocky coast, Geology. 30(10): 895-898.

Baker Engineering. 1998. *Investigation of spur jetties*, submitted to: New York Department of State, Division of Coastal Resources, 38 pp.

Baquerizo, A. M.A. Losada, I.J. Losada. 2002. Edge wave scattering by a coastal structure. Fluid Dynamics Research, 31: 275-287.

Beach, R. R., R. W. Sternberg. 1988. Suspended sediment transport in the surf zone: response to cross-shore infragravity motion. Marine Geology, 80: 61-79.

Benumof, B.T., G.B. Griggs. 1999. The dependence of seacliff erosion rates on cliff material properties and physical processes: San Diego County, California. Shore and Beach, 67: 29-41.

Bokuniewicz, H.J. 2004. Isolated Groins at East Hampton, NY. Journal of Coastal Research, 33: 215-222

Bowen, A.J., D.L. Inman. 1969. Rip currents: laboratory and field observations. American Geophysical Union, 1: 5479-5491.

Bowen, A.J., R.T. Guza. 1978. Edge waves and surf beat. Journal of Geophysical Research, 83(C4): 1913-1920.

Bromirski, P.D. 2001. Vibrations from the "Perfect Storm". Geochemistry, Geophysics and Geosystems, 2: doi:10.1029/2000GC000119.

Bromirski, P.D, F.K. Duennebier. 2002. The near-coastal microseism spectrum: Spatial and temporal wave climate relationships. Journal of Geophysical Research, 107(B8): 2166-2185.

Bromirski, P.D., R.E. Flick, N. Graham. 1999. Ocean wave height determined from inland seismometer data: Implications for investigating wave climate changes in the NE Pacific. Journal of Geophysical Research, 104 (C9): 20753-20766.

Buonaiuto, F.S. 2003. Morphological evolution of Shinnecock Inlet, NY. Ph.D. Dissertation, Stony Brook University, 84 pp. + appendices.

Darbyshire, J., E.O. Okeke. 1969. A study of primary and secondary microseisms recorded in Anglesey. Journal of Geophysical Research, 17(1): 63-92.

Deane, G.B. 2000a. Long time-base observations of surf noise. Journal of the Acoustic Society of America, 107(2): 758-769.

Deane, G.B. 2000b. A model for the horizontal directionality of breaking wave noise in the surf zone. Journal of the Acoustic Society of America, 107(2):177-192.

Gerstoft, P., M. C. Fehler, K.G. Sabra. 2006. When Katrina hit California. Geophysical Research Letters, 33: L173808.

Hasselmann, K. 1963. A statistical analysis of the generation of microseisms. Reviews of Geophysics, 1: 177-209.

Hirsch, J. 2005. Seismic signature of ocean surf as it relates to wave energy and coastal erosion. Technical report, Stony Brook University, 12 pp.

Howell, B.F. 1990. *An introduction to seismological Research: history and development*, Cambridge University Press, Cambridge, 193 pp.

Kana, T. W. 1995. A mesoscale sediment budget for Long Island, New York. Marine Geology, 126: 87-110.

Kinsman, B. 1965. *Wind waves: their generation and propagation on the ocean surface*, Prentice-Hall, Englewood Cliffs, NJ, 676 pp.

Komar, P.D. 1998. *Beach processes and sedimentation*, Prentice hall, Upper Saddle River, NJ, 554 pp.

Longuett-Higgins, M.S., R.W. Stewart. 1964. Radiation stresses in water waves, a physical discussion with applications. Deep-Sea Research, 11: 529-562.

MacMahan, J.H., A.J.H.M. Reniers, E.B. Thornton, T.P. Stanton. 2004. Surf zone eddies coupled with rip current morphology. Journal of Geophysical Research, 109(C07004): doi:10.1029/2003JC002083

Oliver, J., M. Ewing. 1957. Microseisms in the 11- to 18-second period range. Bulletin of the SeismologicalSociety of America, 47 (2): 111-127.

Ruessink, B.G. 1998. The temporal and spatial variability of infragravity energy in a barred nearshore zone. Continental Shelf Research, 18: 585-605

Schubert, C.E., H.J. Bokuniewicz. 1991. Infragravity wave motion in a tidal inlet. Coastal Sediments, Special Conference, Seattle, WA, 1434-1446, June 25-27 1991.

Schüttrumpt, H. 2006. Hydraulic influence of navigation channels in flood defense (sic) structures, 31st Congress of the International Navigation Association (PIANC), Estroil, Portugal.

Tabulevich, V.N. 1992. *Microseismic and infrasound waves*, Research Reports in Physics, Springer-Verlag, NY, 150 pp.

Tanski, J., H.J. Bokuniewicz, and C.E. Schubert. 1990. An overview and assessment of the coastal processes data base for the south shore of Long Island, NY Sea Grant Program, Spec. Rpt., 104: 77 pp.

Tindle, C.T., M.J. Murphy. 1999. Microseisms and ocean wave measurements. Journal of Oceanic Engineering, 24(1): 112-115.

Ursell, F. 1952. Edge waves on a sloping beach. Proceedings of the royal society of London. Series A. Mathematical and Physical Sciences, 214(1116): 79-97

Van Enckevort, I.M.J., B.G. Ruessink, G. Coco, K. Suzuki, I.L. Turner, N.G. Plant, R.A. Holman. 2004. Observations of nearshore crescentric sandbars. Journal of Geophysical Research, 109 (appendix D): 1-17.

Webb, S.C. 1998. Broadband seismology and noise under the ocean. Review of Geophysics, 36(1): 105-142.

Wiechert, E., 1904 Verhandlugen der zweiten internationalen seimologischen Konferenenz, Strassburg, 1903, *Beitr. Gph. Erganz*, 2, 41-43.

Chapter 4: Origins and prediction of rip currents

Introduction

In this chapter, I consider how the observed characteristics of rip currents and wave activity on Long Island's ocean shoreline may relate to various theories of rip current formation and what this might mean for the task of predicting rip currents.

Although rip currents are associated with channels through offshore bars, they are also commonly seen along straight beaches seemingly uncoupled to local geomorphology; a trait noted for our study areas on the south shore of Long Island. Along the steep beaches of Long Island's ocean coast, a fairly infrequent occurrence of rip currents (0.14%) leading to an expected rip-current density of two developed rip currents per day per kilometer of shoreline gave the first clues as to the rip-current regime. The rip currents themselves are, generally, both narrow (15 m) and short (50 m off the coast), appearing as a line of foam oriented perpendicular to the coast. Despite their short duration (average 52-75 seconds respectively) some have been observed to migrate alongshore, almost exclusively west. It seems likely there is a lack of a strong bathymetric control, both due to the offshore position of the bar and the ephemeral nature of the rips combined with their ability to rapidly migrate. The rip currents general form, as well as their tendency to form as individual events instead of multiples, denotes a type of rip current known as a flash rip current.

The process driving the formation of these flash rip currents remains elusive despite efforts to elucidate the mechanisms (Johnson and Pattiaratchi, 2006; Reniers et al.

2004). Even in cases where rip formation, duration and extent is linked to features of the bar, on sand beaches at least, it is likely that rip currents are initiated by conditions of waves, tides and, perhaps, wind. Once an offshore current has begun, wave-current interactions can instigate feedback strengthening the flow. A persistent flow might then move enough sand to alter the bathymetry and subsequently cut the channel through the offshore bar into which fixed rip currents become established (Thornton et al., 2007; MacMahan et al., 2006; Komar, 1998). When linked to bathymetric variability, rip currents are a forcing mechanism for initiating breaks through the offshore bars and, through a positive feedback, the rip currents can eventually be sustained by the presence of said cut. In light of such a chain of feedback processes, determining a specific rip-current regime for any given location may lead to a widely variable result dependent upon the wave climate and the physical setting for each individual beach being monitored. The ultimate key is most likely to be found in the exploring, more closely, variable conditions of wave and current interactions at the shore.

The variable nature of rip currents leads to a more difficult and pressing issue; difficulty in the prediction of rip currents arises because they can be formed by several mechanisms and, once formed, may modify the nearshore morphology in a way that maintains the current even after the original mechanism via which it formed is no longer affecting the nearshore zone. Fixed rip currents can be monitored at comparative leisure, even though storms will alter the offshore bathymetry to cause changes in their location on the scale of weeks or months (Ranasinghe et al., 2004; Holman et al., 2006). In such cases, predicting with accuracy where the bar cut will be re-established is nearly impossible, although in a semi-enclosed shore in the Netherlands, Quartel (2009) found

that the rip currents often reappeared at their before-storm locations alongshore, probably due to a resonance signature within the embayment. Flash rip currents are even more irksome because no visual clues help establish exactly where along a beach they will first take shape. While the body of work regarding rip currents is extensive, a comprehensive review left the same general questions unanswered when broaching the subject of identifying the ultimate force behind initial rip-current generation, the role of incident waves, and a consensus on factors effecting the spacing of rip currents (MacMahan et al., 2005). It seems likely that the forces generating flash rip currents may be the key to determining the occurrence of both fixed and flash rip currents, but until these processes are illuminated, prediction and safety remain an uncertainty.

My working hypothesis is that flash rip-currents are formed by the modulation of the incident wave field by long-period, infragravity or edge waves. Specifically, the evolution of conditions which can instigate height variations of the incoming shorter period wind waves, perhaps via processes that allow the formation of standing or progressive edge waves as hypothesized previous rip current studies (MacMahan et al. 2008; MacMahan et al., 2006; Johnson and Pattiaratchi, 2006; Aagaard et al., 2003; Dalrymple and Lozano, 1978; Bowen and Inman, 1969). Spectral peaks from data recorded at the seismometers show strong power at frequencies associated to typical incident waves. Further frequencies commonly demonstrating high power, are observed at longer periods indicative of infragravity waves. Substantial difficulty remains in field and model observations of edge waves as, by nature, they are undetectable to the naked eye and are released initially into the surf zone which creates hazardous conditions for both researchers and instruments.

Once initiated in this way their longevity can be increased by wave-current interactions and refractions of the incident waves around the outflowing current (Dalrymple, 1975). Eventually, if established, a persistent flash rip current will modify the nearshore morphology evolving into a fixed, bathymetrically controlled rip current. This last step seems to me to be most likely to occur in the days or weeks after a major storm when the beach is being "reset" by ridge-and-runnel structures at the water line.

Previous Work

Theoretical work has continued for nearly 50 years in attempt to better understand all of the physical properties of nearshore wave action that may influence the formation of rip currents (e.g. Reniers et al., 2004; Murray et al., 2003; Falqués et al. 1999; Hammack et al., 1991; Dalrymple and Lozano, 1978; Dalrymple, 1975; LeBlond and Tang, 1974; Arthur, 1962). One model of rip current initiation relies on shear instabilities in the longshore current. Meanders or eddies that develop in longshore currents may establish local areas of offshore flows (Allen et al., 1996) and observed as rip currents (Smith and Largier, 1995). Such instabilities would not necessarily produce narrow, jet-like rip currents but they probably would be more-or-less randomly distributed, like the flash rip currents on Long Island, and it is conceivable that the refraction of incident waves around cross-shore currents could feed back into more focused rip currents. On steep beaches, the longshore current would be expected to be concentrated in a narrow surf zone, enhancing shear instabilities and more prevalent rip currents (Murray et al., 2003).

Dalrymple (1975) focused his studies on exploring the effect of spatial variability in set-down and setup associated with varying radiation stress alongshore owing to the inequity in alongshore wave trains. The superposition of two incident wave trains from different directions sets up a permanent hexagonal surface pattern. Conditions for rip current formation are then realized in the shore-perpendicular troughs in this pattern. Revisiting his 1975 work, Dalrymple and Lozano (1978) established a mechanism by which the waves would be approaching at opposing angles, a major flaw in the 1975 study. They found, that when modeling wave approach, currents flowing perpendicular to the shore act much as a headland would causing the refraction of waves alongshore around the current itself (Dalrymple and Lozano, 1978). The principal characteristics of this model is the generation of multiple, periodic rip currents with a longshore spacing of rip currents, which is approximately one-half the longshore wavelength. When applied to observational data on rip current spacing, the model using edge waves proved more adept as the modulating wave force (3.5% error) than the model using the superposition of two incident wave trains (63.3% error) for several of the study beaches. However, the superposition of two incident wave trains proved to provide much better results for study beaches with more spilling and plunging waves, outperforming the edge wave model. This seems to further support the idea gleaned from aforementioned modern predictive efforts that seemed to demonstrate beach to beach variation in applicability. The work in 1978 was revisited on several occasions by other researches also looking to further identify the role that wave refraction versus other modulation forces acting on the incident waves. Dalrymple (1975) and Dalrymple and Lanan (1976) used linear wave

theory to reach this conclusion and Hammack, et al. (1991) reached the same conclusion using intersecting sets of cnoidal wave trains.

Cnoidal wave crests of the approaching incident waves, instead of being uniform, were connected by lower wave height saddles between consecutive alongshore crests. The lower wave crests within the saddles are refracted towards the larger wave crests constructively joining the larger crest portion and forming zones of consistent low water in lines extending from the shore through the surf zone. The theory was confirmed in laboratory studies (Hammack, et al., 1991); even after the breaking of the larger crests, the hexagonal shape of the wave field was maintained to create small, weak rip currents that didn't extend beyond the surf zone. These results not only supported self modulation within the wave field by the interaction of wave trains directly, but also addressed the narrowness of rip currents via the narrow zones of low wave heights that occurred periodically alongshore. The rip currents that formed quickly, within the time it took for the arrival of eight waves to the simulated beach in a wave flume (Hammack, et al., 1991).

In summary, analytical evidence shows that wave trains approaching the beach at opposite angles should be capable of producing nearshore modulation in the wave fields and generating rip currents. Without this condition of obliquely and oppositely approaching wave trains, the flow directed back oceanward from the incident wave field would not perpetuate as perpendicular to the coast. A further inference from Murray et al. (2003) indicates that the spacing of these rips should decrease on steeper beaches as the width of the surf zone narrows. Another result of this interaction included the

migration of the rip current alongshore and the creation of a diamond shaped pattern in the approaching waves.

Both empirical and model studies have often considered the impact that bound long-waves, released in the nearshore following incident wave break. Infragravity waves might play a role in generating the return flow portion of the circulation cell that results in rip currents. That focus on infragravity energy stems from a seemingly common theme throughout these studies via which the modulation of incoming waves is required to generate focused flow offshore, though the exact nature of processes acting to modulate the wave trains remains a major point of contention among the theorists. Edge waves, wave-wave interaction, wave-currents interactions and set-down/set-up via radiation stress are all prominent examples of modulating forces.

LeBlond and Tang (1974) worked on coupling the approaching incident wave fields with currents established in the nearshore in analytical models in order to determine their interplay in the surf zone. Prior works in the late 1960s focused only in one direction; that of the waves affecting currents, but did not account for the affect the currents themselves had on the incoming wave fields as a process of modulating the approaching wave field. This was largely due to early efforts focusing on the role of standing edge waves (Bowen and Inman, 1969). LeBlond and Tang (1974) generated the rip currents in their simulations in the same manor as the prior work but with the exception of altered wave energy distribution. To further address the idea of the standing edge wave, LeBlond and Tang (1974) took into account rip-current spacing generated from Bowen and Inman (1969) and examined rip spacing on beaches in which standing edge waves are unlikely.

Falqués et al. (1999) examined the role of set-down and setup as well as the strength of the forces in radiation stress in generating rip currents, on the surface, exploring a similar driving mechanism to that of Dalrymple (1975). Without outside perturbations, no instabilities were found capable of generating rips when only taking into account radiation stresses and set-up/set-down. Instead, instability in the surf zone had to be generated to disturb the equilibrium in the radiation stresses and initiate rip current flow. In agreement with Dalrymple and Lozano (1978), this was found to be likely during times of wave refraction. With no wave refraction, the model did not at any time yield rip current formation in the surf zone. The refraction itself had the impact of focusing energy to specific nearshore points generating an increase in the free surface elevation, while simultaneously decreasing the free-surface elevation in more diffuse adjacent regions of the surf zone. The interactions of possible long period, low frequency energy, superimposed on the breaking waves was also addressed briefly, but was not a major component of the work. Energy, exceeding that of wind waves, is often associated with these longer period waves in the surf zone as, unlike the wind waves, the infragravity waves never break (Battjes et al., 1988). Preliminary calculations suggested that the role of edge waves may be, in part, dictated by the traits of the longshore current in determining whether these long period shore bound waves will have an influence in causing the modulation required for rip current formation.

Murray et al. (2003) took a slightly different approach to wave-current interactions that would sustain rip currents. Their model focused on the direct effect that currents will have on the incident incoming waves as the opposing flow will cause energy to be removed from the incident waves and, therefore, a smaller break. Instead of

focusing on all possible physical interactions, they looked only at the effects of current wave interactions in the evolution of radiation stresses for feeding rip currents, and particularly, generating flash rip currents. Using a mathematical model that randomly varied wave heights every 50 seconds, they generated flash rip currents which appeared at random locations and with individual lifetimes on the order of minutes. The duration and frequency of occurrence decreased with increasing beach slope as the width of the surf zone narrows on steeper beaches, the longshore flows that produce the rips also shrink. Theoretically, rip currents would not form if the beach slope was greater than 0.3. (Beach slope is defined as the slope from high tide to a safe wading depth; a vertical distance that I estimate to be about three meters). Tests for modeling started with a prediction that an increase in the variation of incident wave heights would lead to a decrease in the prevalence of rip currents on stretch of beach. This was parameterized by a "rip activity" (RA) which was defined to be the sum of rip current duration per length of shoreline divided by the total time of observation. Torry Pines Beach in southern California was used for observational data against which to test this prediction and supported the assertion that RA diminished with increasing wave height variability. Flash rip currents with durations from one minute up to ten minutes were observed. The second test centered around the surf zone directly. A narrowing of the surf zone would create weaker rip currents that form less readily and are more easily halted in flow. They chose two other beaches with variable slopes (Carlsbad and San Onofre) for field tests. RA's for these data are shown in Figure 1.

Bricker et al. (2007) saw evidence of edge wave in an ADCP array off Hawaii associated with a tsunami. Evidence of edge wave motion has also been detected by

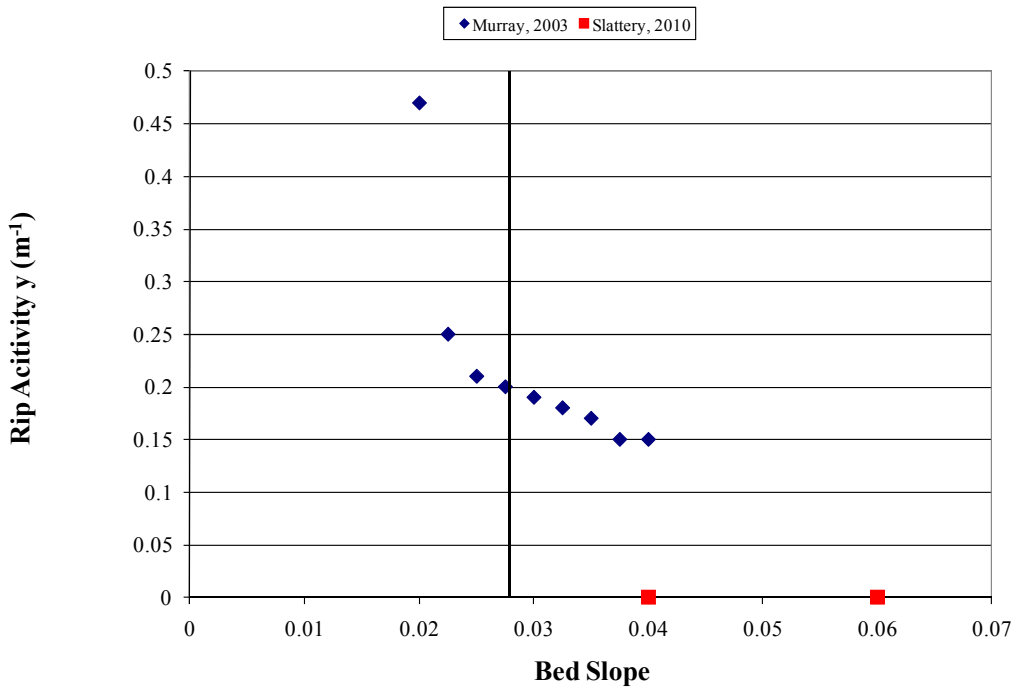

Figure 1. Rip activity. The blue represent observational rip activity from Murray, 2003. The two red dots represent Slattery, 2010 results.

several studies, though it usually needed long term monitoring with expensive alongshore and across shore arrays which could distinguish leaky infragravity waves from bound alongshore energy and seem more prevalent on steeper beaches (Smith and Mocke, 2002; Ruessink, 1998; Battjes, 1988; Oltman-Shay and Guza, 1987). Most, if not all, of these studies suffered from instrumentation failure and retrieval issues as well as being fairly short in duration due to the difficulties of long term deployment of instruments in or near the breaker zone. Edge waves form when energy in the infragravity range, bound to the shorter period incident waves, is released after the incident waves break; able to move as a free wave, these waves don't break, but rather, can be reflected off the shore and refracted back towards the coast becoming trapped in the surf zone (Baquerizo et al, 2002; Komar, 1998). The energy can then move alongshore and become a progressive edge wave, or, in the presence of headlands, groins or jetties reflect again off a structure or headland and resonance will cause a standing edge wave may occur (Baquerizo et al, 2002; Komar, 1998). At East Hampton, the groins to the east of my study site produce a headland (Bokuniewicz, 2004) could have this effect. Once present, the edge wave will produce a pressure field that causes water being transported shoreward by waves to flow toward every other anti-node in the wave and generate focused, offshore flow (Komar, 1998). The edge wave phenomenon is also attributed to undulations in the offshore bar, the shoreline, and possibly rip current pulsations (Quartel, 2009; MacMahan et al., 2004). Observational difficulties have remained the driving force behind the lack actual evidence establishing the presence of edge wave and therefore a relationship between edge waves and incipient rip-currents is lacking (Reniers et al., 2006; MacMahan et al., 2006; MacMahan et al., 2005). Observed spacing during several studies have actually

precluded the edge wave as a mechanism, as the spacing between rip channels was not regular and an order of magnitude (178 m) larger then what would be predicted from edge wave influence (e.g. Holman et al., 2006) to match the expected alongshore wavelength from a standing edge wave, but these studies focused heavily on the position alongshore of fixed rips which are mainly dominated by local bar morphology (Quartel, 2009; Holman et al., 2006; van Enckevort et al., 2004). Since these infragravity waves which result in edge waves are bound to incoming incident waves until breaking, estimating nearshore surf conditions through modeling efforts may prove important.

Methods

To further our grasp of our type of rip current and possible mechanics most responsible for modulation in our study area we explore the work of Murray et al. (2003) in an effort to eliminate or elucidate specific modulating processes. As such we compare our rip-current activity from both Fire Island and East Hampton (Chapter 1, Table 1) to those values found both empirically and experimentally by Murray et al. (2003). To complement the observations of rip currents, the evidence of the seismic existence of Infragravity waves (Chapter 3) will also be considered.

The spectral analysis of seismic records that I used in the Chapter 3 will also be used here. Instead of 10-hour selections from the seismometer, however, seismic readings from only the East Hampton residence study location will be used for the hour in which rip currents were seen to identify spectral peaks and the possible presence of infragravity energy coincident with the presence of rip currents. In addition to the hour in

which the rips were present, nine additional hours preceding and following the hour in which the rip current was observed will be similarly analyzed to determine if any pattern in the changing spectra leads to evidence as to why a rip current was seen at a particular time. These rip-current time periods included May 21st, 2007 1200-2100 GMT and June 2, 2007 0600-1500 GMT. In order to eliminate spectra uncommon to rip-current occurrences, spectra will also be run in one-hour blocks for ten-hour sets for time periods during which no rip currents were seen. These non-rip-current time periods were October 9, 2009 0600-1500 GMT and July 1, 2008 1200-2100 GMT.

SWAN will be used to identify the height, period and direction of waves as they approach shore for the main study region in East Hampton in an attempt to identify any specific incident wave conditions that could be more frequent during times when rips were seen. This could give insight into the wave trains to which infragravity waves are most commonly associated in times of rip current formation. The offshore buoy 44017 will be used as the source of the waves for a small grid containing the area in which the study location is located. For the rip currents seen prior to May 2008, wave direction for initial conditions will be collected from NOAA's WaveWatch III, while post May 2008 wave direction became available from direct buoy measurement.

Results

The results of the SWAN wave model runs can be seen summarized in Table 1. These data represent 34 separate time periods during which rip currents were observed.

Table 1. Summary of SWAN wave model runs for 34 observed rip currents.

Date (m/dd/yyyy)	time (GMT)	Height (m)	Period (s)
4032007	1200	0.96	5.7
4052007	1500	1.41	5.6
4052007	2000	1.25	5.1
4132007	1700	0.46	5.3
4132007	1900	0.38	4.8
4292007	1200	0.91	6
5022007	0	0.45	4.3
5062007	1100	0.93	4.6
5062007	1200	0.98	4.75
5062007	1400	0.8	4.5
5062007	1600	0.97	4.8
5202007	1900	1.25	4.9
5212007	1700	0.67	4.82
5242007	1600	0.73	4.39
5242007	1700	0.91	4.36
5242007	1900	0.75	4.41
5252007	1800	0.66	4.39
6022007	1100	0.76	4.7
6022007	1800	0.61	4.25
6152007	0	1.23	5.41
6152007	1500	1	5.2
6172007	1200	0.56	4.96
6172007	1600	0.53	4.7
7072007	1900	0.68	5.1
5142008	0	1.79	7.2
5212008	1900	1.22	6.1
5212008	2200	1.07	5.5
5282008	2000	0.49	4.78
6072008	0	0.64	4.52
7012008	2000	1.2	6.6
8242008	1500	1.05	6.7
8242008	1600	1	6.7
10032008	1900	1.51	5.86
10212008	2100	1.21	5.6

Due to the nature of the source data the wave conditions fed into and therefore retrieved from the model represent one hour. Wave height varied from a minimum of 0.49 to 1.51 m and having an average wave height of 0.91 m. Wave periods ranged from 4.3 to 7.2 seconds with an average period of 5.19 seconds. The wave directions were typically out of the southeast (18 times) or southwest (12 times) with three additional readings that placed the wave approach at nearly shore parallel (May 6, 2007). From the west approaching waves the most oblique angles only reached 210 degrees (south, southwest) while the east approach became highly oblique to near shore parallel for four occasions (described above 87-94 degrees). No wave approached from the extreme west, and very few fell into quadrant one denoting a slight north approach). Typical wave heights and periods are listed in Chapter 1.

Wave approach for the Long Island south shore is usually from the southeast driving longshore transport from Montauk to the New York harbor for the majority of the year through spring and summer. Our model results show that 21 of the rips current events occurred while wave approach was from the general directions of south and east. However, over one-third of the rip currents happened during a wave approach from the south-southwest, but these angles were generally very close to shore normal (within 30 degrees maximum). It would seem, then, that rip currents are more likely during a south or east swell and much less likely the approach moves west of shore normal conditions. While the average wave conditions were 1.35 m 7.5 second waves at buoy 44017 for the time 2002-2008, rips appear to be more common at below average wave heights and shorter then average periods. It may be that larger waves, which also typically have longer periods, are strong enough to interfere with the generation of infragravity energy

in the surf zone and mute the possible effects that infragravity energy would have on the formation of rip currents.

The morphological and statistical traits of the rip currents themselves make it unlikely that their generation is heavily dependent upon regular, bathymetric control. Rip currents lasting, on average, on the scale of a minute is quite different from traits seen in most studies based on fixed morphological rips which can last on the order of weeks, but seem similar to rips lasting only a few minutes seen by Murray et al. (2003).

Multiple rip currents were very rarely seen over observation distances of up to 100 to 300m on Long Island's ocean shoreline. Based on the wave crests seen, at both East Hampton and Fire Island, the trait of having opposing angles was also not supported. Images from both locations did not directly appear to present the diamond or hexagonal features on days in which rip currents were seen. This observation could be used as evidence that the flash rip currents here are not the product of hexagonal wave patterns impinging on the coast, or of quasi-permanent edge waves both of which are expected to produce multiple rip currents at a periodic spacing. The model of Murray et al. (2003), which is based on random variations in wave heights, seems more appropriate. The beaches here were steep with East Hampton having slope of 0.04 and Fire Island slope of 0.06. This makes both beaches highly reflective and shortens the surf zone.

RA did not seem to increase at increasing beach slope as might be expected if the flash rip currents were caused by instabilities in the longshore currents. The RA for both locations is exceptionally small with East Hampton being smaller at 1.44×10^{-6} and, while slightly larger (4.65×10^{-4}) at Fire Island, both essentially approach a RA of zero (Figure 1; Chapter 1, Table 1). When plotted with his data, our RA vs. beach slope points fell

nearly on the zero line for both Fire Island and East Hampton (Figure 1). This matches well with the findings of Murray et al. (2003) that stated RA is effectively zero at beach slopes above 0.03.

The spectra for two time periods during which rip currents were observed are shown in Figures 2 and 3 and represent 10, single hour spectral graphs. The spectra in Figure 2 (a-j) demonstrate peaks in the infragravity frequencies below 0.05 Hz. There is also evidence of energy between 0.2 and 0.3 Hz, generally associated with incident wave periods, but appears with no definitive single peak. Throughout the time, a more sharply defined peak in the power is apparent at infragravity frequencies for every time period, though some (a and i) show two strong peaks. The relative difference between the peaks in the <0.05 Hz and 0.2-0.3 Hz range seems small with maximum values of spectral power being evident within the infragravity frequencies for about half of the time period (Figure 2 a, b, e, g, and j). Figure 3 has large amounts of power focused in the infragravity frequencies for all hours. This is seen as multiple strong peaks for all times except 1400 and 1500 (i and j) hours, which have a definitive single peak for both. For frequencies associated with incident waves a small increase in power can be seen around 0.35 Hz in hours 0600-1300 and 1400(a-h and j) and in another increase in power appears associated with 0.25 Hz for 1400 and 1500 hours (i and j).

Spectra for two randomly selected time periods that had no rip currents for at least one day prior or post can be seen in figures 4 and 5. In figure 4, spectral peaks are common in the range from 0.15-0.25 Hz throughout all hours October 9, 0600-1500 hours (a-j). Pronounced spectral peaks at the infragravity frequencies become apparent from 0800-1000 hours (c-e) but then once again disappear. There is consistent power 0-

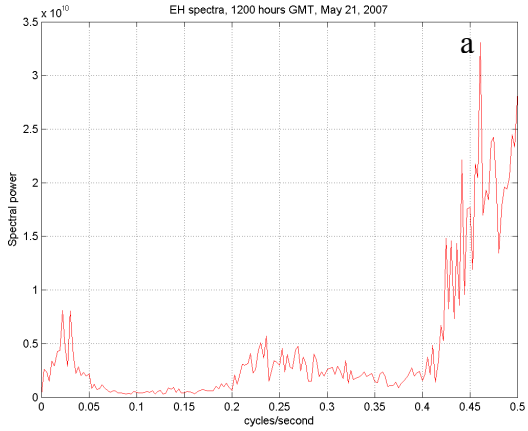
EH spectra, 1200 hours GMT, May 21, 2007
x 10^10
a
Spectral power
cycles/second

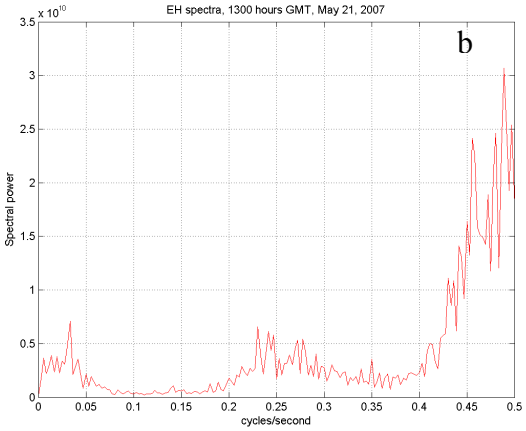
EH spectra, 1300 hours GMT, May 21, 2007
x 10^10
b
Spectral power
cycles/second

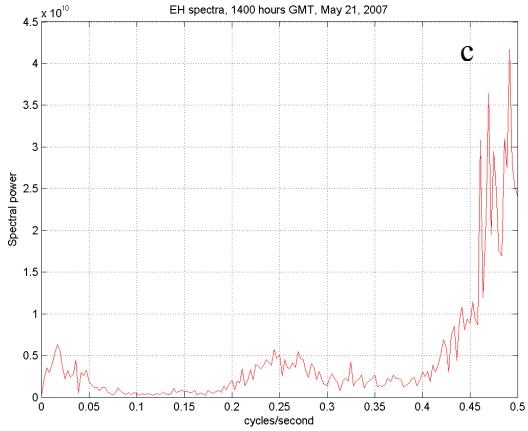
EH spectra, 1400 hours GMT, May 21, 2007
x 10^10
c
Spectral power
cycles/second

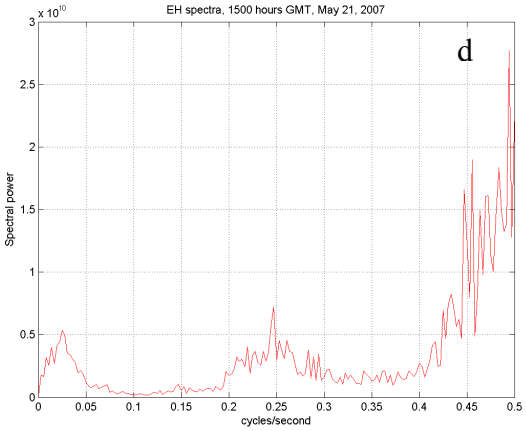
EH spectra, 1500 hours GMT, May 21, 2007
x 10^10
d
Spectral power
cycles/second

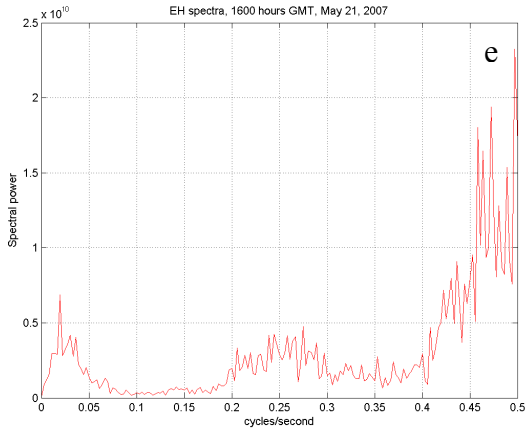
EH spectra, 1600 hours GMT, May 21, 2007
x 10^10
e
Spectral power
cycles/second

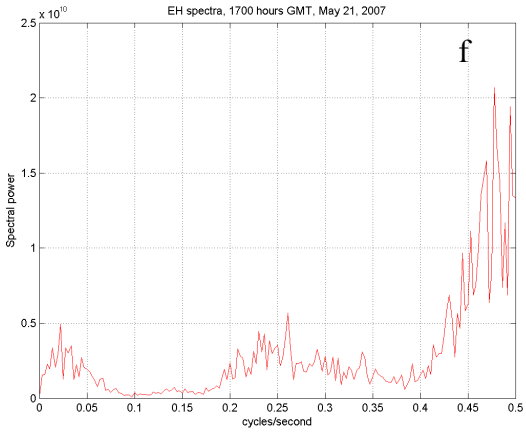
EH spectra, 1700 hours GMT, May 21, 2007
x 10^10
f
Spectral power
cycles/second

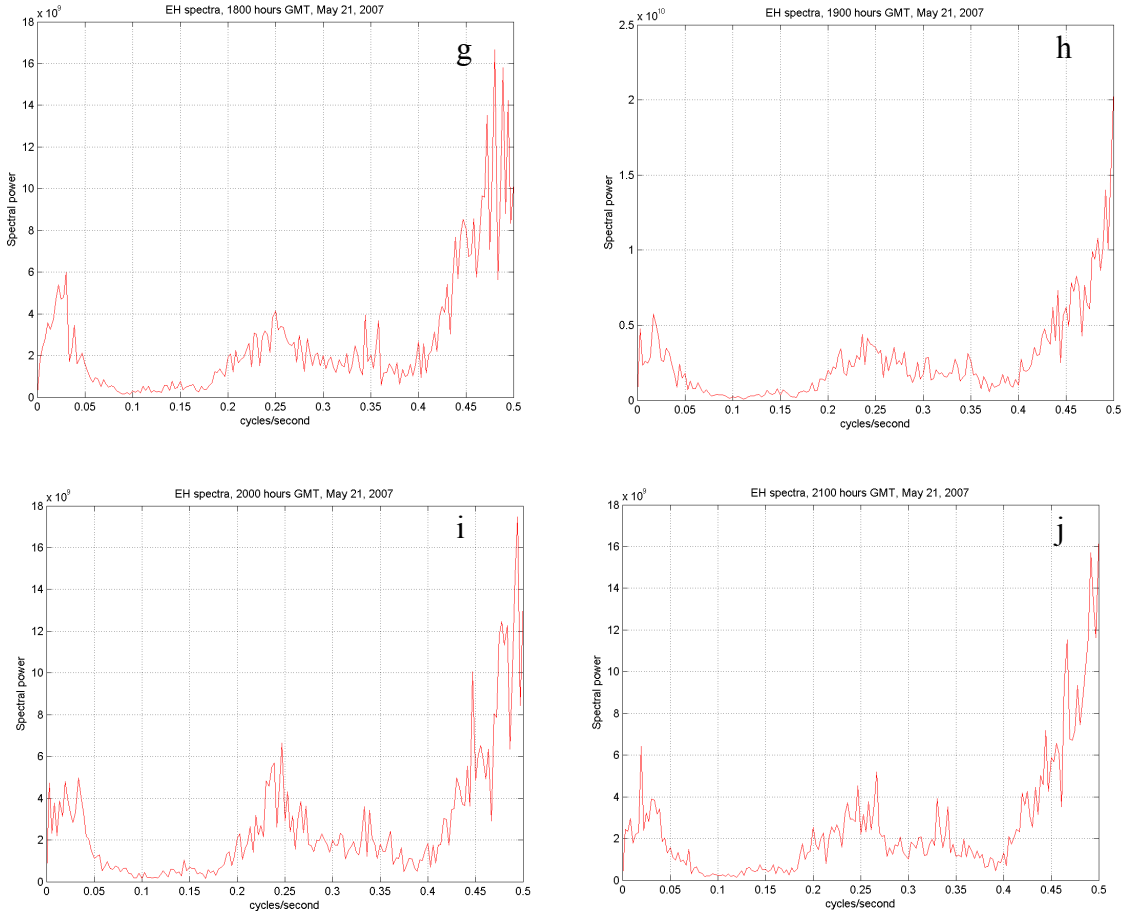

Figure 2. Ten (a-j) single hours of spectra for the period May 21, 2007 from 1300(a)-2100(j) hours. This corresponds to observed rip current at approximately 1700 (F) hours on that day.

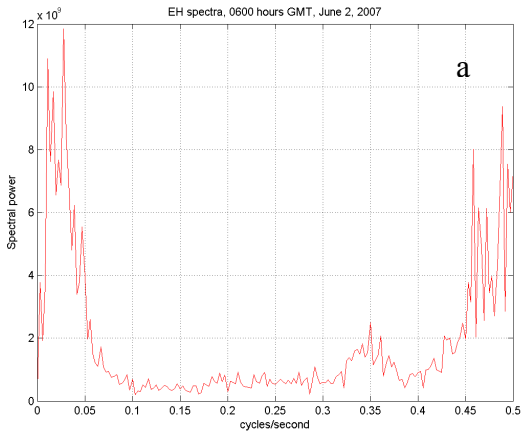
EH spectra, 0600 hours GMT, June 2, 2007
x 10^9
a
Spectral power
cycles/second

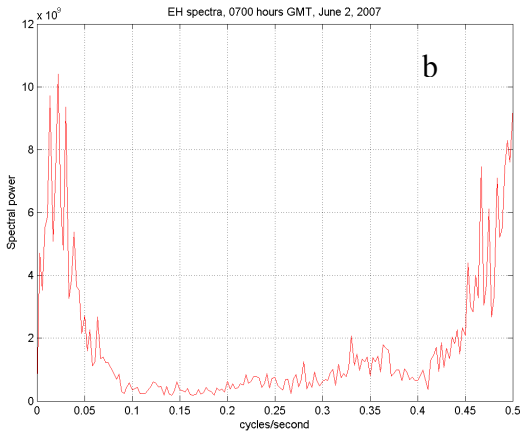
EH spectra, 0700 hours GMT, June 2, 2007
x 10^9
b
Spectral power
cycles/second

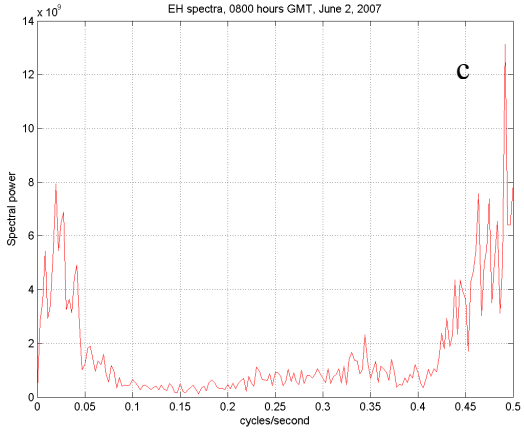
EH spectra, 0800 hours GMT, June 2, 2007
x 10^9
c
Spectral power
cycles/second

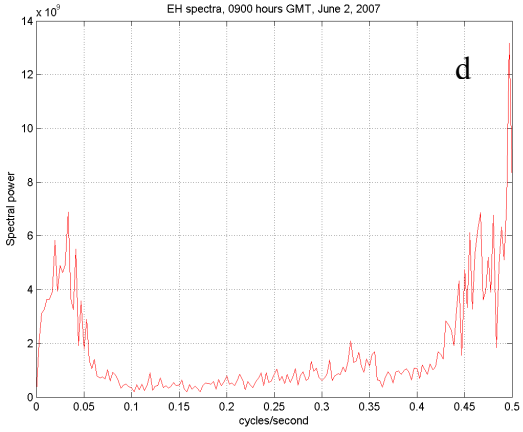
EH spectra, 0900 hours GMT, June 2, 2007
x 10^9
d
Spectral power
cycles/second

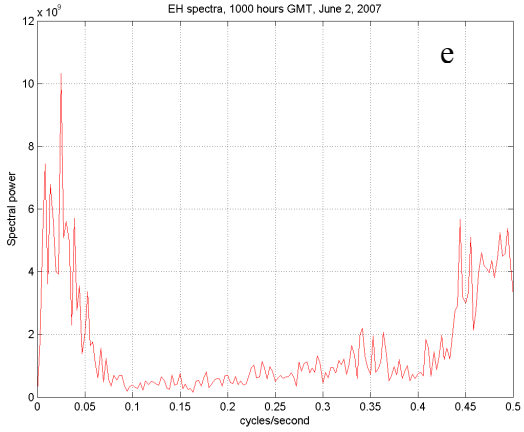
EH spectra, 1000 hours GMT, June 2, 2007
x 10^9
e
Spectral power
cycles/second

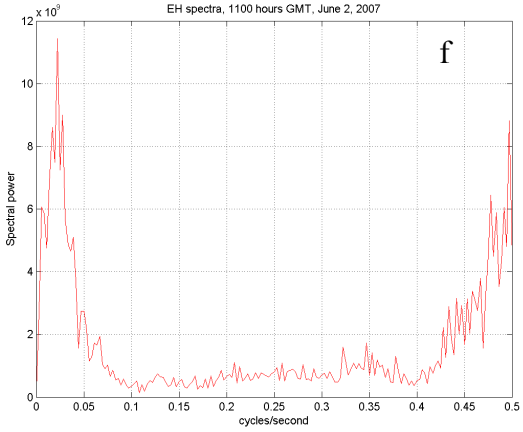
EH spectra, 1100 hours GMT, June 2, 2007
x 10^9
f
Spectral power
cycles/second

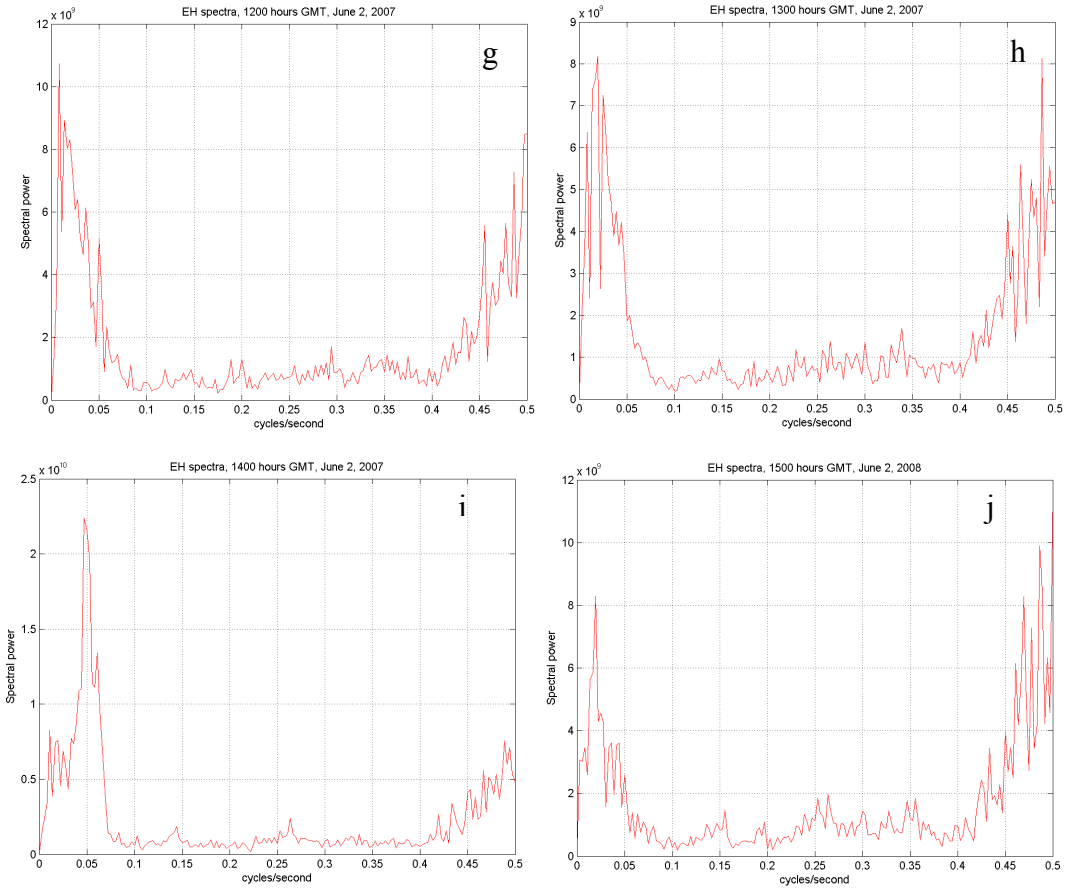

Figure 3. Ten (a-j) single hour spectra from June 2, 2007 from 0600(a)-1500(j) hours that correspond to an observed rip current at 1100 (f) hours.

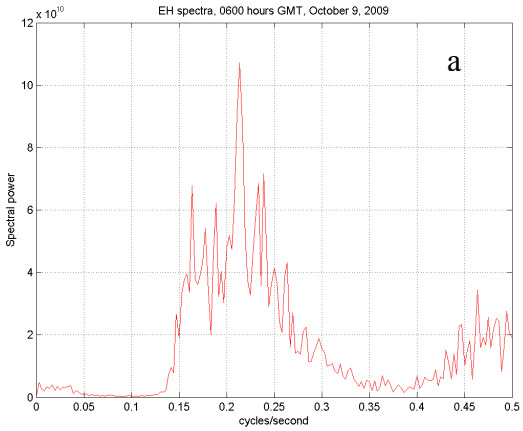
EH spectra, 0600 hours GMT, October 9, 2009
x 10^10
Spectral power
cycles/second
a

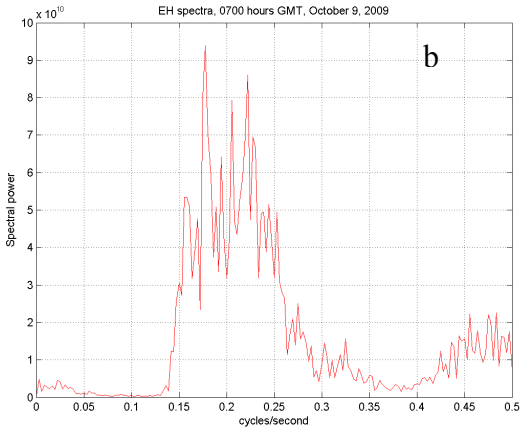
EH spectra, 0700 hours GMT, October 9, 2009
x 10^10
Spectral power
cycles/second
b

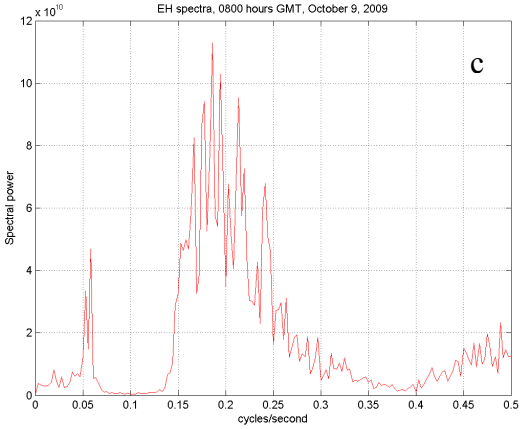
EH spectra, 0800 hours GMT, October 9, 2009
x 10^10
Spectral power
cycles/second
c

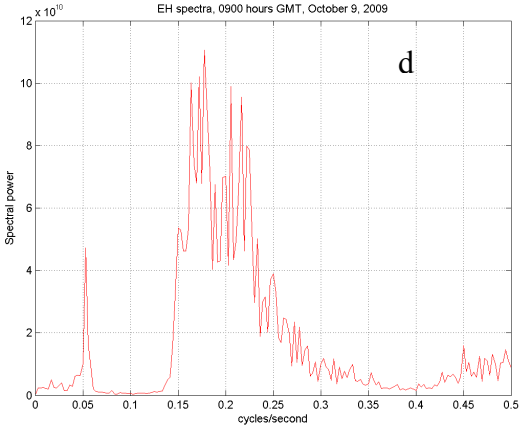
EH spectra, 0900 hours GMT, October 9, 2009
x 10^10
Spectral power
cycles/second
d

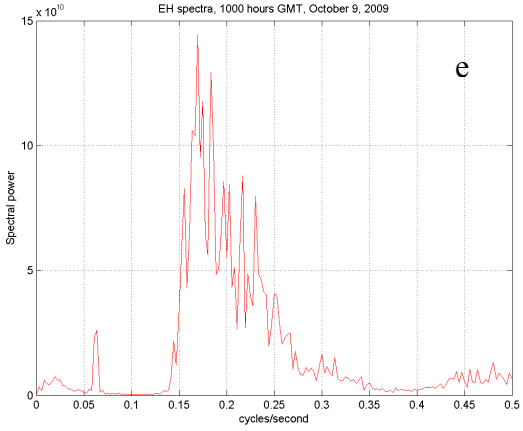
EH spectra, 1000 hours GMT, October 9, 2009
x 10^10
Spectral power
cycles/second
e

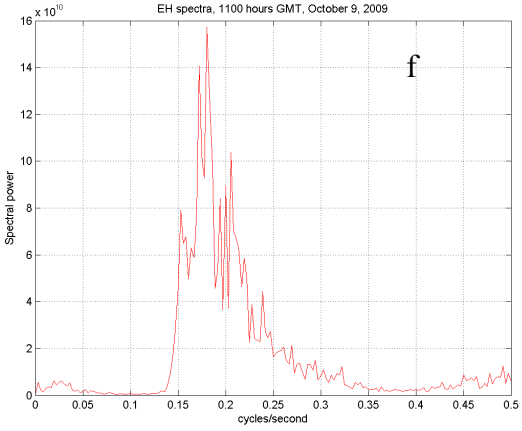
EH spectra, 1100 hours GMT, October 9, 2009
x 10^10
Spectral power
cycles/second
f

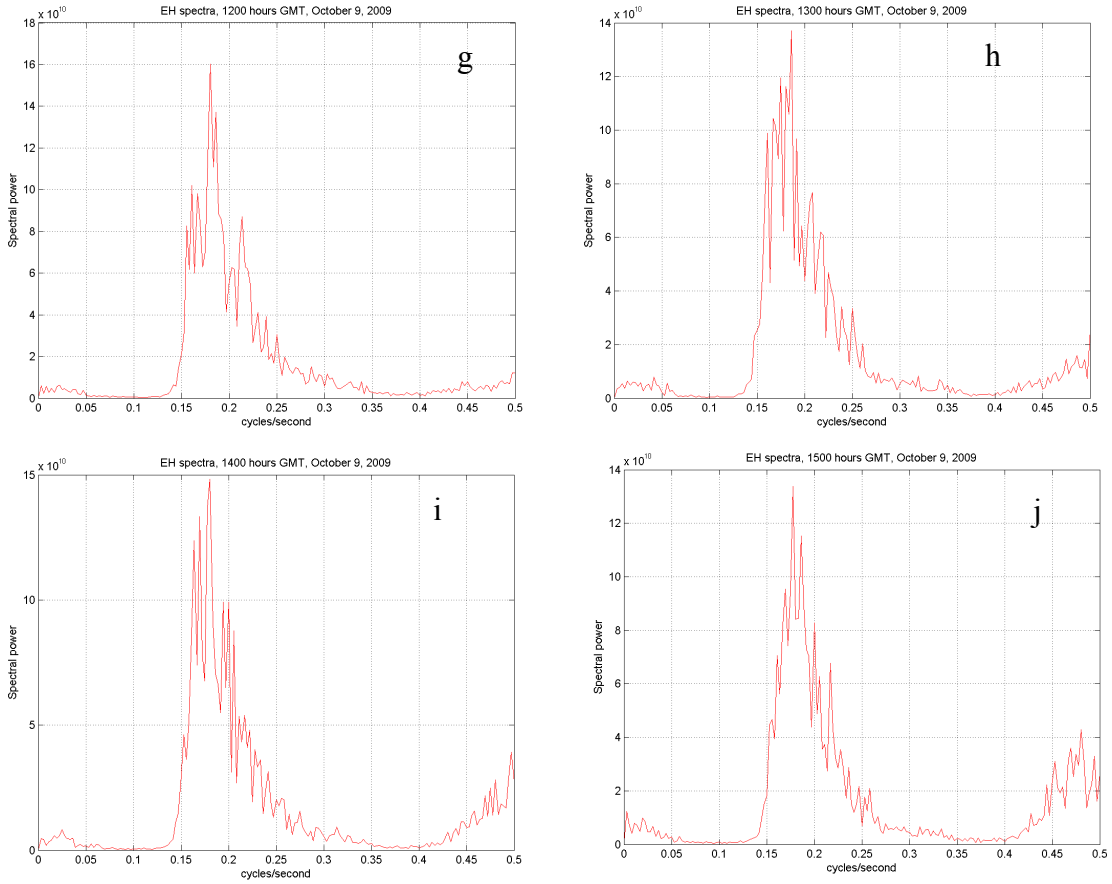

Figure 4. Ten (a-j) single hours of spectra for the period October 9, 2009 from 0600(a)-1500(j) hours. This corresponds to a time period in which no rips were seen through the day.

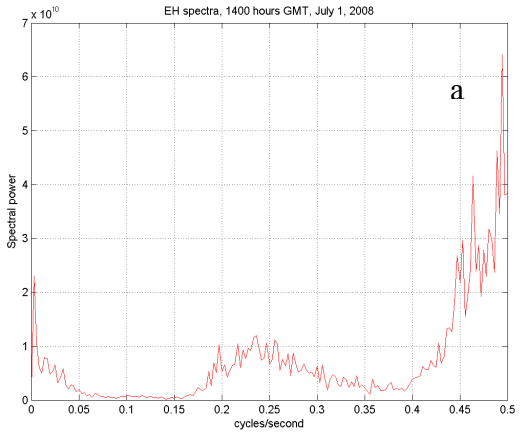
EH spectra, 1400 hours GMT, July 1, 2008
x 10^10
Spectral power
cycles/second
a

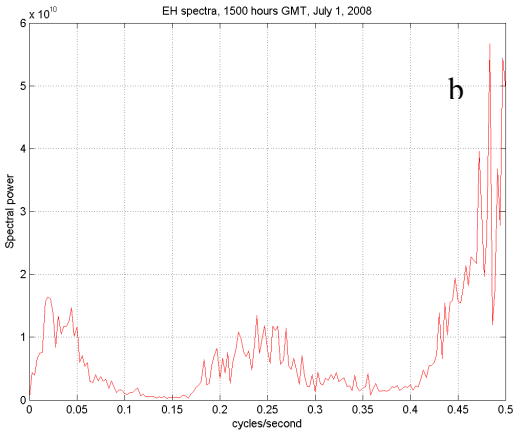
EH spectra, 1500 hours GMT, July 1, 2008
x 10^10
Spectral power
cycles/second
b

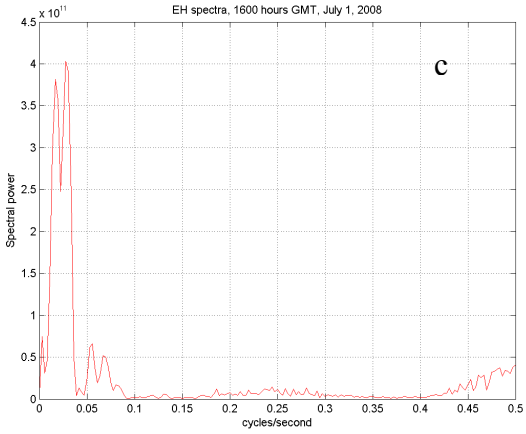
EH spectra, 1600 hours GMT, July 1, 2008
x 10^11
Spectral power
cycles/second
c

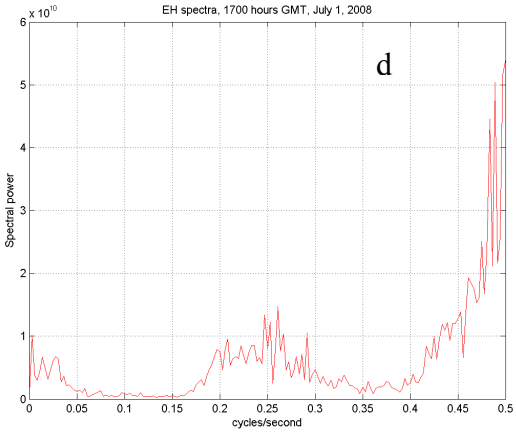
EH spectra, 1700 hours GMT, July 1, 2008
x 10^10
Spectral power
cycles/second
d

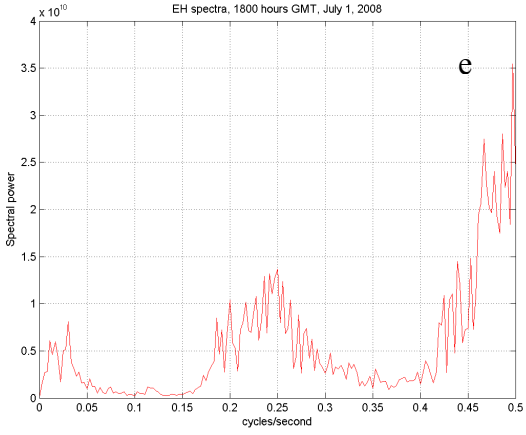
EH spectra, 1800 hours GMT, July 1, 2008
x 10^10
Spectral power
cycles/second
e

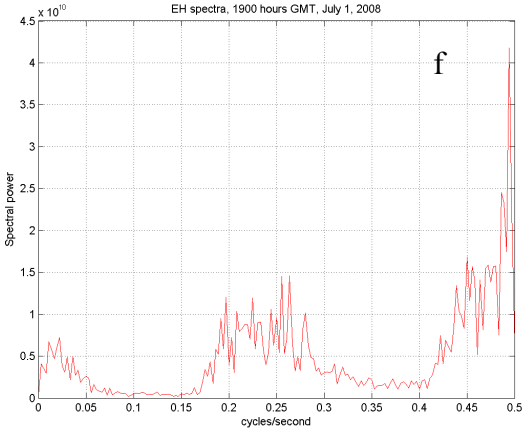
EH spectra, 1900 hours GMT, July 1, 2008
x 10^10
Spectral power
cycles/second
f

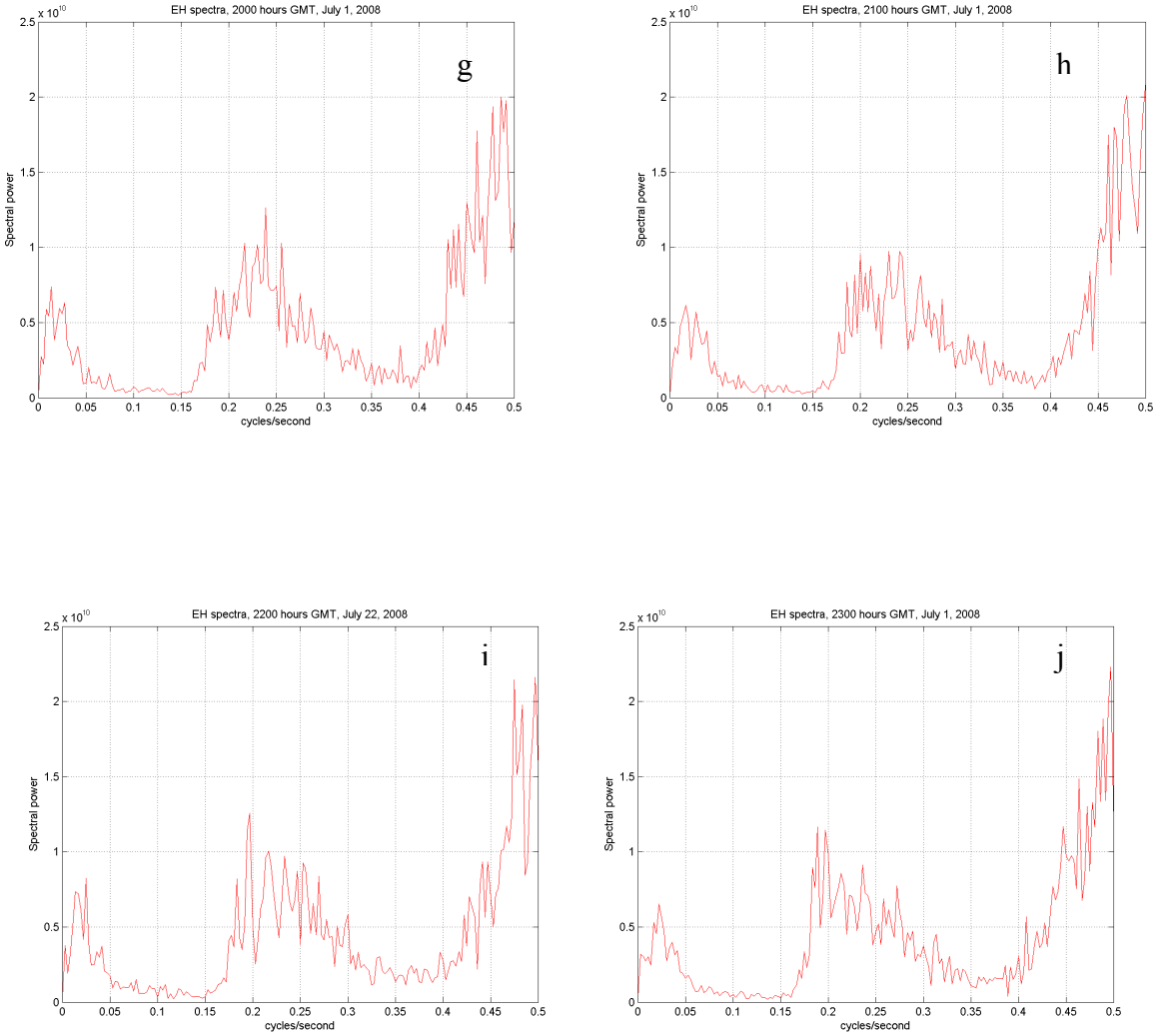

Figure 5. Ten (a-j) single hours of spectra for the period July 21, 2008 from 1400(a)-2300(j) hours. This corresponds to a time period in which no rips were seen through the day.A preliminary magnitude 4.1 earthquake occurred June 30, 2008 at 6:49 p.m. EDT (10:49 GMT), 95 miles north northeast of Las Vegas, Nevada, at a reported depth of 5.1 miles. A tsunami warning, watch, or advisory was not generated. (USGS, Earthquake Hazards Program, Alaska Earthquake Information Center, Pacific Tsunami Warning Center, and West Coast/Alaska Tsunami Warning Centers)

0.05 Hz, but no pronounced peaks are visible for 0600-0700 and 1100-1500 hours (a, b, and f-j). The power at the infragravity frequencies is consistently much lower then the higher frequency power during the whole time period, even when the more pronounced peak is present. Figure 5 covers the non-rip-current period from 1400-2300 hours (a-j) on July 1, 2008. Each spectrum demonstrates a diffuse area of power between 0.2-0.3 Hz, though for 1600 hours (c) it is hard to make-out as the scale changes to reflect a sudden and large increase in power nearer the infragravity frequency range. Power focused at infragravity frequencies is present throughout this study time below 0.05 Hz. Early, 1400-1500 hours (a and b), infragravity power is higher then the region associated with incident waves, though this does not persist or become apparent at any subsequent times, 1600-2300 hours (d-j) except during the aforementioned event that was a degree of magnitude higher then any other signal seen throughout all the times examined.

Discussion

The incident wave fields as predicted nearshore from SWAN during rip currents present no widely constant conditions most likely associated with rip currents except for wave direction. A wide range of periods and waves heights make it unlikely that they, alone, create any stress directly attributable to rip formation. Lack of direct relationships does not preclude a dynamic cooperation between wave height, wave period and wave direction that become more apt to generate rip currents that was elusive during this project.

Any infragravity waves could be edge waves. Dalrymple and Lozano (1978) and Murray et al. (2003) both saw that edge wave models seemed to better address observations for steep beaches when compared with models based on the superposition of two incident wave trains**.** Our rip currents based on RA would support an edge-wave driven system as the forcing mechanism for modulating the incoming wave field. However, observations during the study (Murray et al., 2003) did not take particular note of wave approach from opposing direction at angles to the beach. While not addressed in any of the source material (or this study directly), another possibility dictating rip occurrence on steep beaches may have to do with accommodation space in the nearshore. A steeper beach should have a deeper basin between the offshore bar and the beach which provides more room for the development of offshore flow as undertow to account for the transport of water shoreward. For a more gradual beach the return flow would not have this deep basin in which to move as undertow and, instead, might be more likely to form as a surface flow represented by a rip current.

The position of the offshore bar itself would nearly preclude its involvement in driving rip currents as its location well off shore (over 200 meters) is quite large when compared to the extent of the average rip currents seen (usually under 50 m). Storm resets can alter the beach steepness and shape while altering the presence position and shape of the offshore bar (Howard, 1939). This may account for some of the variability that is seen between the two sites as more fine resolution nearshore bathymetry could account for the preference of rip currents at one location at Fire Island. Moving past these basic traits of both the nearshore in which the rips are acting and the rips

themselves one can look at the basic statistics of the rip currents observed to further elucidate the type of rip regime present.

It seems that the most likely scenario is one in which these frequent (in terms of a new seemingly unique event) short-lived rip currents formed via edge waves can modify the nearshore small scale bathymetry causing alongshore variability. It could be just by chance that one of these many rip currents happens to form over an area where the bathymetry is more conducive to sustaining flash rip currents persistent for 2.5 minutes as observed. Despite this local synergy the scale of the rips were not such that they extended to the offshore bar creating a breach or modifying the offshore bathymetry enough to create an area of preferential rip formation.

Though reports of spacing during multiple rips is highly variable and edge waves are certainly not the only factor in rip current formation, the lack of definitive source of edge waves may lead to the inconsistencies; as mentioned prior, an edge wave may establish rip currents which weaken a point in the offshore bar and establish a rip channel, but when the edge wave diminishes the morphological forcing becomes more important allowing for the continuation of rip-current flow long after the edge wave had dissipated. Another indicator of edge waves can be undulations in both the offshore bar and in the shoreline (Quartel, 2009). While the exact formation is unknown, evidence strongly supports a relationship between edge waves and breaking nearshore wave conditions (Ruessink, 1998).

Also taken into consideration was the direct physical setting present along the study area. The biggest missing component of this project was the critical lack of surf-zone bathymetry data. In studies where this type of high temporal resolution bathymetry

was used, surveys as frequent as every 20 days showed drastically different surf zone bathymetry traits. While MacMahan et al. (2008) seemed to link low-energy rip currents to small bathymetric variations the scale was still much greater having average rip channel widths on the order of over 100 m (the entire extent of our viewable East Hampton area). Such wide rips aren't seen anywhere along our coastal study and their wide extent may have allowed them to be more easily linked to smaller bathymetric perturbations. Even where a surf zone bathymetric survey was available, multiple runs on the scale of days would be required to really have a fully accurate portrayal of the rapidly evolving system. A rip current or several rip currents could have been newly formed by the ephemeral long-wave modulations of the incident waves, or it may be the result of the interaction of flash rip currents with incoming waves (i.e. wave-current interactions) or it may be a fixed rip with local, bathymetric control.

Rip current warning systems are largely based on visual observations of the incident waves and have an unacceptably large incidence of false alarms with a widely used model dating back to Lushine (1991) who utilized wind direction and velocity, swell height and time of low water to try and predict rip current threat based on the anecdotal relationship between these factors and rip current rescues/deaths. Lascody (1998) further adapted the Lushine Rip Current Scale (LURCS), adding wave period to his East Central Florida (ECFL LURCS), after noting that longer wave periods seemed related to life guard reports of rip current rescues. There was a high incidence of false positives using both Lushine's original model and Lascody's renovated version. Further application of LURCS was attempted by Engle et al. (2002), by further modifying the technique to incorporate wave direction and increasing tidal factoring to account for rescue trends that

showed a higher incidence of rescues associated with low tide. While this met with much greater success along beaches in Valusia County, FL the system showed poor portability and Nelko and Dalrymple, (2009) were unable to successfully implement the methodology for Ocean City, MD. This presents another aspect of rip current prediction and study; that of its seemingly endless variability between study locations (beaches). Ultimately, researchers may discover that each individual beach experiences a confluence of distinct factors that impact rip current formation and persistence requiring an extensive database of observations regarding rip currents before any attempt can be made at categorizing rip currents (such as the effort expressed in chapter 1). This realization, too, may also mean that the traits of observed incident waves are not the direct and immediate causes of rip currents, but rather, imperfect surrogates for more fundamental process. No system may be widely applied. Regardless of the causes for success and failure of model and prediction efforts, it's clear that incident wave conditions and climatological forcing are only part of the causative factors and bathymetry, too, doesn't relate ubiquitously with the formation and persistence of recorded rip currents.

Recently, the NWS on Long Island has launched a project to forecast surf conditions in order to better predict rip current conditions at some of the anecdotally more active beaches. Loosely based on the LURCS model ideology, they are honing the model for local application based on daily reports from life guards and some hindcasting. This has allowed them to create a point system in order to easily predict rip danger, not just based on rip presence, but also on relative rip strength. The point system takes into account several physical traits that were identified as influences on rip current

hazardousness like wave direction, wave height and tidal stage (Nelson Vaz, NWS, 2010 personal communication).

When flash rip currents do occur it seems that they are more likely to survive along favorable beach morphology. They might overlap, for instance, with pre-existing undulations in the shoreline. Shoreline undulations have been documented at a wide range of sizes (Seaver et al. 2007; Gravens, 1999). Important wavelengths were found ranging from a few hundreds meters to kilometers. Based on power spectra, Gravens (1999) had found wavelengths of 2135 m, 1830 m, 1065 m and 1045m as well as shorter wavelengths of lesser importance. Seaver et al. (2007) also found wavelengths of 2172 m, 1837 m, 1062 m and 1038 m. and shorter. The fortuitous superposition of a few important undulations would create a re-entrant along the shoreline into which a flash rip current might become trapped.

Alternatively, Flash rip currents might excavate their own re-entrants, as I have documented earlier, these flash rip currents are confined close to shore. As a result, it seems to me that flash rip currents are most likely to turn into fixed rip currents when ridges-and-runnels are present at the shoreline providing a nearshore structure that could be modified by the currents. This happens days or weeks after a major storm when the berm beach is being reset with sand previously moved offshore by storm erosion. In the morphological classification of Wright and Short (1983), the appearance of the ridge-and-runnel morphology is parameterized by a local Irribarren Number combining the beach slope and wave steepness. Such a parameter might be useful, therefore, in forecasting the risk of rip currents although it would have to be tailored to the local situations.

The angle of wave attack should also be a relevant parameter. High angles of attack drive longshore currents and the conventional wisdom has it that longshore currents curtail the lifetime of cross-shore rip currents (MacMahan, 2006).

Conclusions

The preceding builds upon the body of work presented in chapters 1-3 addressing, specifically, the possibility of edge wave influence on modulation of the nearshore wave fields. The ten-hour spectral segments show indications of ephemeral features generating focused energy at infragravity periods. Too, our observational rip current data when compared with data from Murray et al. (2003) indicate rips more common for a flash rip type setting and less likely to support those models assuming strong bathymetric forcing. SWAN model results indicated that rips seemed most prevalent during wave approach from the southeast, essentially the dominant conditions for the Long Island south shore. Wave height did not seem to play any role in the occurrence of rips though the rips did seem to occur at lower then average wave heights.

In all, the evidence for edge wave presence and influence appears to be a strong direction for focus on the Long Island south shore in ultimately trying to define conditions for rip formation.

References

Aagaard, T., K.R. Bryan. 2003. Observations of infragravity wave frequency selection. Continental Shelf Research, 23: 1019-1034.

Allen, J.S., P.A. Newberger, R.A. Holman. 1996. Nonlinear shear instabilities of alongshore currents on plane beaches. Journal of Fluid Mechanics, 310: 181-213.

Arthur, R.S. 1962. A note on the dynamics of rip currents. Journal of Geophysical Research, 67(7): 2777-2779.

Baquerizo, A., M.A. Losada and I.J. Losada. 2002. Edge wave scattering by a coastal structure. Fluvial Dynamics Research, 31: 275-287.

Battjes, J. A. 1988. Surf-zone dynamics. Annual Review of Fluid Mechanics, 20: 257-293.

Bokuniewicz, H.J. 2004. Isolated Groins at East Hampton, NY. Journal of Coastal Research, 33: 215-222

Bowen, A.J., D.L. Inman. 1969. Rip currents: laboratory and field observations. American Geophysical Union, 17: 5479-5491.

Bricker, J. D., S. Munger, C. Pequignet, J.R. Wells, G. Pawlak, K.F. Cheung. 2007. ADCP observations of edge waves off Oahu in the wake of the November 2006 Kuril Islands tsunami. Geophysical Research Letters, 34 (L23617): doi 10.1029/2007GL032015, 2007.

Dalrymple, R.A., C.J. Lozano. 1978. Wave-current interaction models for rip currents. Journal of Geophysical Research, 83(C12): 6063-6071.

Dalrymple, R.A. 1975. A mechanism for rip current generation on an open coast. Journal of Geophysical Research, 80(24): 3485-3487.

Dalrymple, R.A., G.A. Lanan. 1976. Beach cusps formed by intersecting waves. Geological Society of America Bulletin, 87: 57-60.

Engle, J., J. MacMahan, R. J. Thieke, D. M. Hanes, R. G. Dean. 2002. Formulation of a rip current predictive index using rescue data. Proceedings of the National Conference on Beach Preservation Technology (FSBPA), Biloxi, MS.

Falques, A., A. Montoto, D. Vila. 1999. A note on hydrodynamic instabilities and horizontal circulation in the surf zone. Journal of Geophysical Research, 104(C9): 2060-20615.

Gravens, M. B. 1999. Periodic Shoreline Morphology, Fire Island, New York. Proceedings of Coastal Sediments, '99, American Society of Civil Engineers, NY, 2: 1613-1626 pp.

Hammack, J., N. Scheffner, H. Segur. 1991. A note on the generation and narrowness of periodic rip currents. Journal of Geophysical Research, 96: 4909-4914.

Holman R.A., G. Symonds, E.B. Thornton, R. Ranasinghe. 2006. Rip spacing and persistence on an embayed beach. Journal of Geophysical Research, 111: 1-17.

Howard, A.D. 1939. Hurricane modifications of the offshore bar of Long Island, NY. Geographical Review, 29(3): 400-415.

Johnson, D., C. Pattiaratchi. 2006. Boussinesq modeling of transient rip currents. Coastal Engineering, 53: 419-439.

Komar, P.D. 1998. *Beach processes and sedimentation*, Prentice hall, Upper Saddle River, NJ, 554 pp: 335:350, 457:492.

Lascody, R. L. 1998. East Central Florida Rip Current Program. National Weather Digest, 22(2): 25-30.

Leblond, P.H., C.L. Tang. 1974. On energy coupling between waves and rip currents. Journal of Geophysical Research, 79(6): 811-816.

Lushine, J.B. 1991. A study of rip current drownings and related weather factors. National Weather Digest, 16: 13-19.

Macmahan, J.H., E.B. Thornton, A.J.H.M. Reniers, T.P. Stanton, G. Symonds. 2008. Low-Energy Rip Currents Associated With Small Bathymetric Variations. Marine Geology, 255: 156-164.

MacMahan, J.H., E.B. Thornton, A.J.H.M Reniers. 2006. Rip Current Review. Coastal Engineering, 53: 191-208.

MacMahan, J.H., E.B. Thornton, T.P. Stanton, A.J.H.M. Reniers. 2005. RIPEX: observations of a rip current system. Marine Geology, 218: 113-134.

MacMahan, J.H., A.J.H.M. Reniers, E.B. Thornton, T.P. Stanton. 2004. Infragravity rip current pulsations. Journal of Geophysical Research, 109(C01033): 1-9.

Murray, A.B., M. LeBars, C. Guillon. 2003. Tests of a new hypothesis for non-bathymetrically driven rip currents. Journal of Coastal Research, 19: 269-277.

Nelko, V., R.A. Dalrymple. Last accessed July 18, 2010. Rip currents prediction in Ocean City, MD. http://www.ripcurrents.fiu.edu/NEW%20SITE%20JUNE%202009/Symposium2010/Abstracts/Rip%20Currents%20Prediction%20in%20Ocean%20City,%20MD.pdf.

Oltman-Shay, J., R.T. Guza. 1987. Infragravity edge wave observation on two California beaches. Journal of Physical Oceanography, 17: 644-663.

Quartel, S. 2009. Temporal and special behavior of rip channels in a multiple-barred coastal system. Earth Surface Processes and Landforms, 34: 163-176.

Ranasinghe, R., G. Symonds, K. Black, R. Holman. 2004. Morphodynamics of Intermediate beaches: a video imaging and numerical modeling study. Coastal Engineering, 51: 629-655.

Reniers, A.J.H.M., J.A. Roelvink, E.B. Thornton. 2004. Morpholdynamic modeling of an embayed beach under wave group forcing. Journal of Geophysical Research, 109(C01030): doi: 10.1029/2002JC001586.

Ruessink, B.G. 1998. The temporal and spatial variability of infragravity energy in a barred nearshore zone. Continental Shelf Research, 18: 585-605.

Seaver, K. H. J. Bokuniewicz, F. Buoniauto. 2007. Evolution of erosional hot spots on a barrier island: Fire Island, New York. Coastal sediments '07, N.C. Kraus and J.D. Rosati, editors. Amer. Soc. Civil Engs, 3: 1722-1730 pp.

Smith, J.A., J.L. Largier. 1995. Observations of nearshore circulation: rip currents. Journal of Geophysical Research, 100: 10, 967-10, 975.

Smith, G.G., G.P. Mocke. 2002. Interaction between breaking/broken waves and infragravity-scale phenomena to control sediment suspension transport in the surf zone. Marine Geology, 187: 329-345.

Thornton, E.B., J. MacMahan, A.H. Sallenger Jr. 2007. Rip currents, mega-cusps, and eroding dunes. Marine Geology, 240: 151-167.

Van Enckevort, I.M.J., B.G. Ruessink, G. Coco, K. Suzuki, I.L. Turner, N.G. Plant, R.A. Holman. 2004. Observations of nearshore crescentric sandbars. Journal of Geophysical Research, 109 (appendix D): 1-17.

Wright, L.D., A.D. Short. 1983. Morphodynamices of Beaches and Surf Zones in Australia. In *Handbook of Coastal Processes and Erosion*, P.D. Komar (editor). CRC Press, Boca Raton, FL, 35-64 pp.

Chapter 5: Lessons learned and future work

Introduction

The ultimate goal of this project was to gain better an understanding of forces involved in the generation of rip currents present along the Long Island south shore. In all, what can be said about the rip currents on Long Island south shore is that the majority are infrequent and small, generally lasting only a very short time and likely not associated with offshore bathymetry based on scale. However, should one find themselves suddenly within a flash rip they would certainly be in danger of rapid offshore transport. Edge waves seem most likely the cause of these rip currents, and, though seemingly common, these waves only cause rips when certain criteria are met. Specifically, higher energy carried in the infragravity waves as compared with incident waves, coupled with the infragravity energy focused at a dominant frequency, seems to be the formula that links edge waves to rip current incidence. There remains a chance of event driven rip currents of a different morphological (bathymetrically controlled) type following erosional events as sand moves back to the beach forming a ridge and runnel type offshore pattern. There is an incredible amount of room for expansion of this project, but the foundation has been laid to integrate forecasting of waves and infragravity wave traits to rip current occurrence and hopefully save multiple live both in the United States and abroad. The research has created a strong foundation for insight into forces contributing to flash rip formation, a land based system capable of monitoring possible forcing mechanisms and elucidating some of the more difficult aspects of attempting to model nearshore conditions that may lead to rip currents. While the ultimate solution to protecting people

from these deadly processes remains elusive, I believe that the experience gained in my research identifies a number of challenges and promising next steps. In this chapter, I will evaluate the ability of the various components of my study to be integrated into one functional system by focusing on those time period in which rip currents were observed as compared to conditions when no rip currents were evident and trying to decode the complex relationships between incident wave fields, infragravity waves and rip currents. I will discuss the lessons learned and the potential for future research in this chapter.

Comparisons that didn't pan out

The relatively low number of rip currents made it difficult to directly compare some physical traits to rip occurrence. No definitive relationship was found with tidal stage or seasonal trends. As mentioned in chapter 4, the rips seemed slightly event driven; there were time periods that had increased rip activity, but this did not continue over multiple years. Other comparisons, such as the relationship to wave direction were also unclear. While it did seem more likely for rips during swell from the south east, this corresponds to the dominant conditions present along the south shore most of the time anyway, so one would expect that even random chance would allow for this weak association. High-resolution wind data was not available, and when looking at the regional wind, no apparent relationship emerged. Large wave conditions at Fire Island were examined to try and further describe the transition during and after storms to a more dynamic near shore bathymetry in the form of ridge in runnels. No rip currents were seen during this time period that might provide a compelling case regarding the role of storms

in generating ridge-and-runnels from our camera, although it has been observed outside of the camera ranges. I also never found any evidence of increased bar breaks in the days (7-14) following a storm passage. It is possible, though, that any of these may be expanded on with further observation over a longer time period for a larger rip current sample set.

Comments on a Video Monitoring

The previous chapters have outlined work to address each of the three research components, individually, in order to assess the validity of each method towards the ultimate goal, better rip-current safety. Initial observations via direct monitoring of the surfzone, as described in chapter 1, indicated that flash rip currents were the dominant (if not exclusive) type of rip currents for both south shore study areas. As I have shown, a fairly infrequent occurrence of rips leading to an expected rip current density of a few rip currents per day per kilometer of shoreline gave the first clues as to the rip regime. The rip currents themselves are, generally, both narrow and short appearing as a line of foam oriented perpendicular to the coast. The rips general form, as well as their tendency to form as individual events instead of multiples, denotes a type of rip known as a flash rip. Monitoring flash rip currents requires a continuous series of observations with sampling periods on the order of seconds and image averaging may ultimately destroy the signal. In addition, coverage must be over a stretch of shoreline wide enough to detect multiple rips on the order of 100+ m apart. This means putting the camera at an elevated position near the shore, like the lighthouse, or having multiple cameras. The video technique is

promising and, indeed, in 2005 a patent was issued to Gregory Perrier for a conceptual application of this concept (Patent No. U.S. 6,931,144 B2). Complications, however, were many and diverse throughout the study. The camera itself presented a problem of upkeep as the glass would be susceptible to fouling which could affect the focus and cause the far-frame to be unusable. While this wasn't a frequent issue it presented a hurdle early in the project in producing quality images until it was discovered that the inner lens itself was shipped covered in dust and after disassembling the lens, cleaning and replacing the problem was largely inert. Rainy conditions presented the same problem as rain drops on the camera would cause both focus and blurring issues for the images being recorded. This was unfortunate as storms, in general, are associated to with increased surfzone activity and therefore, possibly, including rip currents. If so, these storms would have an unknown impact on the study's findings. Though, since people won't generally be enjoying the surf in rough weather the hazard of the rip is probably negligible. The camera itself stopped working on several occasions and the circuit board had to be returned in summer of 2008 for circuitry work.

Gathering data from the images was labor-intensive, requiring an experienced and trained analyst. Considerable energy went into trying to create an automated recognition system in cooperation with the computer science department at Stony Brook University, but this ultimately failed. The idea was to train the program to recognize pixel color to pick out rip currents in the surfzone. While there was some success with picking out rips successfully the false positives made the system ineffective and visual inspection of the images was, instead, used. The failure of the automated system could be traced to the inherent variability within the visual signature of the rip which was sometimes white

water, sometimes a gap in the foam line, sometimes sediment laden water etc. In addition, the character of the signature on the image varied with sun angle, sea surface roughness, cloudiness, etc. so that training the system to pick up rip currents in the range of conditions proved impossible. Ultimately fruitless, computer trained identification still holds great reward should it be able to fully develop an accurate methodology for rip recognition and make an extremely tedious and time consuming task a minor portion of the study. Having more time to focus on generation of rips instead of 1000's of hours simply scanning and re-scanning images would be monumental in furthering the efficiency of rip current studies. Current technology simply doesn't seem to have caught up with needs in surfzone studies from an imaging standpoint. More difficulties arise because of the various guesses under which rip currents appear on the images. The problem with these types of rips remains linkage to a forcing process. It seems likely there is a lack of a strong bathymetric control, likely both due to the offshore position of the bar and the ephemeral nature of the rips combined with their ability to rapidly migrate, leaving, instead a more reasonable alternative theory regarding rip generation via modulation of incident waves. While this modulation has been attributed to an array of possible causes, our focus included long period energy trapped in the surf zone.

Comments on seismic monitoring

Chapter 3 of this research has demonstrated the ability of a land based seismometer to record energy at the coast via vibrations from breaking waves. This system, essentially replacing surfzone pressure sensor deployments, was capable of

monitoring both shorter period (3-15 seconds) coastal energy associated with incident waves and longer period (>20 seconds) energy associated with edge waves and surf beat. I have shown that spectral peaks at from data recorded at the seismometers detected strong power associated with frequencies associated to typical incident waves. Further frequencies commonly demonstrating high power have been focused at a dominant frequency associated with infragravity energy. Initial results pertaining to the presence of this phenomenon were verified via a second seismometer 3 km from the initial location that showed similar spectral peaks, alluding to a common forcing, which due to the relative distance could only be approaching swell. A distal location at the Long Island north shore only showed a similar spectra signal when forced by a strong single event (large earthquake) but otherwise had little commonality between spectral signals, which should be expected as Stony Brook should only get a very faint seismic signal from the water waves in nearby Long Island Sound. In conjunction with the video monitoring, the seismic records provide insight into nearshore physical conditions that may give rise to instance of rip currents and further enhance our current, weak abilities to predict rip occurrences. Currently, both of these methods give a real-time picture of possible rip currents and are only steps towards prediction by trying to understand the association between infragravity energy in the nearshore and the presence of rips. To reach the next step of prediction, having an idea of wave conditions most likely to produce infragravity waves and corresponding rip currents is required. For this, forecasts including information about the incoming wave conditions (to which the infragravity energy is initially bound) needs to accompany these data. *In situ* wave gages in the surf zone are

needed to further verify and calibrate the seismic signature to local surf conditions. Unfortunately, resources were not available to do this for my study.

The seismometer required little maintenance beyond the occasional power outage at the home in which it was located and a replacement of the computer to which it was attached. These issues were minor inconveniences that were easily handled. By far, the seismometer took the least time to install, maintain and analyze as compared to the herculean task of individually scanning the photos and keeping up with glitches associated with the camera system. Further work should be done to address the applicability of seismic stations in alongshore arrays to replace current methodology using pressure sensors, but for the discrete point type study addressed in this manuscript it functioned exceptionally well and is a great alternative to the more cumbersome in-situ surfzone techniques. I see especially strong uses for this methodology along high population coasts as the system could easily be installed in several hotels alongshore in out of the way corners that would create little inconvenience for the hotel/resort staff and focus on areas that are more likely to attract high volumes of people to the beach causing a much higher chance of persons encountering rip currents.

The importance of the seismic signal represents two ideas that may further elucidate the exact nature of edge waves in Long Island. First, the signal is concentrated at one dominant frequency, but is not ubiquitous in the records showing that the edge wave can be formed and destroyed in a relatively short period of time based on what is surely a confluence of several factors including wave approach, height, period, and the chance that the infragravity wave is indeed trapped. Second, the fact that the signal is ephemeral over a consistent, low power infragravity signal that is ubiquitous means that

the phenomenon is not associated directly with wave beat, but is, in fact, a free wave acting in the nearshore. While it's true that no rip currents were seen during this time period it could be that our visible frame was simply too small to catch rips that formed just off screen.

Comments on wave modeling

Chapter 3 focused on the implementation of the SWAN wave model to identify nearshore wave transformations. The model was shown to accurately describe wave heights as open ocean wave approached the Long Island south shore at three separate locations. Root mean squared error (rms) and scatter index (SI), were used to evaluate the model accuracy. SWAN accuracy varied between the sites. At the straight beach location in Westhampton Beach (rms:0.398, SI:0.4313) the model performance was affected by a short, three-day period with increased divergence. Removing this time period increased the model's accuracy (rms: 0.307, SI:0.323) and error is linked to lack of available local wind data for additional forcing. The two sites located at the Shinnecock inlet (rms:0.2701, 0.340; SI:0.414, 0.452) demonstrated better rms and SI then the Westhampton beach over the whole period, but exceeded the results from one location after the three-day period with high divergence was removed. Around the inlet, maximum wave heights seemed to be limited, most likely due to wave interactions around said inlet causing an apparent limit on the maximum wave height achievable for SWAN. Since the model accuracy tests are based on trends in the data; the inability to describe peak wave heights didn't result in as high an rms and SI as the trending

divergence seen at Westhampton over the three day even. Currently, SWAN has shown the ability to reasonable depict nearshore wave conditions and should be viable as a source for describing said conditions. SWAN modeling, however, proved to be of limited use in the study of rip currents for two reasons. The direction of wave attacks in the surf zone was not adequately resolved and the SWAN results are essentially monochromatic incident waves. The modulation of these waves and the generation of infragravity waves is not reproduced.

Overall, the incident wave fields as predicted nearshore from SWAN during rip currents present no widely constant conditions most likely associated with rip currents except for wave direction. A wide range of periods and waves heights make it unlikely that they, alone, create any stress directly attributable to rip formation. Lack of direct relationships does not preclude a dynamic cooperation between wave height, wave period and wave direction that become more apt to generate rip currents that was elusive during this project.

SWAN performed admirably in the verification tests, on par or better then STWave. To really address its validity, nearshore devices aimed specifically at monitoring wave conditions are needed. SWAN was initially chosen based on preliminary findings that showed its accuracy in the nearshore, but limitations in the model may have made it less valuable for our study. Rip currents are often seen to be wide, on the order of 150 meters, but the rips seen over this study were much smaller. Generally they did not exceed 15 m in width and didn't extend offshore very far. As such, the resolution required to get an accurate depiction of the exact location in which rip currents were observed was limited both by the model (not accurate below 25 m), the

bathymetry data that had to be interpolated to the 25 meter resolution and so may not have been exactly representative of nearshore conditions and computation efficiency. Especially considering the high variability of bathymetry in the nearshore, the money and time needed to help ensure the models integrity was beyond the scope of this project and most likely beyond the scope of most nearshore projects.

References

Aagaard, T., K.R. Bryan. 2003. Observations of infragravity wave frequency selection. Continental Shelf Research, 23: 1019-1034.

Aagaard, T., B. Greenwood, J. Nielsen. 1997. Mean currents and sediment transport in a rip channel. Marine Geology, 140: 25-45.

Adams, P.N., R.S. Anderson, J. Revenaugh. 2002. Microseismic measurement of wave energy delivery to a rocky coast. Geology, 30(10): 895-898.

Allen, J.S., P.A. Newberger, R.A. Holman. 1996. Nonlinear shear instabilities of alongshore currents on plane beaches. Journal of Fluid Mechanics, 310: 181-213.

Arthur, R.S. 1962. A note on the dynamics of rip currents. Journal of Geophysical Research, 67(7): 2777-2779.

Baker Engineering. 1998. *Investigation of spur jetties*, submitted to: New York Department of State, Division of Coastal Resources, 38 pp.

Baquerizo, A. M.A. Losada, I.J. Losada. 2002. Edge wave scattering by a coastal structure. Fluid Dynamics Research, 31: 275-287.

Batten, B.K. 2003. Morphologic typologies and sediment budget for the ocean shoreline of Long Island, New York. Ph.D. Dissertation, Stony Brook University, 92 pp. +appendices.

Battjes, J. A. 1988. Surf-zone dynamics. Annual Review of Fluid Mechanics, 20: 257-293.

Beach R. R., R. W. Sternberg. 1988. Suspended sediment transport in the surf zone: response to cross-shore infragravity motion. Marine Geology, 80: 61-79.

Benumof, B.T., G.B. Griggs. 1999. The dependence of seacliff erosion rates on cliff material properties and physical processes: San Diego County, California. Shore and Beach, 67: 29-41.

Bokuniewicz, H.J. 2004. Isolated Groins at East Hampton, NY. Journal of Coastal Research, 33: 215-222

Booij, N, R.C. Ris, L.H. Hothuijsen. 1999. A third-generation wave model for coastal regions 1. Model description and validation. Journal of Geophysical Research, 104(C4): 7649-7666.

Bowen, A.J., D.L. Inman. 1969. Rip currents: laboratory and field observations. American Geophysical Union. 1: 5479-5491.

Bowen, A.J., R.T. Guza. 1978. Edge waves and surf beat. Journal of Geophysical Research, 83(C4): 1913-1920.

Brander, R.W., A.D. Short. 2000. Morphodynamics of a large-scale rip current system at Muriwai Beach, New Zealand. Marine Geology, 165: 27-39.

Brewster, B. C. 1995. *The United States lifesaving association manual of open water lifesaving*, BRADY/Prentice Hall, Upper Saddle River, New Jersey, 07458, 316 pp.

Bricker, J. D., S. Munger, C. Pequignet, J.R. Wells, G. Pawlak, K.F. Cheung. 2007. ADCP observations of edge waves off Oahu in the wake of the November 2006 Kuril Islands tsunami. Geophysical Research Letters, 34 (L23617): doi 10.1029/2007GL032015, 2007.

Bromirski, P.D., R.E. Flick, N. Graham. 1999. Ocean wave height determined from inland seismometer data: Implications for investigating wave climate changes in the NE Pacific. Journal of Geophysical Research, 104 (C9): 20753-20766

Bromirski, P.D. 2001. Vibrations from the "Perfect Storm". Geochemistry, Geophysics and Geosystems, 2: doi:10.1029/2000GC000119.

Bromirski, P.D, F.K. Duennebier. 2002. The near-coastal microseism spectrum: Spatial and temporal wave climate relationships. Journal of Geophysical Research, 107(B8): 2166-2185.

Buonaiuto, F.S. M.P. Slattery, H.J. Bokuniewicz. Wave Modeling of Long Island Coastal Waters. Journal of Coastal Research, *Accepted with revisions August 2008*.

Buonaiuto, F.S. 2003. Morphological evolution of Shinnecock Inlet, NY. Ph.D. Dissertation, Stony Brook University, 84 pp. + appendices.

Dalrymple, R.A. 1975. A mechanism for rip current generation on an open coast. Journal of Geophysical Research, 80(24): 3485-3487.

Dalrymple, R.A., G.A. Lanan. 1976. Beach cusps formed by intersecting waves. Geological Society of America Bulletin, 87: 57-60.

Dalrymple, R.A., C.J. Lozano. 1978. Wave-current interaction models for rip currents. Journal of Geophysical Research, 83(C12): 6063-6071.

Darbyshire, J., E.O. Okeke. 1969. A study of primary and secondary microseisms recorded in Anglesey. Journal of Geophysical Research, 17(1): 63-92.

Davis, R.E., R. Dolan.1993. Nor'easters. American scientist, 81: 428-439.

Deane, G.B. 2000a. Long time-base observations of surf noise. Journal of the Acoustic Society of America, 107(2): 758-769.

Deane, G.B. 2000b. A model for the horizontal directionality of breaking wave noise in the surf zone. Journal of the Acoustic Society of America, 107(2):177-192.

Engle, J., J. MacMahan, R. J. Thieke, D. M. Hanes, R. G. Dean. 2002. Formulation of a rip current predictive index using rescue data. Proceedings of the National Conference on Beach Preservation Technology (FSBPA), Biloxi, MS.

Falques, A., A. Montoto, D. Vila. 1999. A note on hydrodynamic instabilities and horizontal circulation in the surf zone. Journal of Geophysical Research, 104(C9): 2060-20615.

Gravens, M. B. 1999. Periodic Shoreline Morphology, Fire Island, New York. Proceedings of Coastal Sediments, '99, American Society of Civil Engineers, NY, 2: 1613-1626 pp.

Gerstoft, P., M. C. Fehler, K.G. Sabra. 2006. When Katrina hit California. Geophysical Research Letters, 33: L173808 Sep 8 2006.

Hammack J., N. Scheffner, H. Segur. 1991. A note on the generation and narrowness of Periodic rip currents. Journal of Geophysical Research, 96(C3): 4909-4914.

Hasselmann, K. 1963. A statistical analysis of the generation of microseisms. Reviews of Geophysics, 1: 177-209.

Hirsch, J. 2005. Seismic signature of ocean surf as it relates to wave energy and coastal erosion. Technical report, Stony Brook University, 12 pp.

Holman R.A., G. Symonds, E.B. Thornton, R. Ranasinghe. 2006. Rip spacing and persistence on an embayed beach. Journal of Geophysical Research, 111: 1-17.

Howard, A.D. 1939. Hurricane modifications of the offshore bar of Long Island, NY. Geographical Review, 29(3): 400-415.

Howell, B.F. 1990. *An introduction to seismological Research: history and development*, Cambridge University Press, Cambridge, 193 pp

Jin, Kang-Ren, Zhen-Gang Ji. 2001. Calibration and verification of the spectral wind-wave model for Lake Okeechobee. Ocean Engineering, 28: 571-584.

Johnson, D., C. Pattiaratchi. 2006. Boussinesq modeling of transient rip currents. Coastal Engineering, 53: 419-439.

Kana, T.W. 1995. A mesoscale sediment budget for Long Island, New York. Marine Geology, 126: 87-110.

Kinsman, B. 1965. *Wind waves: their generation and propagation on the ocean surface*, Prentice-Hall, Englewood Cliffs, NJ, 676 pp.

Komar, P.D. 1998. *Beach processes and sedimentation*, Prentice hall, Upper Saddle River, NJ, 554 pp.

Lascody, R. L. 1998. East Central Florida Rip Current Program. National Weather Digest, 22(2): 25-30.

Leblond, P.H., C.L. Tang. 1974. On energy coupling between waves and rip currents. Journal of Geophysical Research, 79(6): 811-816.

Long Island Shores. Last accessed March 22, 2010. http://www.lishore.org/sites.htm.

Longuett-Higgins, M.S., R.W. Stewart. 1964. Radiation stresses in water waves, a physical discussion with applications. Deep-Sea Research, 11: 529-562.

Lushine, J.B. 1991. A study of rip current drownings and related weather factors. National Weather Digest, 16: 13-19.

Macmahan, J.H., E.B. Thornton, A.J.H.M. Reniers, T.P. Stanton, G. Symonds. 2008. Low-Energy Rip Currents Associated With Small Bathymetric Variations. Marine Geology, 255: 156-164.

MacMahan, J.H., E.B. Thornton, A.J.H.M Reniers. 2006. Rip Current Review. Coastal Engineering, 53: 191-208.

MacMahan, J.H., E.B. Thornton, T.P. Stanton, A.J.H.M. Reniers. 2005. RIPEX: observations of a rip current system. Marine Geology, 218: 113-134.

MacMahan, J.H., A.J.H.M. Reniers, E.B. Thornton, T.P. Stanton. 2004. Infragravity rip current pulsations. Journal of Geophysical Research, 109(C01033): 1-9.

MacMahan, J.H., A.J.H.M. Reniers, E.B. Thornton, T.P. Stanton. 2004. Surf zone eddies coupled with rip current morphology. Journal of Geophysical Research, 109(C07004): doi:10.1029/2003JC002083

Murray, A.B., M. LeBars, and C. Guillon. 2003. Tests of a new hypothesis for non-bathymetrically driven rip currents. Journal of Coastal Research, 19: 269-277.

National Oceanic and Atmospheric Administration, National Data Buoy Center. Last accessed, March 2, 2010. http://www.ndbc.noaa.gov/station_hisoty.php?station=44017

Nelko, V., R.A. Dalrymple. Last accessed July 18, 2010. Rip currents prediction in Ocean City, MD. http://www.ripcurrents.fiu.edu/NEW%20SITE%20JUNE%202009/Symposium2010/Abstracts/Rip%20Currents%20Prediction%20in%20Ocean%20City,%20MD.pdf.

Oliver, J., M. Ewing. 1957. Microseisms in the 11- to 18-second period range. Bulletin of the Seismological Society of America, 47 (2): 111-127.

Oltman-Shay, J., R.T. Guza. 1987. Infragravity edge wave observation on two California beaches. Journal of Physical Oceanography, 17: 644-663.

Palmsten, M.L. 2001. Application of the SWAN wave model to a high-energy continental shelf. MA thesis University of South Florida, 135 pp.

Quartel, S. 2009. Temporal and special behavior of rip channels in a multiple-barred coastal system. Earth Surface Processes and Landforms, 34: 163-176.

Ranasinghe, R., G. Symonds, K. Black, R. Holman. 2004. Morphodynamics of Intermediate beaches: a video imaging and numerical modeling study. Coastal Engineering, 51: 629-655.

Reniers, A.J.H.M., J.A. Roelvink, E.B. Thornton. 2004. Morpholdynamic modeling of an embayed beach under wave group forcing. Journal of Geophysical Research, 109(C01030): doi: 10.1029/2002JC001586.

Ris, R.C., L.H. Holthuijsen, N. Booij. 1999. A third-generation wave model for coastal regions 2. Verification. Journal of Geophysical Research, 104(C4): 7667-7681.

Rogers, W.E., J.M. Kaihatu, H.A.H. Petit, N. Booij, L.H. Holthuijsen. 2002. Diffusion reduction in an arbitrary scale third generation wind wave model. Ocean Engineering, 29: 1357-1390.

Rogers, W.E., P.A. Hwang, D.W. Wang. 2003. Investigation of wave growth and decay in the SWAN model: three regional-scale applications. Journal of Physical Oceanography, 33: 366-389

Ruessink, B.G. 1998. The temporal and spatial variability of infragravity energy in a barred nearshore zone. Continental Shelf Research, 18: 585-605.

Seaver, K. H. J. Bokuniewicz, F. Buoniauto. 2007. Evolution of erosional hot spots on a barrier island: Fire Island, New York. Coastal sediments '07, N.C. Kraus and J.D. Rosati, editors. Amer. Soc. Civil Engs., 3: 1722-1730 pp.

Schubert, C.E., H.J. Bokuniewicz. 1991. Infragravity wave motion in a tidal inlet. Coastal Sediments, Special Conference, Seattle, WA, 1434-1446, June 25-27 1991.

Schüttrumpt, H. 2006. Hydraulic influence of navigation channels in flood defense (sic) structures, 31st Congress of the International Navigation Association (PIANC), Estroil, Portugal.

Smith, J.A., J.L. Largier, 1995. Observations of nearshore circulation: rip currents. Journal of Geophysical Research, 100: 10, 967-10, 975.

Smith, G.G., G.P. Mocke. 2002. Interaction between breaking/broken waves and infragravity-scale phenomena to control sediment suspension transport in the surf zone. Marine Geology, 187: 329-345.

Tabulevich, V.N. 1992. *Microseismic and infrasound waves*, Research Reports in Physics, Springer-Verlag, NY, 150 pp.

Taney, N.E. 1961. Geomorphology of the south shore of Long Island, New York. U.S. Army Corps of Engineers, Beach Erosion Board, TM No. 128: 67 pp.

Tanski, J., H.J. Bokuniewicz, C.E. Schubert. 1990. An overview and assessment of the coastal processes data base for the south shore of Long Island. NY Sea Grant Program, Spec. Rpt., 104: 77 pp.

Thornton, E.B., J. MacMahan, A.H. Sallenger Jr. 2007. Rip currents, mega-cusps, and eroding dunes. Marine Geology, 240: 151-167.

Tindle, C.T., M.J. Murphy. 1999. Microseisms and ocean wave measurements. Journal of Oceanic Engineering, 24(1): 112-115.

Tsien, H-S. 1986. Differential transport of sand on the south shore of Long Island. M.S. Thesis, Stony Brook University, 140 pp.

Turner, I.L., D. Whyte, B.G. Ruessink, R. Ranasinghe. 2007. Observations of rip spacing, persistence and mobility at a long, straight coastline. Marine Geology, 236: 209-221.

United States Life Saving Association (USLA). 2010. http://www.usla.org/ripcurrents/.

United States Army Corps of Engineers (USACE). Last accessed, March 22, 2010. http://sandbar.wes.army.mil/public_html/pmab2web/htdocs/newyork/westhampton/ny001/ny001.html.

Ursell, F. 1952. Edge waves on a sloping beach. Proceedings of the royal society of London. Series A. Mathematical and Physical Sciences, 214(1116): 79-97.

Van Enckevort, I.M.J., B.G. Ruessink, G. Coco, K. Suzuki, I.L. Turner, N.G. Plant, R.A. Holman. 2004. Observations of nearshore crescentric sandbars. Journal of Geophysical Research, 109 (appendix D): 1-17.

Van Enckevort, I.M.J., B.G. Ruessink. 2001. Effects of hydrodynamics and bathymetry on video estimates of nearshore sandbar position. Journal of Geophysical Research, 106(C8): 16969-16979.

Webb, S.C. 1998. Broadband seismology and noise under the ocean. Review of Geophysics, 36(1): 105-142.

Wiechert, E., 1904 Verhandlugen der zweiten internationalen seimologischen Konferenenz, Strassburg, 1903, *Beitr. Gph. Erganz*, 2, 41-43.

Wright, L.D., A.D. Short. 1983. Morphodynamices of Beaches and Surf Zones in Australia. In *Handbook of Coastal Processes and Erosion*, P.D. Komar (editor). CRC Press, Boca Raton, FL, 35-64 pp.

Yu, J., D.N. Slinn. 2003. Effects of wave-current interaction on rip currents. Journal of Geophysical Research, 108(C3): 33(1)-33(19).

Zarillo, G.A., J.T. Liu. 1988. Resolving bathymetric components of the upper shoreface on a wave-dominated coast. Marine Geology, 82: 169-186.

Appendix A
Equations used throughout text

Chapter 2:
Action Balance Equation

$$\frac{\partial}{\partial t}N+\frac{\partial}{\partial x}c_x N+\frac{\partial}{\partial y}c_y N+\frac{\partial}{\partial \sigma}c_\sigma N+\frac{\partial}{\partial \theta}c_\theta N=\frac{S}{\sigma} \quad (1)$$

Where :

$\frac{\partial}{\partial t}N$	is local rate of change
$\frac{\partial}{\partial x}c_x N+\frac{\partial}{\partial y}c_y N$	is propagation of action in x and y space
$\frac{\partial}{\partial \sigma}c_\sigma N$	represents variability in relative frequency with change in depth and current interactions in x space
$\frac{\partial}{\partial \theta}c_\theta N$	represents wave transformations due to refraction around currents and bathymetry
S	represents source term for generation, dissipation and nonlinear wave-wave interactions
σ	is relative frequency

Chapter 3:
Wavelength L_e of an edge wave

$$L_e=\frac{gT_e^2}{2\pi}\sin\left[(2n+1)\beta\right] \quad (1)$$

Where:

T_e	is the period of an edge wave
n	is the edge wave mode
β	Is the beach slope

Expected wavelength of alongshore cusps where $T_e = 2T_i$ and n=0

$$L_e=\frac{g2T_i^2}{\pi}\sin(\beta) \quad (2)$$

Resonant period of an edge wave

$$\frac{2L}{\sqrt{gh}}$$

Where:

L	is across shore width of resonant basin
h	is water depth

Appendix B
Example of SWAN control file

```
$*************HEADING*************************************
$
PROJ 'ssli' '1'
$
$
$ --|-----------------------------------------------------------|--
$   | This SWAN file for South shore of Long Island               |
$   |                                                           |
$ --|-----------------------------------------------------------|--
SET 0 90 0 200 1 9.81 1025 0 1 Nautical
MODE STAT TWOD
COORD SPHERICAL CCM
$
$************MODEL INPUT*************************************
$
CGRID REG -74.25 40.0 0. 2.75 1.3 660 312 CIRCLE 10 0.05 40 70
$
INPGRID BOTTOM -74.25 40.0 0. 1100 520 0.0025 0.0025
READINP BOTTOM 1. 'C:\SWAN\myproj\verifyFeb1999\02199912\SSgrid0025.bot' 1 0 FREE
$
BOU SHAPE JONSWAP 3.3 PEAK DSPR DEGREES
$
BOUN SIDE E CON PAR 1.62 5.28 90
$
BOUN SIDE S CON PAR 1.62 5.28 155.67
$
GEN1 188 0.59 0.12 250 0.0036 0.0012 1 0.13
$
OFF WCAP
$
$************ OUTPUT REQUESTS ************************
$
POINT 'whole' FILE 'C:\SWAN\myproj\verifyFeb1999\02199912\loc.loc'
TABLE 'whole' HEAD XP YP DIST HS HSWELL DEP TM01 DIR WLEN STEEPNESS RTP DSPR
TABLE 'whole' HEAD 'C:\SWAN\myproj\verifyFeb1999\02199912\bigloc.tbl' XP YP DIST HS TM01
DIR DEP RTP WLEN STEEPNESS
$
POINT 'bouys' FILE 'C:\SWAN\myproj\verifyFeb1999\02199912\bouys.loc'
TABLE 'bouys' HEAD XP YP DIST HS HSWELL DEP TM01 DIR WLEN STEEPNESS RTP DSPR
TABLE 'bouys' HEAD 'C:\SWAN\myproj\verifyFeb1999\02199912\bouys.tbl' XP YP DIST HS TM01
DIR DEP RTP WLEN STEEPNESS
$
TEST 1,0
COMPUTE
STOP
$
```